2012 ABIGAIL ESENAM ASANGBA

PLANT CELL WALL DEGRADING ENZYMES AND THEIR POTENTIAL APPLICATION TO BIOFUEL PRODUCTION

BY

ABIGAIL ESENAM ASANGBA

THESIS

Submitted in partial fulfillment of the requirements
for the degree of Master of Science in Animal Sciences
in the Graduate College of the
University of Illinois at Urbana-Champaign, 2012

Urbana, Illinois

Advisor:

Professor Isaac Cann

ABSTRACT

The soaring high price of petroleum price as well as the impact of the fossil fuel combustion process on atmospheric carbon dioxide (CO_2) has necessitated the development of alternative fuel energy. Even with the most recent technology, oil, natural gas, and coal will emit not only climate-threatening greenhouse gases and other pollutants, but also the quantity of undiscovered stocks will always be a matter of great concern

Plants have evolved photosynthetic mechanisms in which solar energy is used to fix CO_2 into carbohydrates. Thus, combustion of biofuels, derived from plant biomass, can be considered a potentially carbon neutral process. Plants cell walls which are composed mostly of lignocellulosic materials (lignin, cellulose, and hemicellulose) are recalcitrant and are difficult to breakdown. This therefore represents a major limitation in the conversion of plant biomass to biofuels. Microbes have evolved a plethora of enzymatic strategies for hydrolyzing plant cell wall into its constituent sugars for subsequent fermentation to biofuels. Therefore, microorganisms are considered an important source of biocatalysts in the emerging biofuel industry.

Caldicellulosiruptor bescii and *Themoanaerobacterium bryantii* are both thermophilic anaerobes capable of secreting enzymes for degrading plant cell walls. To gain insight into the cellular machinery that these organisms elaborate to degrade cellulose and the hemicellulosic polymer xylan, genes with various putative functions from both organisms were identified, cloned and expressed the recombinant proteins in *Escherichia coli*.

A hemicellulase gene cluster from *T. bryantii* encoding genes predicted to have endoxylanase activity, β-xylosidase activity, α-glucoronidase activity, acetyl xylan esterase activity as well as oxido-reductase activity was isolated for further studies. We hypothesized that the endoxylanase

should work synergistically with the other accessory enzymes in the cluster to break down xylan releasing mainly xylose for the utilization of the organism. As expected the endoxylanase was able to hydrolyze a number of xylan containing polysaccharides releasing undecorated xylo-oligosaccharides with the β-xylosidases converting the xylobiose released to xylose.

A putative β-glucosidase Cb486 from *C. bescii* was screened for enzymatic properties, and it was shown to exhibit activity against pNP-α-L-arabinopyranoside, pNP-β-D-fucopyranoside, pNP-β-D-galactopyranoside, pNP-β-D-glucopyranoside, pNP-β-D-xylopyranoside and pNP-β-D-cellobioside suggesting that Cb486 is a multi-functional enzyme. We therefore hypothesized that Cb486 incubated with endoglucanases or endoxylanases should be able to enhance the release of glucose or xylose from cellulose and xylans respectively. As expected, Cb486 was also able to work synergistically with a number of endo-glucanases from the genome of *C. bescii* to release glucose from cellulosic substrates as well as xylose from xylan containing substrates.

To my mother and siblings

ACKNOWLEDGEMENTS

This project would not have been possible without the support of many people. Many thanks to my adviser, Dr. Isaac K.O. Cann, who read my numerous revisions and helped, make some sense of the confusion. I also want extend my appreciation to my committee members; Dr. Roderick I. Mackie, Dr. Alfred Roca and Dr. Sidonie N. Lavergne, who offered guidance and support. My appreciation also goes to all Cann Lab members especially Xiaoyun Su, Michael Iakiviak and Atsushi Miyagi who helped me obtain the best results with the various assays.

Thanks to the University of Illinois Graduate College for awarding me a graduate research assistantship for my Master's program. My appreciation also goes to Energy Biosciences Institute (EBI), for providing me with the financial means to complete this project as well as paying my monthly stipend.

And finally, my appreciation goes to my parents, siblings and numerous friends who helped me in diverse ways, always offering support and love.

TABLE OF CONTENTS

CHAPTER I: INTRODUCTION……...1

CHAPTER II: LITERATURE REVIEW……..……4

CHAPTER III: BIOCHEMICAL ANALYSIS OF THERMOSTABLE HEMICELLULASES FROM *THERMOANAEROBACTERIUM BRYANTII*……..……..……..19

CHAPTER IV: BIOCHEMICAL ANALYSIS OF A MULTIFUNCTIONAL THERMOSTABLE GLYCOSIDE HYDROLASE FAMILY ONE MEMBER FROM *CALDICELLULOSIRUPTOR BESCII*……..……..….38

CHAPTER V: DISCUSSION…….……56

CHAPTER VI: CONCLUSIONS……...……62

CHAPTER VII: FIGURES AND TABLES……..…….……63

REFERENCES ...……..…..……...92

CHAPTER I

INTRODUCTION

OVERVIEW OF BIOFUELS

The human society has an insatiable appetite for fuels and today's supply of liquid fuels worldwide is almost completely dependent on petroleum. Bioenergy production has therefore become a topic of intense interest due to increased concern regarding limited petroleum-based fuel supplies and the contribution of the use of these fuels to atmospheric CO_2 levels. Bioethanol has been produced since the 1970's in Brazil on a large scale, from processing of sugar cane, via extraction of sucrose, conversion to glucose, and fermentation to ethanol, followed by distillation (Lee 1997). The use of bioethanol can reduce our dependence on fossil fuels, while at the same time decreasing net emissions of carbon dioxide, the main greenhouse gas (Lynd *et al*., 1991).

Brazil's bioethanol production consumes large quantities of sugar cane, while in the USA; corn is used (Wheals *et al*., 1999). Other starch-rich grains, such as wheat and barley, are mostly used in Europe (Galbe and Zacchi, 2002). The use of such sugar-rich feedstock causes the escalation of food prices, owing to competition on the market [Catic and Rujnic-Sokele 2008; Knocke and Vogt 2009). Therefore, future expansion of biofuel production must be increasingly based on bioethanol from lignocellulosic materials, such as agricultural byproducts, forest residues, industrial waste streams or energy crops [Claassen *et al*., 1999; Solomon *et al*., 2007). These feedstocks, which are being used in second-generation (2G) bioethanol production, are abundant, and their cost is lower than that of food crops (Tan *et al*., 2008).

The most abundant polysaccharide in the plant cell wall is cellulose followed by hemicellulose and then pectin (Linden *et al*., 1994). Microorganisms have to synthesize a

number of different enzymes for the hydrolysis of cellulose or hemicellulose in order to invade or live successfully in the plant tissues (Khandeparker and Numan, 2008). Thus, to effectively degrade plant cell wall polysaccharides, some specialist microorganisms develop a cell associated multiprotein complex called cellulosome (Lamed and Bayer, 1988) or xylanosome (Lin and Thompson, 1991) that contains cellulases, xylanases, and cellulose-binding factors. Another strategy is to induce multi-functionalization of certain enzymes to hydrolyze different kinds of substrates (Khandeparker and Numan, 2008) whereby one enzyme is able to hydrolyze a number of different linkages. The utilization of hemicellulose and lignin, in addition to cellulose, may greatly improve the productivity and yield of fuels from biomass (Linden *et al*., 1994). The hemicellulose fraction is made up mainly of pentose sugars that are potentially important value-added products of fermentation to biofuels. Xylan is the major hemicellulose component in plant cell walls as well as the most abundant renewable polysaccharide after cellulose in nature (Biely, 1985; Saha 2003). Hydrolysis of xylan therefore is essential in the breakdown process of plant material and this can be carried out either by acid or enzymes. Acid hydrolysis is faster but is accompanied by the formation of toxic compounds that hinder subsequent microbial fermentations (Biely, 1985). The xylan main chain differs from the cellulose main chain by having D-xylose instead of the D-glucose found in cellulose (Biely, 1985). Cellulose is a highly homogeneous polymer and it consists of β-1, 4-linked glucose units that make interstrand hydrogen bonds to form a highly stable crystalline lattice (Laureano-Perez *et al.*, 2005). Xylan, on the other hand, is a heteropolymeric hemicellulosic polymer that consists predominantly of the pentose sugars arabinose and xylose, although it may also contain glucuronyl, feruloyl, and acetyl groups (Ebringerova & Heinze, 2000). The structure of xylan is therefore more complex than cellulose (Biely, 1985). The main problem with the utilization of hemicellulose is the high

degree of substitution found on the hemicellulose backbone (Linden *et al*., 1994). These substituent groups are important in the hydrolysis of xylans due to the fact that they are rate limiting in the hydrolysis process (Debeire *et al*., 1990). They interfere with the enzymatic degradation of the hemicellulose to monomeric sugars through steric hindrance (Linden *et al*., 1994). Endo-1, 4-β-xylanase, β-xylosidase and several other accessory enzymes such as α-L-arabinofuranosidase, α-glucuronidase, acetylxylan esterase, ferulic acid esterase and *p*-coumaric acid esterase that are required for the hydrolysis of various substituted xylans are responsible for the total biodegradation of xylan (Saha, 2003). Endoxylanase and β-xylosidase however have the most important activities during the hydrolysis of xylan among all the xylanolytic enzymes (Sunna and Antranikan 1997). Monosaccharide released from cellulose and hemicellulose by enzymes is mediated by glycoside hydrolases that are a large class of enzymes that exhibit both broad and stringent substrate specificities (Yeoman *et al*., 2010). They are able to accelerate the rate of hydrolysis of glycosidic linkages by up to 17 orders of magnitude over the uncatalyzed hydrolysis (Wolfenden *et al*., 1998). Glycoside hydrolases are classified into different families based on their amino acid sequences and three-dimensional folds (Cantarel *et al*., 2009). There are currently 129 GH families organized into 14 clans (CAZy; http://www.cazy.org/).

CHAPTER II:

LITERATURE REVIEW

PLANT CELL WALL

CELLULOSE

Cellulose accounts for up to 40% of plant biomass and consequently is the most abundant natural polymer on earth and comprises a linear polymer of glucopyranose molecules linked by β-1-4 glycosidic linkages that have alternating orientations (Fig 1) making cellobiose the fundamental repeating unit (Mansfield *et al*., 1999). Cellulose microfibrils form interstrand hydrogen bonds that along with Van der Waals forces result in a highly crystalline structure. Glucan chains occur in hexagonal arrays of 36 (3 nm×5 nm width) with exceptionally high DPs (degrees of polymerization) (Ding and Himmel, 2006). Crystallinity is thought to influence biomassrecalcitrance and varies widely among plant cell walls from approximately 40–50%in plant cellulose to 65–80%in bacterial and algal cellulose (reviewed by Klemm *et al*., 2005). This crystalline form limits enzyme accessibility and, therefore, limits the efficiency of enzymatic hydrolysis. Cellulose hydrolysis is further limited by the intimate associations between cellulose, hemicellulose, pectin, and lignin (Brett and Waldren, 1996) that further reduces the accessibility of cellulase enzymes to the cellulose fibers. The hemicellulose fraction of lignocellulose represents a significant source of mostly pentose sugars that are potentially important value-added products for fermentation to biofuels.

HEMICELLULOSE

Hemicelluloses are non-cellulosic polysaccharides and they are found in plant tissues (Woodward, 1984). Hemicelluloses constitute 20–30% of the biomass of dicotyledonous plants, such as trees, up to 50%for some tissues of monocotyledonous plants, and approximately 25% of the available biomass of the bioenergy-specific crops, Miscanthus, switchgrass, fescue and fibre sorghum (Timell, 1964). It is hydrogen-bonded to itself as well as to cellulose and this is thought to stabilize the cell wall matrix and render it insoluble to water. It is also bonded to lignin through ferulic acid residues that covalently link lignin to the arabinosyl and 4-O-methyl glucuronyl residues of hemicellulose, further enhancing the stability of the cell wall (Linden *et al*., 1994) (Fig 1).

Hemicellulose composition varies with plant species and tissue type and it can be classified into four major groups (Mohnen *et al*., 2008) based on polysaccharide composition (Ebringerova *et al*., 2005). (i) Mannans comprise galactomannan, glucomannan and galactoglucomannan. Galactomannans have β-1,4-mannose backbones with α-1,6-galactose branches; glucomannans contain both mannose and D-glucose β-1,4-linked backbones; and galactoglucomannans have β-1,4-mannose and β-1,4-glucose backbones with α-1,6-galactose branches attached to the mannose backbone. For example, the secondary cell walls of conifers (i.e. softwoods) consist of galactoglucomannan [10–30% (w/w)]. (ii) Mixed-linkage glucans comprise a backbone of D-glucose residues having both β-1,3 and β-1,4 linkages. For example, the primary cell walls of grasses contain 2–15% (w/w) of mixed-linkage glucans. (iii) Xylans have β-1,4-linked D-xylose backbones that may include arabinan and glucuronic acid side chains. For example, in grasses, the primary cell walls contain 20–40% (w/w) glucuronoarabinoxylan, whereas the secondary cell walls contain 40–50% (w/w)

glucuronoarabinoxylan. In dicots (e.g. hardwoods), the secondary cell walls contain 20–30% glucuronoxylan. (iv) Xyloglucan has a *β*-1,4-glucan backbone with xylose-containing branches that can contain other monosaccharide substitutions, such as galactose, arabinose and fucose. For example, the primary cell walls of conifers (i.e. softwoods) contain 10% (w/w) xyloglucans and the primary cell walls of dicots (e.g. hardwoods) contain 20–25% (w/w).

STRUCTURE AND OCCURRENCE OF XYLAN

Hemicelluloses that are based on a xylose backbone, regardless of source, are termed xylans (Linden *et al*., 1994). Plant cell walls contain xylan as the most abundant hemicellulosic polysaccharide that represents more than 30% of the dry weight (Joseleau *et al*., 1992). Xylan has a variable structure ranging from linear 1, 4-β-linked poly-xylose chains to highly branched hetero-polysaccharides (Bouveng, 1961). These substituents include α-L-arabinose and α-D glucuronic acid residues, the 4-O methyl ester derivative of α-D glucuronic acid, cinnamate-based esters, some short oligosaccharides and acetyl esters and they are attached to the number 2 and 3 hydroxyl (Linden *et al*., 1994). The α-L-arabinose is linked to the O-3 positions of the D-xylose residue and the α-D glucuronic acid or 4-O methyl ester derivative of α-D glucuronic acid is linked to the O-2 position (Biely, 1985; Linden *et al*., 1994). The degree of branching or the proportions of the various residues varies greatly depending on the source of the plant tissue and this has a major influence on the solubility and functionality of the xylan (Biely, 1985; Linden *et al*., 1994; Dodd & Cann, 2009). The more substituted xylans cannot self-hydrogen bond, and become more water soluble. Xylans substituted to a low degree hydrogen bond not only to themselves, rendering them insoluble, but also to cellulose, screening it from degradation

while highly substituted xylans do not hydrogen bond to cellulose very well and may have only a limited protective effect against cellulose degradation (Linden *et al*., 1994). Several hardwood xylans are acetylated; e.g., birch xylan contains >1 mol of acetic acid per mol of D-xylose (Biely 1985). Acetylation occurs mostly at the *O*-3 than the *O*-2 position and acetylation at both positions has been reported (Bouveng 1961).

Xylan being the major hemicellulose component in plant cell walls (Biely, 1985; Saha 2003; Yeoman *et al*., 2010) can vary dramatically in composition, with the major classes including homoxylans, glucuronoxylan, arabinoxylan, and glucuronoarabinoxylan (Dodd and Cann, 2009; Yeoman *et al*., 2010). The xylan polymer comprises of a linear backbone of *β*-1, 4-D-xylopyranoside residues that are commonly substituted by acetyl, arabinofuranosyl, and 4-*O*-methyl-glucuronyl groups (Yeoman *et al*., 2010). The proportions of the various residues vary greatly depending on the source of the plant tissue (Dodd and Cann, 2009). The architecture becomes more complex with the various hemicellulose components forming intimate interactions with each other as well as plant cell wall cellulose and pectin (Marcus *et al*., 2008). In this respect, optimizing the enzymatic conversion of lignocellulose to fermentable sugars must take into account hemicellulose depolymerization (Yeoman *et al*., 2010). In addition, hemicellulose can account for 37–48% of a plant's primary cell wall (Chesson *et al.*, 1986) and represents an abundant and exploitable source of pentose sugars (Yeoman *et al*., 2010).

OTHERS

Lignin is a complex, variable, hydrophobic, cross-linked, three-dimensional aromatic polymer of *p*-hydroxyphenylpropanoid units connected by C–C and C–O–C links (Lee, 1997). Lignin accounts for 15–30% dry weight of lignocellulose, in which it forms a matrix that is closely associated with the cellulose filaments, and is covalently attached to hemicelluloses. Lignin is formed by radical polymerisation of guaiacyl (G) units from precursor coniferyl alcohol, syringyl (S) units from precursor sinapyl alcohol, and *p*-hydroxyphenyl (H) units from precursor *p*-coumaryl alcohol (Faix, 1991). This polyphenolic compound is essential for the growth of land plants because it provides mechanical support to the whole plant and is responsible for the hydrophobic proprieties of water-conducting cells in the xylem. Although beneficial for plants, the presence of lignin increases the industrial processing costs for cell wall deconstruction (Vanholme *et al*., 2010). Most pretreatments do not extensively degrade lignin because of the nature of its linkages. Studies on lignin-reduced mutants of alfalfa and sorghum plants have demonstrated that lower lignin content is positively correlated with enzymatic digestibility following pretreatment (Chen and Dixon, 2007; Dien *et al*.,2009).

Pectin is a complex heteropolysaccharide that hydrates and further cements the primary cell wall matrix and accounts for 30–40% of non-cellulosic polysaccharides in the primary cell walls of herbaceous dicotyledons and non-graminaceous monocots with significantly lesser amounts found in grasses, woody tissue and secondary cell walls (Vogel and Jung, 2001; Mohnen, 2008). Various pectic polysaccharides can be detected in the cell wall, including homogalacturonan (HG), xylogalacturonan (XGA), apiogalacturonan, rhamnogalacturonan I (RGI), and rhamnogalacturonan II (RGII) (Harholt *et al*., 2010). HG is considered the most abundant pectic polysaccharide in plant cell walls, accounting for greater than 60% of the total pectin amount (Cafall and Mohnen, 2009).The primary roles of cell walls are to give physical

strength to the plant and to provide a barrier against the outside environment. The main role of pectin is to participate in these two functions together with the other polymers (Harholt *et al*., 2010)

ANAEROBIC THERMOPHILES

A number of thermophilic anaerobes have been shown to utilize cellulose for growth. These include *Clostridium thermocellum*, *Clostridium Stercorarium* and *Caldicellulosiruptor saccharolyticus, Thermoanaerobacterium bryantii* (Madden**,** 1983; Freier *et al*., 1988; Rainey *et al*., 1994, Stroot *et al*., unpublished) and *Caldicellulosiruptor bescii* was isolated from a hot spring in the Valley of Geysers (Russia) (Svetlichiny et al, 1990).

CALDICELLULOSIRUPTOR BESCII

C. bescii grows at temperatures up to 90°C and is the most thermophilic bacterium capable of growth on crystalline cellulose with an optimum temperature of 80°C (Yang et al, 2009). It also utilizes xylan, pectin and starch and is also able to grow efficiently on untreated plant biomass (Yang *et al*., 2009; Svetlichiny *et al*., 1990). The bacterium is capable of using cellulose and xylan simultaneously. It's potential to degrade plant cell wall and its end products composed of glucose and xylose make *it* an important microorganism not only in the study of biomass deconstruction, but also for industrial development of ethanol and other biofuels (Yang *et al*, 2009).

THERMOANAEROBACTERIUM BRYANTII

The cells of the type strain mel9^T of *Thermoanaerobacterium bryantii* isolated from corn cannin waste are straight rods, Gram negative, and motile by peritrichously arranged flagella (Stroot *et al*., unpublished). They occur in singles or pairs and grow under anaerobic conditions. The cultures are catalase negative and nitrate is not reduced. Indole is not produced. Thiosulfate is reduced to sulfide. Sulfate and sulfur are not reduced. The optimum temperature is 62 - 65 °C and the upper limit is 69 °C. Growth does not occur at 37 °C or 75 °C. The optimum pH occurs at 6·8-7·0. The doubling time is 60 min. The cells utilize the following as sole carbon and energy sources: glucose, galactose, lactose, maltose, mannose, sucrose, trehalose, xylose, cellobiose, raffinose, melibiose, dextrin and maltodextrin. The end products of fermentation on a minimal medium with 1 % (w/v) glucose as the carbon source are butyrate (24 mM), acetate (10 mM), ethanol (14 mM), and butanol (2·7 mM). The G+C content is 37·7% (Stroot *et al*; unpublished).

THERMOSTABLE HEMICELLULASES

Hemicellulose is a highly branched mixture of complex polysaccharides, including xylans, glucans, xyloglucans, callose, mannans, and glucomannans (Yeoman *et al*., 2010). Xylan comprising a complex mixture of polysaccharides is laden with numerous types of glycoside linkages and therefore requires the synergistic action of a complex set of enzymes for its complete hydrolysis (Yeoman *et al*., 2010). These include endo-β-1, 4-xylanases and β-D-xylosidases acting on the backbone and also debranching enzymes such as α-L-arabinofuranosidases, α-glucuronidases, and esterases (Dodd and Cann, 2009) (Fig 2).

XYLANASES

Almost all xylanases that have been described to date are endo-acting; to our knowledge only two bacteria have been reported to produce exo-acting xylanases, in both cases these enzymes were mesophilic (Gasparic *et al*., 1995; Kubata *et al*., 1994, 1995).

ENDO-1, 4-B-XYLANASE

One of the critically important enzymatic activities required for the depolymerization of xylans is endo-1, 4-*β*-xylanase (xylanase) activity (Dodd and Cann, 2009). Xylanases have been classified into GH families 5, 7, 8, 10, 11, and 43 on the basis of their amino acid sequences, structural folds, and mechanisms for catalysis (Cantarel *et al*., 2009). Xylanases catalyze the endo-hydrolysis of 1,4-β-D-xylosidic linkages in a seemingly random fashion, although more recent evidence would suggest the cleavage sites used by GH10 and GH11 enzymes are

influenced by side chain substituents (Dodd and Cann, 2009; Kolenova *et al*., 2006; Maslen *et al*., 2007). Xylanases have long been utilized in the, food, paper, and fine chemical industries and are well recognized as critical components in the deconstruction of lignocellulose for biofuels production (Garcia-Aparicio *et al*., 2007). Crystal structures have been solved for numerous xylanases from GH families 10 and 11 (Manikandan *et al*., 2005), with GH family 10 xylanases forming a (β/α)8 TIM-barrel fold and GH family 11 enzymes largely consisting of β-sheets (Yeoman *et al*., 2010). GH10 and GH11 xylanases represent the best studied xylanase families and they differ in the number of subsites they possess, with GH10 having four or five subsites (Biely *et al*., 1981, 1997b; Derewenda *et al*., 1994) and GH11 having at least seven subsites (Vrsanska *et al*., 1982; Bray & Clarke, 1992). Despite these inherent differences xylanase-mediated catalysis from both families occurs via a retention mechanism (Henrissat and Davies, 1997) with two glutamate residues, one acting as the proton donor, and the other acting as a catalytic nucleophile (CAZy; http://www.cazy.org/). Using commercially available non-decorated xylo-oligosaccharide substrates to assess xylanase activity is convenient. However, the results provide only limited information since the substrates do not represent the natural xylan substrates that these enzymes would encounter in the deconstruction of plant cell walls (Dodd and Cann, 2009). A recent study assessed the activity of several GH10 and GH11 proteins with purified xylo-oligosaccharides substituted with MeGA and revealed that GH10 enzymes cleave xylan chains when 4-O-methyl α-glucuronic acid (MeGA) is linked to xylose at the +1 subsite, whereas GH11 enzymes cleave xylan when MeGA is appended at the +2 subsite (Kolenova *et al*., 2006). These results suggest that GH10 enzymes are able to hydrolyze xylose linkages closer to side chain residues and thus help to explain why GH10 enzymes release shorter products than GH11 enzymes when incubated with arabinoglucuronoxylan substrates (Biely *et al*., 1997b).

Xylan side chain decorations are recognized by endo-xylanases, and the degree of substitution in xylan will influence the products of hydrolysis for xylanases (Dodd and Cann, 2009).

XYLOSIDASES

Xylan-1,4-*β*-xylosidase (*β*-xylosidase) enzymes release xylose monomers from the non-reducing end of xylo-oligosaccharides (Dodd and Cann, 2009). *β*- Xylosidases occur in five different GH families (GH 3, 39, 43, 52, and 54) (Henrissat, 1991) and their reaction mechanisms result either in inversion (GH 43) or retention (GH 3, 39, 52, and 54) of stereochemical configuration at the anomeric carbon (Dodd and Cann, 2009). The most abundant and best characterized *β*- xylosidases are from GH3 and GH43 (Sunna & Antranikian, 1997). For those families that structural information has been determined or inferred, the common structural conformation exhibited is a (β/α)8 fold (families 30, 39, and 51), although GH family 43 enzymes form a fivefold β-propeller (Yeoman *et al*., 2010). The catalytic residues for GH families 30, 39, and 51 comprise a pair of glutamate amino acids, while family 52 enzymes utilize a glutamate residue as the catalytic nucleophile and an aspartate as the proton donor (Bravman *et al*., 2001; Czjzek *et al*., 2005; Zverlov *et al*., 1998b; CAZy; http://www.cazy.org/). β-D-xylosidases are important in the relief of end-product inhibition of xylanases caused by xylobiose and the performance of β-xylosidases is typically inhibited by increasing concentrations of their end-product, xylose (Yeoman *et al*., 2010). Interestingly, a thermophilic β-xylosidase from the fungus *Scytalidium thermophilum* was, however, found to be immune to xylose-mediated inhibition (Zanoelo *et al*., 2004).

GLUCURONIDASES

Xylose residues within arabinoglucuronoxylan may be substituted at *O*-2 with 4-O-methyl α-glucuronic acid (Dodd and Cann, 2009). α-Glucuronidases catalyze the cleavage of the α-1,2-glycosidic bond between 4-O-methyl α-glucuronic acid and the terminal nonreducing end xylopyranosyl unit of small xylo-oligosaccharides (Mierzwa *et al*., 2005; Sunna and Antranikan, 1997; Puls *et al*., 1987). The substrate specificity of α-glucuronidases differ depending on the enzyme source (Sunna and Antranikian, 1997). The enzymes from *Agaricus bisporus* and **S. olivochromogenes* require a low-molecular weight glucuronoxylan substrate (Puls *et al*., 1987; Johnson *et al*., 1989). They release 4-O-methyl α-glucuronic acid from 4-0-methylglucuronose-substituted xylo-oligomers, but not from the polymer (Puls *et al*., 1987). They however have a negligible activity on polymeric xylan and *para*-nitrophenyl α-D-glucuronopyranoside, although interestingly, a thermostable α-glucuronidase from the bacterium *Thermotoga maritima* was found to hydrolyze *para*-nitrophenyl α-D-glucuronopyranoside, with an optimum temperature of 80°C (Suresh *et al*., 2003). These enzymes utilize an inverting mechanism for catalysis, and although the proton-donating residue is known to be a glutamate, the nucleophile has yet to be determined (Biely *et al*., 2000; CAZy; http://www.cazy.org/). Relatively few thermostable α-glucuronidases have been described compared to other lignocellulosic enzymes. Both the fungi *Aureobasidium pullulans* and *Thermoascus aurantiacus* produce α-glucuronidases, each with optimal catalytic activity at 65°C (Khandke *et al*., 1989).

α-L-ARABINOFURANOSIDASES

In contrast to α-L-arabinanases, α-L-arabinofuranosidases are exo-acting enzymes that hydrolyze terminal α-1,5-glycosidic linkages to arabinofuranosides in arabinan as well as α-1,2 and α-1,3-linkages to arabinofuranosides of arabinan, arabinoxylan, and arabinogalactan (Matsuo *et al*., 2000). Arabinofuranosidases are classified into five GH families: 3, 43, 51, 54, and 62 (CAZy; http://www.cazy.org/). These enzymes work synergistically with other hemicellulolytic enzymes removing L-arabinose side chains that would otherwise restrict the activity of the backbone-degrading enzymes (Yeoman *et al*., 2010). The production of arabinofuranosidase in several actinomycetes seems to be induced, among others, by arabinan, xylan, and wheat bran (Mackenzie *et al*., 1987; Zimmermann *et al*., 1988). Similarly, several rumen bacterial isolates investigated by Williams and Whithers (1982) showed high levels of arabinofuranosidase activity when grown in the presence of arabinose or arabinose-containing polysaccharides. On the other hand, only low levels of arabinofuranosidase activities were detected when the isolates were grown with glucose or cellobiose as substrate. An arabinofuranosidase from *Aspergillus awamori* was purified and this 1, 4-β-D-arabinoxylan arabinofuranohydrolase is highly specific for arabinoxylans and is able to release only arabinose from arabinoxylan (Kormelink *et al*., 1991a). During the arabinose release, the xylan backbone is not degraded and there is no production of xylo-oligosaccharides. The enzyme is not active toward α-L-1,3- or α-l,5-linked arabinose from arabinans, arabinogalactans, or *para*-nitrophenyl-α-L-arabinofuranoside (Kormelink *et al*., 199 la, b).

ACETYL XYLAN ESTERASES

Plant cell wall polysaccharides, particularly those comprising the hemicellulose fraction, such as xylans, mannans, and glucomannans, as well as pectin, are commonly acetylated and on occasion feruloylated, with O-bound acetyl groups comprising up to 7% of plant cell walls by dry weight (Brett and Waldren, 1996). Xylans, the major hemicellulosic component, in particular, are typically rich in acetyl and 4-O-methyl substituents in the β-1,4-linked backbone. In fact studies of hardwood xylans suggest that as much as 60–70% of xylose residues are esterified with acetic acid. Acetylated xylans are also common to perennial plants (Biely *et al*., 1986, Shao and Wiegel, 1995). A high degree of xylan acetylation increases the solubility of xylan by preventing inter-chain hydrogen bond (Poutanen *et al*., 1990). This has however been overlooked in most microbial xylan degradation studies (Biely 1985). Acetylxylan esterases (EC 3.1.1.6) remove the 0-acetyl substituents at the C-2 and C-3 positions of xylose residues in acetylxylan (Sunna and Antranikian, 1997; Biely 2003).

THERMOSTABLE CELLULASES

Cellulose-degrading enzymes are widespread in nature and are predominantly produced by microorganisms such as bacteria, archaea, and fungi that harvest energy from decaying plant matter (Yeoman *et al*., 2010). These microorganisms can be aerobic, anaerobic, mesophilic or thermophilic. Efficient cellulose hydrolysis requires the concerted action of three different classes of enzymes, including endoglucanases and exoglucanases that operate at the solid: liquid interface and β-glucosidases that operate on the soluble degradation products of cellulose (Yeoman *et al*., 2010).

ENDOGLUCANASES

Endo-1,4-β-D-glucanases help speed up the cellulolytic process, acting synergistically with cellobiohydrolases (CBHs). In the cellulolytic deconstruction of cellulose, endoglucanases attack the cellulose polymer in a random manner, disrupting the regular crystalline nature of the substrate (Yeoman *et al*., 2010).

EXOGLUCANASES

β-1,4-Exoglucanases or cellobiohydrolases (CBHs) are of significant importance to cellulolytic systems, facilitating the production of mostly cellobiose that can readily be converted to glucose by β-glucosidases (Yeoman *et al*., 2010). For biotechnological applications, enzymes exhibiting broad substrate specificity are desirable. In this regard, two CBHs have been isolated from *C. thermocellum* that were found to cleave lichenan, xylan, and para-nitrophenyl derivatives of cellobiose and lactopyranose in addition to CMC (Tuka *et al*., 1990).

To date, the most thermostable CBH has been isolated from the culture supernatant of the thermophilic bacterium *Thermotoga sp*. strain FjSS3-B1. The enzyme has maximal activity at 105°C and maintains a half-life of 70 min at 108°C (Ruttersmith and Daniel, 1991).

β-GLUCOSIDASES

β-glucosidases (EC 3.2.1.21) and β-galactosidases (EC 3.2.1.23) constitute a major group among glycosyl hydrolase families which hydrolyze terminal non-reducing β-D-glucose and β- D-galactose respectively in oligosaccharides and glycoconjugates. The β-glucosidases fall predominantly in GH1, GH3, GH9, GH30 and GH116 families, while β-galactosidase in

GH1, GH2, GH35 and GH42 (Canteral *et al*., 2009). β-Glucosidase enzymes are responsible for the hydrolysis of b-glucosidic linkages in aryl-, amino-, or alkyl-b-D-glucosides, cyanogenic glucosides, and oligo- or disaccharides (Yeoman *et al*., 2010). In the enzymatic hydrolysis of cellulose, β-glucosidases hydrolyze cellobiose to free glucose molecules after it has been degraded to cellobiose by endoglucanases and exoglucanases.

CHAPTER III:

BIOCHEMICAL ANALYSIS OF THERMOSTABLE HEMICELLULASES FROM *THERMOANAEROBACTERIUM BRYANTII*

ABSTRACT

Thermoanaerobacterium bryantii is capable of metabolizing hemicellulose and cellulose, the major components of the plant cell wall. The enzymes that allow this bacterium to capture energy from the two polysaccharides, therefore, have potential application in plant cell wall depolymerization, a process critical to biofuel production. For this purpose, a genome sequence of *T. bryantii* was generated. The genomic data depicted a bacterium endowed with multiple forms of plant cell wall-degrading enzymes. A hemicellulase gene cluster encoding genes predicted to have endoxylanase activity, β-xylosidase activity, α-glucoronidase activity, acetyl xylan esterase activity as well as oxido-reductase activity was isolated for further studies. We hypothesized that the endoxylanase should work synergistically with the other accessory enzymes in the cluster to breakdown xylan releasing mainly xylose for the utilization of the organism.

To test this hypothesis, the gene encoding the predicted endoxylanase was expressed, and the protein was biochemically characterized either alone or in combination with accessory enzymes. The endoxylanase was able to hydrolyze a number of xylan containing polysaccharides releasing xylo-oligosaccharides with the β-xylosidases converting the oligosaccharides released to xylose. The β-xylosidases were also able to convert the xylo-oligosaccharides released from aldouronic acids by the α-glucuronidase to xylose.

INTRODUCTION

Plant biomass represents the lignocellulosic materials that comprise the cell walls of plants. They are the most abundant source of carbohydrate in the world (Linden *et al*., 1994). The most abundant polysaccharide is cellulose followed by hemicellulose and then pectin (Linden *et al*., 1994). Xylan is the most abundant hemicellulosic polysaccharide in plant cell walls. It represents more than 30% of the dry weight of the plant cell wall (Joseleau *et al*., 1992). Cellulose is a highly homogeneous polymer and it consists of *β*-1, 4-linked glucose units, that make interstrand hydrogen bonds to form a highly stable crystalline lattice (Laureano-Perez *et al.,* 2005). Xylan, on the other hand, is a heteropolymeric and consists predominantly of the pentose sugars arabinose and xylose, although it may also contain glucuronyl, feruloyl, and acetyl groups (Ebringerova & Heinze, 2000). The utilization of hemicellulose and lignin, in addition to cellulose, may greatly improve the productivity and yield of fuels from biomass (Linden *et al*., 1994). The use of biofuels provides a means to reduce the dependence on fossil fuels as well as a reduction in global emission of greenhouse gases into the environment (Lynd *et al*., 1991). Of the many bioenergy feedstocks, switchgrass and *Miscanthus* are expected to become significant substrates in the future for bioconversion to bioethanol (Somerville *et al*., 2010).

Thermoanaerobacterium bryantii is a thermophilic anaerobe that was isolated from corn canning waste. This organism was found to have cells that are straight rods, Gram negative and motile by peritrichously arranged flagella. The optimum temperature is 62 - 65 °C and the upper limit is 69 °C. A hemicellulase gene cluster from this organism was studied. As expected the only endoxylanase in the cluster was able to hydrolyze a number of xylan containing polysaccharides releasing xylo-oligosaccharides that were further hydrolyzed by β-xylosidases to xylose. The

endoxylanases were also able to convert the xylobiose released from aldouronic acids by the α-glucuronidase to xylose.

MATERIALS AND METHODS

MATERIALS

Thermoanaerobacterium bryantii was obtained from our culture collection housed at the Department of Animal Sciences, University of Illinois at Urbana-Champaign. The culture was stored on maintenance slants in liquid nitrogen vapor at 105°C (XLC1110; MVE Cryogenics). The clones of all recombinant proteins used were obtained from Xiaoyun Su, a member of the Cann lab. The Talon Metal Affinity Resin was purchased from Clontech Laboratories, Inc. (Mountain View, CA). Amicon Ultra-15 centrifugal filter units with 10,000 MWCO and 50,000 MWCO were obtained from Millipore (Billerica, MA). Xylo-oligosaccharides, cello-oligosaccharides, aldouronic acids, oat spelt xylan, larch wood xylan, rye arabino xylan, birch wood xylan, xyloglucan and wheat arabinoxylan (WAX) (medium viscosity, 20 centistokes) were obtained from Megazyme (Bray, Ireland). Gel filtration standards were obtained from Bio-Rad (Hercules, CA). All other reagents were of the highest possible purity and were purchased from Sigma-Aldrich (St. Louis, MO).

PURIFICATION OF Tb888, Tb882, Tb884, Tb887, Tb881, Tb885 AND Tb886

Clones of the various gene products were obtained from Xiaoyun Su, a member of the Cann lab. The resulting plasmid constructs were introduced into *E. coli* BL-21 CodonPlus (DE3)

RIL competent cells by heat shock, and grown overnight in lysogeny broth (Bertani, 2004; Bertani 1951) (LB) (10mL) supplemented with ampicillin (100μg/mL) and chloramphenicol (50μg/mL) at 37°C with aeration. After 6 h, the starter cultures were diluted into fresh LB (1 L) supplemented with ampicillin and chloramphenicol and cultured at 37°C with aeration until the optical density at 600 nm reached 0.3. The culture was then incubated at 16°C with aeration and protein expression was induced by the addition of isopropyl β-D-thiogalactopyranoside (IPTG) at a final concentration of 0.1mM. After 16 h, the cells were harvested by centrifugation (4000 x g, 15 min, 4°C), re-suspended in 35mL lysis buffer (50mM sodium phosphate, 300mM NaCl, pH 7.5), and the cells were ruptured by two passages through a French pressure cell (American Instrument Company Inc., Silver Spring, MD). The cell lysate was then clarified by centrifugation at 30,000 x g for 30 min at 4°C and purified utilizing TALON® Polyhistidine-Tag Purification Resin from Clontech (Mountain View, CA) as described by the manufacturer. Aliquots of eluted fractions were analyzed by sodium dodecyl sulfate-polyacrylamide gel electrophoresis (SDS-PAGE) using the method described by Laemmli (Laemmli, 1970) and protein bands were visualized by staining with Coomassie brilliant blue G-250. Elution fractions were pooled and dialyzed against storage buffer and assays were performed immediately. The protein concentrations were quantified by absorbance spectroscopy according to methods described previously by Gill and von Hippel (21), with the following extinction coefficients: 67,840$M^{-1}cm^{-1}$, 99,490$M^{-1}cm^{-1}$, 125,055$M^{-1}cm^{-1}$, 128,160$M^{-1}cm^{-1}$, 39,100$M^{-1}cm^{-1}$, 50,435$M^{-1}cm^{-1}$ and 59,610$M^{-1}cm^{-1}$ for Tb888, Tb882, Tb884, Tb887 Tb881, Tb885 and Tb886 respectively. The absorbance value for each protein solution was measured at 280 nm with a NanoDrop 1000 apparatus from Thermo Fisher Scientific Inc. (Waltham, MA).

EVALUATION OF XYLANASE ACTIVITY OF Tb888 ON AGAR PLATES

Enzyme-catalyzed hydrolysis of plant cell wall polysaccharides was evaluated by spotting purified Tb888 (0.25µM, 0.5µM, 1µM and 2µM) onto agar plates (0.8%) containing oat spelt xylan (0.5%), or pectin (0.5%). The plates were incubated at 60 °C for 16 hours followed by staining with Congo red (0.1%) for 5 minutes and then destained with 1M NaCl (Teather et al, 1982). This was done by Xiaoyun Su.

HYDROLYSIS ON MODEL XYLANS BY Tb888

Tb888 (50nM final concentration) was incubated with each of the above substrates (1% wt/vol, final concentration) in citrate buffer (50 mM sodium citrate, 150 mM NaCl, pH 5.5) at 60 °C for 9mins with aliquots taken at every 3mins intervals. The concentration of released reducing ends was estimated using the para-hydroxybenzoic acid hydrazide (PAHBAH) assay as described previously (Lever, 1972) with xylose as the standard. For qualitative analysis, the incubation was carried out for 16 hours in citrate buffer (50 mM sodium citrate, 150 mM NaCl, pH 5.5) at 60 °C with 25nM final enzyme concentration of Tb888. The hydrolysis products were resolved by thin layer chromatography (TLC). Following incubation at 60 °C for 16h, hydrolysis products were centrifuged for 10 min and spotted onto a DC-Plastikfolien Silica Gel 60 F254 TLC plate from Merck (Whitehouse Station, NJ) to resolve the products using monomeric xylose (X1) and xylo-oligosaccharides (X2-X6) (25 µg each) as standards. The mobile phase consisted of n-butanol: acetic acid:H_2O, 10:5:1 (vol/vol/vol) and 20cm x 10cm TLC plates were used. The products were then visualized by spraying the plates with a 1:1 (v/v) mixture of methanolic orcinol (0.2% w/v) and sulfuric acid (20% v/v) followed by heating the plates at 65 °C for 10 min.

DETERMINATION OF OPTIMUM PH OF Tb888

Tb888 (25nM final concentration) was incubated with wheat arabino xylan (WAX) (1% wt/vol, final concentration) in citrate buffer (50 mM sodium citrate, 150 mM NaCl, pH 4.0-6.0) or phosphate buffer (50 mM sodium phosphate, 150 mM NaCl, pH 6.0-8.0) at 60 °C for 9mins with aliquots taken at every 3mins. The concentration of released reducing ends was estimated using the para-hydroxybenzoic acid hydrazide (PAHBAH) assay as described previously (Lever, 1972) with xylose as a standard. Specific activities of Tb888 at the different pH values were calculated from known concentrations of the standard (xylose). These were then plotted against their corresponding pH values to determine the optimum pH of Tb888.

DETERMINATION OF OPTIMUM TEMPERATURE OF Tb888

Tb888 (25nM final concentration) was incubated with wheat arabino xylan (WAX) (1% wt/vol, final concentration) in citrate buffer (50 mM sodium citrate, 150 mM NaCl, pH 5.5) at 60 °C for 9mins with aliquots taken at every 3mins. The concentration of reducing ends was estimated using the para-hydroxybenzoic acid hydrazide (PAHBAH) assay as described previously (Lever, 1972) with xylose as a standard. Specific activity of Tb888 at the different temperatures was calculated from known concentrations of the standard (xylose). The specific activities were then plotted against their corresponding temperatures to determine the optimum temperature of Tb888.

DETERMINATION OF SUBSTRATE SPECIFICITIES OF B-XYLOSIDASES (Tb882, AND Tb884) WITH PNP-LINKED SUGARS

The substrate specificities of Tb882, and Tb884 with *para*-nitrophenyl (*p*NP)-linked substrates were assayed using a thermostated Cary 300 UV-visible spectrophotometer from Varian Inc. (Palo Alto, CA). Fifteen different substrates from Sigma-Aldrich (St. Louis, MO) were screened: *p*NP-α-L-arabinopyranoside, *p*NP- α-L-arabinofuranoside, *p*NP-β-D-fucopyranoside, *p*NP-α-L-fucopyranoside, *p*NP-α-D-galactopyranoside, *p*NP-β-D-galactopyranoside, *p*NP-α-D-glucopyranoside, *p*NP-β-D-glucopyranoside, *p*NP-β-D-maltopyranoside, *p*NP-α-D-maltopyranoside, *p*NP-α-D-mannopyranoside, *p*NP-β-D-mannopyranoside, *p*NP-α-L-rhamnopyranoside, *p*NP-β-D-xylopyranoside, and *p*NP-β-D-cellobioside. The different *p*NP substrates (2.0 mM, final concentration) were incubated at 50°C in the presence or absence of Tb882, and Tb884 (50nM, final concentration) in a buffer composed of 50 mM Na-citrate buffer and 150 mM NaCl (pH 5.5) for 30 min, and the rate of *p*NP release was determined by monitoring the absorbance at 400 nm continuously.

DETERMINATION OF OPTIMUM pH VALUES FOR Tb882 AND Tb884

To determine the optimum pH values of Tb882 and Tb884, *p*NP-β-D-xylopyranoside (2.0mM final concentration) was prepared in citrate buffer (50mM Na-citrate with 150mM NaCl, pH 4.0-6.0) or phosphate buffer (50mM Na-phosphate with 150mM NaCl, pH 6.0-8.0). The data was collected using Cary 300 UV-Vis spectrophotometer (Varian). Each reaction was initiated by adding 25µl of Tb882 (50nM final concentration) or Tb884 (5nM final concentration) to 100µl of the substrate and mixed by pipetting up and down several times at 60 ºC. The release of

*p*NP was continuously monitored by recording the UV signal at 400 nm for 5 minutes. Each experiment was carried out in triplicate. Initial velocities of the enzyme-catalyzed reactions were obtained by adjusting the protein concentrations such that the slopes of the resulting progress curves (change in absorbance per unit of time) were linear. Initial rate obtained at each pH was converted to relative activity and plotted against pH using GraphPad Prism v5.02 from GraphPad Software (San Diego, CA). The extinction coefficient for *para*-nitrophenol at pH 5.5 and at a wavelength of 400 nm was measured to be 0.673 mM^{-1} cm^{-1}**.**

DETERMINATION OF OPTIMUM TEMPERATURE VALUES FOR Tb882 AND Tb884

To determine the optimum temperatures of Tb882 and Tb884, *p*NP-β-D-xylopyranoside (2.0mM final concentration) was prepared in citrate buffer (50mM Na-citrate with 150mM NaCl, pH 6.0 (Tb882) or pH 5.5 (Tb884)). The data was collected using Cary 300 UV-Vis spectrophotometer (Varian). Each reaction was initiated by adding 25µl of Tb882 (50nM final concentration) or Tb884 (5nM final concentration) to 100µl of the substrate and mixed by pipetting up and down several times at various temperatures ranging from 40°C to 95 ºC. The release of *p*NP was continuously monitored by recording the UV signal at 400 nm for 5 minutes. Each experiment was carried out in triplicate. Initial velocities of the enzyme-catalyzed reactions were obtained by adjusting the protein concentrations such that the slopes of the resulting progress curves (change in absorbance per unit of time) were linear. Initial rate obtained at each temperature was converted to relative activity and plotted against temperature using GraphPad Prism v5.02 from GraphPad Software (San Diego, CA). The extinction coefficient for *para*-nitrophenol at pH 5.5 and at a wavelength of 400 nm was measured to be 0.673 mM^{-1} cm^{-1}.

HYDROLYSIS OF XYLO-OLIGOSACCHARIDES BY Tb882 AND Tb884

The capacity of Tb882 and Tb884 to hydrolyze xylo-oligosaccharides was assessed by resolving and detecting the hydrolysis products utilizing thin layer chromatography (TLC). Initial biochemical studies had revealed that the optimum pH for activity of Tb882, and Tb884 were 6.0 and 5.5, respectively. Thus, for measuring the hydrolysis of xylo-oligosaccharides, reaction mixtures (10 μl) were prepared in citrate buffer (50mM sodium phosphate, 150mM NaCl, pH 6.0 (Tb882) or pH 5.5 (Tb884)) with X1-X6 (20mM) and reactions were initiated by the addition of Tb882 and Tb884 (2μM, final concentration). Following incubation at 60 °C for 16h, hydrolysis products were centrifuged at 30,000 x g for 10mins and spotted onto a DC-Plastikfolien Silica Gel 60 F254 TLC plate from Merck (Whitehouse Station, NJ) to resolve the products as described above.

STEADY-STATE KINETIC PARAMETERS OF Tb888, Tb882 AND Tb884

For the steady kinetic study of Tb888, 25nM final concentration of Tb888 was incubated with various concentrations (0-50mg/ml) of BWX or LWX prepared in citrate buffer (50mM Na-citrate with 150mM NaCl, pH 5.5) at 60°C for 9mins with aliquots taken every 3mins. The concentration of reducing ends was estimated using the para-hydroxybenzoic acid hydrazide (PAHBAH) assay as described previously (Lever, 1972) with xylose as a standard. Kinetic studies of Tb882 and Tb884 proteins were performed using a Cary 300 UV-Vis spectrophotometer equipped with a circulating water bath from Varian Inc. (Palo Alto, CA). *p*NP-β-D-xylopyranoside (0-10 mM) was incubated in citrate buffer (50 mM sodium citrate, 150

mM NaCl, pH 6.0 (Tb882) or pH 5.5 (Tb884) in a 1 cm path-length quartz cuvette and reactions were initiated by the addition of Tb882 (50nM) or Tb884 (10nM). Hydrolysis of each *p*NP substrate was continuously monitored by recording the UV signal at 400 nm. The extinction coefficient for *para*-nitrophenol at pH 5.0 and a wavelength of 400 nm was measured as 319 M^{-1} cm^{-1}. Initial rate data were then plotted against the substrate concentration and kinetic values were estimated by applying a nonlinear curve fit using GraphPad Prism v5.01 from GraphPad Software (San Diego, CA).

HYDROLYSIS OF MODEL XYLANS BY Tb888, Tb882 AND Tb884

Each substrate (1% wt/vol, final concentration) was incubated alone or co-incubated with Tb888 (5nM final concentration) or Tb882 (50nM final concentration) or Tb884 (5nM final concentration) or all three enzymes in various combinations in citrate buffer (50 mM sodium citrate, 150 mM NaCl, pH 5.5) at 60 °C for 16 hours. The concentration of reducing ends was estimated using the *para*-hydroxybenzoic acid hydrazide (PAHBAH) assay as described previously (Lever, 1972) with xylose as a standard. For qualitative identification of the hydrolysis products, the reactions were resolved by thin layer chromatography (TLC). Following incubation at 60 °C for 16h, hydrolysis products were centrifuged for 10 min and spotted onto a DC-Plastikfolien Silica Gel 60 F254 TLC plate from Merck (Whitehouse Station, NJ) to resolve the products using monomeric xylose (X1) and xylo-oligosaccharides (X2-X6) as described above.

HYDROLYSIS OF ALDOURONIC ACID BY Tb887, TB882, Tb884 AND Tb888

The enzyme, Tb887 (final concentration of 0.5µM in 50 mM Na-citrate with 150 mM NaCl, pH 5.5) or Tb882, or Tb884 or Tb888 (final concentration of 50nM in 50 mM Na-citrate with 150 mM NaCl, pH 5.5), was incubated with the aldouronic acid mixture (final concentration of 1.0 mg/ml) at 60°C individually or together to determine their potential synergistic activity. After 1 h, the reactions were terminated by boiling for 10 min. The hydrolysis products were analyzed by thin layer chromatography as described above. Xylose and xylo-oligosaccharides (X2 to X6) were used as standards.

RESULTS

DOMAIN ARCHITECTURE OF FIVE XYLAN DEGRADING ENZYMES

Using a bioinformatics approach, glycoside hydrolase (GH) genes predicted to encode polysaccharide degrading enzymes in the genome of *Thermoanaerobacterium bryantii* were identified. A number of genes coding for putative glycoside hydrolases involved in xylan degradation were identified (Fig 4 and Table 1a) and expressed. The primers for cloning genes into pET46b are shown in Table 1b. A gene encoding a putative endoxylanase (ORF888) was identified and based on its amino acid sequence analysis was found to be composed of a single GH 10 catalytic domain (Fig 5A). Proteins with GH10 catalytic domain are known to have endo-1,4-β-xylanase (EC 3.2.1.8) or endo-1,3-β-xylanase (EC 3.2.1.32) activity. Two other genes encoding putative beta-xylosidase function were also identified; one composed of a single GH39 catalytic domain (ORF882) (Fig 5A) and the other encoding a single GH52 catalytic domain (ORF884) (Fig 2A). Known activities of the proteins with GH39 catalytic domain include; β-

xylosidase (EC 3.2.1.37), α-L-iduronidase (Hydrolysis of unsulfated α-L-iduronosidic linkages in dermatan sulfate) (EC 3.2.1.76); and those with GH52 catalytic domain are known to have mainly β-xylosidase (EC 3.2.1.37) activity. Each of these genes was expressed with an N-terminal hexa-histidine tag (6-His tag) in *E. coli* BL-21 CodonPlus RIPL cells to facilitate purification of the gene product. The putative endoxylanase protein degraded xylan during initial screening of multiple substrates. The initial screening of artificial substrates using the putative β-xylosidases revealed activity in two of these substrates. The enzymes were screened to determine whether they function synergistically to degrade xylan.

PURIFICATION OF A PUTATIVE ENDOXYLANASE AND ACCESSORY ENZYMES FROM *T. BRYANTII*

The product of each gene was expressed as a polypeptide with an N-terminal hexahistidine tag to facilitate protein purification. The predicted molecular masses of Tb888, Tb882, Tb884, Tb887, Tb881, Tb885 and Tb886 were 42.4, 60.2, 78.4, 79.3, 38.4, 48.9 and 45.5kDa respectively. These are in agreement with the sizes of the purified protein estimated by comparison with molecular weight markers through SDS-PAGE analysis (Fig 5B).

OPTIMAL TEMPERATURE AND pH VALUES OF A PUTATIVE ENDOXYLANASE AND ACCESSORY ENZYMES FROM *T. BRYANTII*

The optimal temperature values as determined for Tb888, Tb882 and Tb884 are shown in Fig 6 (A, C and E) respectively and the pH values are shown in Fig 6 (B, D and F) respectively.

Tb888 POSSESSES AN ENDO-XYLANASE ACTIVITY

To determine whether the putative endoxylanase possesses its predicted activity, it was spotted on agar plates containing oat spelt xylan (Fig 7A) and pectin (Fig 7B) and incubated for 16 hrs. A clear zone observed indicated activity on these plates. This result suggested a possible xylanase activity in this protein.

To confirm this possible xylanase activity, the enzyme was examined for release of products from six different xylan sources (Fig 7C). The substrates were soluble wheat arabinoxylan (WAX), oat spelt xylan (OSX), birch wood xylan (BWX), larch wood xylan (LWX), rye arabinoxylan (RAX) and xyloglucan (XGC). As shown in Fig 7D, Tb888 released products ranging from xylose (X1) to xylo-oligosaccharides of various lengths (X2 to X6) from all the substrates in exception of xyloglucan that has a backbone of β-1,4 glucose residues instead of the backbone of β-1,4 xylose residues in the other substrates.

Hydrolysis products of RAX showed the presence of products whose migration patterns were similar to xylobiose (X2), some amount of xylotriose (X3), xylotetraose (X4), xylopentaose (X5), xylohexaose (X6) and of xylose (X1). There was no migration similar to X6 detectable in the resolved products of OSX, LWX, WAX and BWX. No X5 was seen in the hydrolysis products of OSX. In all five substrates, a product with similar migration to X2 seems to be the main product.

ENZYMATIC ACTIVITIES OF ACCESSORY ENZYMES (Tb882 AND Tb884) FOR *p*NP HYDROLYSIS

Six different proteins were predicted to participate with endoxylanases to release fermentable sugars from xylans. These included two putative xylosidases (Tb882 and Tb884), two putative oxido-reductases (Tb885 and Tb886), a putative glucuronidase (Tb887) and a putative acetyl esterase xylanase (Tb881).

A screen of sixteen *p*NP substrates using both putative xylosidases resulted in the observation of activities in two of these substrates (*p*NP-α-L-arabinopyranoside and *p*NP-β-D-xylopyranoside) with both showing higher activity in the *p*NP-β-D-xylopyranoside (Fig 8A and 8B). Tb882 or Tb884 was each co-incubated with arabino- and xylo- oligosaccharides to confirm their xylosidase activity. Resolving the hydrolysis products on TLC showed the release of xylose as the only product from the xylo-oligosaccharides (X2 to X6) and some amount of X2 in the case of Tb882 (Fig 8C). Both enzymes however showed no activity on the arabino-oligosaccharides confirming that both enzymes are xylosidases and not arabinofuranosidases (data not shown). Co-incubation with xylose produced no long chain oligosaccharides, implying that each enzyme lacks transglycosylation, at least under the conditions tested in the present studies.

STEADY-STATE KINETIC STUDY OF Tb888, Tb882 AND Tb884

To determine the catalytic properties of these proteins, their steady-state kinetic parameters with the following substrates were determined. The substrates were LWX and BWX for Tb888 or *p*NP-xylopyranoside for Tb882 and Tb884. Initial rate data of Tb888, Tb882 and Tb884 were obtained for each of the substrate concentrations, and plots of the initial velocity of

substrate hydrolysis (nmol/s) versus substrate concentration (mM) were generated (Fig 9A, 9B, 9C and 9D). Tb888 exhibited a higher affinity for larch wood xylan with a K_m of 1.51 mg/ml and 2.87mg/ml for birch wood xylan (Table 2a). Tb884 always showed higher activity on all the substrates tested compared to Tb882. This was confirmed by the lower K_m of 0.38 ± 0.03 mM observed for Tb884 on pNP-xylopyranoside in comparison to the 1.29 ± 0.08 mM recorded for Tb882. Furthermore, Tb884 also showed a much higher catalytic efficiency of 394.97 s^{-1} mM^{-1} compared to the 51.21 s^{-1} mM^{-1} determined for Tb882. Table 2b shows a summary of the kinetic parameters.

SYNERGISTIC ACTIVITIES OF Tb888 WITH ACCESSORY ENZYMES (Tb882 AND Tb884) IN XYLAN HYDROLYSIS

The capacity of the Tb888 enzyme to function synergistically with the two β-xylosidases from *T. bryantii* was investigated (Fig 10A, 10B, 10C and 10D). TLC analysis of the hydrolysis products of Tb888 alone with RAX revealed the presence of mainly xylobiose (X2), some amount of xylotriose (X3), xylotetraose (X4), xylopentaose (X5), and a small amount of xylose (X1). Incubation of RAX with either Tb882 or Tb884 alone however yielded no xylose or xylo-oligosaccharides. Co-incubation of Tb888 with either Tb882 or Tb884 on the other hand resulted in an increased release of xylose with a concurrent decrease in the released amounts of the xylo-oligosaccharides especially in the presence of all three enzymes. The pattern of products released was similar to when the enzymes were co-incubated with WAX. However, no X6 was detected on the TLC plate from the hydrolysis of WAX and RAX in the presence of any of the enzymes. On co-incubation of BWX with either Tb882 or Tb884 alone, there was a slight amount of xylose released. Co-incubation of Tb888 and Tb882 with BWX did not seem to produce a lot

more xylose. However in the presence of Tb888 and Tb884 or Tb882 and Tb884, there was an increase in the release of xylose.

Hydrolysis of OSX produced almost no products similar to X5 and X6 with only a very small amount of X4 that was barely detectable when it was co-incubated with Tb888 and Tb882 or Tb884 or both. Resolved hydrolysis products of LWX showed no product migration similar to X6 in the presence of any of the proteins. Hydrolysis product from incubation with either Tb882 or Tb884 alone showed the release of a product with migration similar to xylose. Co-incubation of LWX with Tb888 and Tb882 or Tb884 or both showed a relative increase in the product whose migration was similar to xylose with a relative decrease in the amount of products migrating in similarity to xylo-oligosaccharides. The product with the same migration pattern as X3 was almost undetectable in the presence of Tb888 and Tb884 or all three enzymes.
On OSX, LWX and BWX, Tb882 was shown to release a product whose migration was not similar to the migration of any of the sugar standards on the TLC plate and was also not found from the hydrolysis of the three substrates by either Tb888 or Tb884. On co-incubation of each of the three substrates with the three enzymes however showed the disappearance of the unknown product. The two xylosidases (Tb882 and Tb884) clearly work synergistically with the xylanase (Tb888) to release mainly xylose from xylans. In some substrates (OSX, LWX and BWX) the unknown product seen from co-incubation with Tb888 and Tb882 is removed when the incubation is done in the presence Tb884. This shows that the two xylosidases are not redundant in their functions in the organism on different substrates.

Figure 11 (A-E) shows the resolved products of hydrolysis using HPLC. Quantifying the released xylobiose and xylose in each case, similar patterns as seen on the TLC plate were revealed. Tb882 or Tb884 work synergistically with Tb888 to release more xylose. In all cases,

co-incubating Tb888 with Tb884 released relatively more xylose than when it was co-incubated with Tbb882. The two β-xylosidases (Tb882 and Tb884) when incubated together with the xylanase (Tb888) released more xylose than when co-incubated with it individually.

HYDROLYSIS OF ALDOURONIC ACIDS BY Tb887, Tb882, Tb884 AND Tb888

The catalytic activity of the Tb887 was determined by its capacity to release xylo-oligosaccharides from aldouronic acids and also to function synergistically with β-xylosidases (Tb882 and Tb884) and endoxylanase (Tb888) to release xylose from aldouronic acids. Analysis of the hydrolysis products on TLC (Fig 12) showed that Tb887 is able to release mainly xylobiose and some amount of xylose and xylotriose from aldouronic acids. Incubating Tb882 or Tb884 alone with the aldouronic acids led to an increased amount of xylose compared to that with the control or substrate without enzyme suggesting that Tb882 and Tb884 are both able to cleave xylose from the aldouronic acid mixture or that there were xylo-oligosaccharides lacking the glucuronic acid side chain in the substrate. As expected, co-incubating Tb887 with Tb882 or Tb884 led to an increase in the amount of xylose released in each case. Some amount of xylobiose is still seen on the TLC plate when Tb887 and Tb882 are incubated together with the substrate. This is however not the case when Tb884 is used in place of Tb882 where all the xylobiose get converted to xylose. Using both xylosidases (Tb882 and Tb884) with Tb887 also converts all the xylobiose produced by Tb887 to xylose. This shows a synergism between each xylosidase and Tb887 in the release of xylose from aldouronic acids as expected.

DISCUSSION

Most xylanases are endo-acting; only two bacteria have been reported to produce exo-acting xylanases, and in both cases these enzymes were mesophilic (Gasparic *et al*., 1995; Kubata *et al*., 1994, 1995). One of the critically important enzymatic activities required for the depolymerization of xylans is endo-1, 4-*β*-xylanase (xylanase) activity (Dodd and Cann, 2009). The polypeptide Tb888, with a GH10 catalytic domain, based on its amino acid sequence, was predicted to function as a xylanase. We set out, therefore to determine if this protein has a xylanase activity. Spotting it on two agar plates containing pectin or oat spelt xylan overnight, clearing zones observed suggested activity on both substrates. Tb888 was also able to release xylose when incubated with five different model xylans (WAX, BWX, OSX, LWX and RAX) with the highest activity seen on WAX and RAX. No activity was observed when Tb888 was incubated with XGC and this was not a surprise since XGC has a backbone of β-1-4 glucose residues instead of the backbone of β-1-4 xylose residues in the other substrates.

Tb882 and Tb884 were both designated as putative *β*-xylosidases based on the analysis of their amino acid sequences. Tb882 and Tb884 were screened on fifteen artificial substrates and were both found to be active on *p*NP-α-L-arabinopyranoside and *p*NP-β-D-xylopyranoside with both enzymes showing more activity on the *p*NP-β-D-xylopyranoside. Tb882 and Tb884 were found to be able to hydrolyze xylo-oligosaccharides (X2-X6) producing mainly xylose units from the oligosaccharides. Incubation of the enzymes with xylose, however, produced no long chain oligosaccharides, suggesting that both enzymes lack transglycosylation activity.
Tb882 or Tb884 or both were able to work synergistically with Tb888 to release xylose units from xylans (BWX, LWX, OSX, WAX and RAX) as well as xylo-oligosaccharides. The two β-xylosidases (Tb882 and Tb884) were able to hydrolyze the xylobiose released by Tb888 to

xylose units from the polysaccharides. In some substrates (OSX, LWX and BWX) there was an unknown product seen from co-incubation with Tb888 and Tb882 that was removed when the incubation was done in the presence of Tb884. This shows that the two β-xylosidases are not redundant in their functions in the organism on different substrates.

In summary, the Tb888 enzyme hydrolyzes the xylan into a variety of oligosaccharides that serve as substrates for further degradation by the other enzymes (Tb882 and Tb884). The β-xylosidases Tb882 and Tb884 degrade xylobiose and other xylooligosaccahrides into xylose, and therefore releasing fermentable sugars for metabolism by the bacterium.

CHAPTER IV:

BIOCHEMICAL ANALYSIS OF A MULTIFUNCTIONAL THERMOSTABLE GLYCOSIDE HYDROLASE FAMILY ONE MEMBER FROM *CALDICELLULOSIRUPTOR BESCII*

ABSTRACT

Very few cultivated microorganisms can degrade lignocellulosic biomass without chemical pretreatment. It has been shown that *Caldicellulosiruptor bescii* DSM 6725, an anaerobic bacterium that grows optimally at 75°C, efficiently utilizes various types of untreated plant biomass, as well as crystalline cellulose and xylan. Genome sequence data shows that the bacterium harbors a large number of plant cell degrading enzymes in its genome. A putative β-glucosidase Cb486 was cloned from *Caldicellulosiruptor bescii*, expressed and purified from *Escherichia coli* cells. The protein was characterized for enzymatic properties, and it was shown to exhibit activity against *p*NP-α-L-arabinopyranoside, *p*NP-β-D-fucopyranoside, *p*NP-β-D-galactopyranoside, *p*NP-β-D-glucopyranoside, *p*NP-β-D-xylopyranoside and *p*NP-β-D-cellobioside suggesting that Cb486 is a multi-functional enzyme. Thin layer chromatography analysis showed that the enzyme can effectively hydrolyze cello- and xylo-oligosaccharide substrates, indicating the facilitation in saccharification of cellulose and hemicellulose. As expected, Cb486 was also able to work synergistically with a number of endo-glucanases from the genome of *C. bescii* to release glucose from cellulosic substrates as well as xylose from xylan containing substrates.

INTRODUCTION

Cellulose represents the most abundant polysaccharide in the plant cell wall (Linden *et al*., 1994). It accounts for up to 40% of plant biomass and consequently is the most abundant natural polymer on earth and comprises a linear polymer of glucopyranose molecules linked by β-1-4 glycosidic linkages that have alternating orientations (Fig 1) making cellobiose the fundamental repeating unit (Mansfield *et al*., 1999). Cellulose microfibrils form interstrand hydrogen bonds that along with Van der Waals forces result in a highly crystalline structure which is thought to influence its recalcitrance (Ding and Himmel, 2006). The intimate association of of cellulose with hemicellulose, pectin and lignin further limits its degradation by the various cellulose enzymes (Brett and Waldren, 1996). A complete enzymatic degradation of cellulose consists of at least three related enzyme groups. Endo-glucanases (EC 3.2.1.4) randomly hydrolyze internal glycosydic bonds to decrease the length of the cellulose chain and multiply polymer ends. Exo-glucanases (EC 3.2.1.91) split-off cellobiose from cellulose termini and β-glucosidases (EC 3.2.2.21) hydrolyze cellobiose and oligomers to render glucose. Certain microorganisms are able to induce multi-functionalization of some of their enzymes to hydrolyze different kinds of substrates (Khandeparker and Numan, 2008) whereby one enzyme is able to hydrolyze a number of different linkages.

Caldicellulosiruptor bescii DSM 6725, an anaerobic bacterium that grows optimally at 75°C, has been shown to efficiently utilize various types of untreated plant biomass, as well as crystalline cellulose and xylan (Yang *et al*, 2009). It harbors a large number of plant cell was degrading enzymes in its genome. In this study, a putative β-glucosidase Cb486 cloned from *C. bescii*, was expressed and purified from Escherichia coli. It was found to be active on a number of substrates. Chromatography analysis showed that it could effectively hydrolyze cello- and

xylo-oligosaccharide substrates, indicating the facilitation in saccharification of cellulose and hemicellulose. As expected it was also able to work synergistically with four endo-glucanases and one endo-xylanase from the genome of *C. bescii* to release glucose from cellulosic substrates and xylose from xylan containing substrates respectively.

MATERIALS AND METHODS

MATERIALS

Clones of Cb486 were obtained from Atsushi Miyagi of the Cann Lab. The Talon Metal Affinity Resin was purchased from Clontech Laboratories, Inc. (Mountain View, CA). Amicon Ultra-15 centrifugal filter units with 10,000 MWCO and 50,000 MWCO were obtained from Millipore (Billerica, MA). Xylo-oligosaccharides, cello-oligosaccharides, avicel, konjac glucomannan and wheat arabinoxylan (WAX) (medium viscosity, 20 centistokes) were obtained from Megazyme (Bray, Ireland). Gel filtration standards were obtained from Bio-Rad (Hercules, CA).

PURIFICATION OF Cb486

The plasmid construct, pET*46-Cb846*, was introduced into *E. coli* BL-21 CodonPlus (DE3) RIL competent cells by heat shock, and grown overnight in lysogeny broth (Bertani, 2004; Bertani 1951) (LB) (10 mL) supplemented with ampicillin (100 μg/mL) and chloramphenicol (50 μg/mL) at 37°C and with aeration. After 6 h, the starter cultures were diluted into fresh LB (1 L) supplemented with ampicillin and chloramphenicol and cultured at 37°C with aeration until the optical density at 600 nm reached 0.3. The culture was then incubated at 16°C with aeration

and protein expression was induced by the addition of isopropyl β-D-thiogalactopyranoside (IPTG) at a final concentration of 0.1mM. After 16 h, the cells were harvested by centrifugation (4000 x g, 15 min, 4°C), re-suspended in 35mL lysis buffer (25 mM Tris-HCL pH 7.8, 750 mM of NaCl, 5% glycerol, 20 mM imidazole, 1.25% Tween-20), and the cells were ruptured by two passages through a French pressure cell (American Instrument Company Inc., Silver Spring, MD). The cell lysate was then clarified by centrifugation at 30,000 x g for 30 min at 4°C and purified utilizing TALON® Polyhistidine-Tag Purification Resin from Clontech (Mountain View, CA) as described by the manufacturer. Aliquots of eluted fractions were analyzed by sodium dodecyl sulfate-polyacrylamide gel electrophoresis (SDS-PAGE) using the method described by Laemmli (Laemmli, 1970) and protein bands were visualized by staining with Coomassie brilliant blue G-250. Elution fractions were pooled and dialyzed against storage buffer and assays were performed immediately. The protein concentrations were quantified by absorbance spectroscopy according to methods described previously by Gill and von Hippel (21), with the following extinction coefficient of 119,180$M^{-1}cm^{-1}$. The absorbance value for each protein solution was measured at 280 nm with a NanoDrop 1000 apparatus from Thermo Fisher Scientific Inc. (Waltham, MA).

DETERMINATION OF CATALYTIC ACTIVITIES OF CB486 WITH PNP-LINKED SUGARS

The specific activities of Cb486 with *para*-nitrophenyl (*p*NP) - linked substrates were assayed using a thermostated Cary 300 UV-visible spectrophotometer from Varian Inc. (Palo Alto, CA). Fifteen different substrates from Sigma-Aldrich (St. Louis, MO) were screened: *p*NP-

α-L-arabinopyranoside, *p*NP- α-L-arabinofuranoside, *p*NP-β-D-fucopyranoside, *p*NP-α-L-fucopyranoside, *p*NP-α-D-galactopyranoside, *p*NP-β-D-galactopyranoside, *p*NP-α-D-glucopyranoside, *p*NP-β-D-glucopyranoside, *p*NP-β-D-maltopyranoside, *p*NP-α-D-maltopyranoside, *p*NP-α-D-mannopyranoside, *p*NP-β-D-mannopyranoside, *p*NP-α-L-rhamnopyranoside, *p*NP-β-D-xylopyranoside, and *p*NP-β-D-cellobioside. The different *p*NP substrates (1.0 mM, final concentration) were incubated at 50°C in the presence or absence of Cb486 (50nM, final concentration) in a buffer composed of 50mM Na-citrate and 150 mM NaCl (pH 5.5) for 30 min, and the rate of *p*NP release was determined by monitoring the absorbance at 400 nm continuously.

DETERMINATION OF OPTIMUM pH OF Cb486

To determine the optimum pH of Cb486, *p*NP-β-D-galactopyranoside (1.0mM final concentration) was prepared in citrate buffer (50mM Na-citrate with 150mM NaCl, pH 4.0-6.0) or phosphate buffer (50mM Na-phosphate with 150mM NaCl, pH 6.0-8.0). The data was collected using Cary 300 UV-Vis spectrophotometer (Varian). Each reaction was initiated by adding 25µl of Cb486 (10nM final concentration) to 100µl of the substrate and mixed by pipetting up and down several times at 60 ºC. The release of *p*NP was continuously monitored by recording the UV signal at 400 nm for 5 minutes. Each experiment was carried out in triplicate. Initial velocities of the enzyme-catalyzed reactions were obtained by adjusting the protein concentrations such that the slopes of the resulting progress curves (change in absorbance per unit of time) were linear. Initial rate obtained at each pH was converted to relative activity and plotted against pH using GraphPad Prism v5.02 from GraphPad Software (San Diego, CA). The

extinction coefficient for *para*-nitrophenol at pH 5.5 and at a wavelength of 400 nm was measured to be 0.673 mM^{-1} cm^{-1}.

DETERMINATION OF OPTIMUM TEMPERATURE OF Cb486

To determine the optimum temperature of Cb486, *p*NP-β-D-galactopyranoside (1.0mM final concentration) was prepared in citrate buffer (50mM Na-citrate with 150mM NaCl, pH 5.5). The data was collected using Cary 300 UV-Vis spectrophotometer (Varian). Each reaction was initiated by adding 25µl of Cb486 (10nM final concentration) to 100µl of the substrate and mixed by pipetting up and down several times at various temperatures ranging from 40°C to 95 ºC. The release of *p*NP was continuously monitored by recording the UV signal at 400 nm for 5 minutes. Each experiment was carried out in triplicate. Initial velocities of the enzyme-catalyzed reactions were obtained by adjusting the protein concentrations such that the slopes of the resulting progress curves (change in absorbance per unit of time) were linear. The initial rate obtained at each temperature was converted to relative activity and plotted against temperature using GraphPad Prism v5.02 from GraphPad Software (San Diego, CA). The extinction coefficient for *para*-nitrophenol at pH 5.5 and at a wavelength of 400 nm was measured to be 0.673 mM^{-1} cm^{-1}.

THERMOSTABILITY OF Cb486

The thermostability assay of Cb486 was carried out as follows. Five micromolar Cb486 was kept at different temperatures (50 ºC, 55 ºC, 60 ºC, 65 ºC, 70 ºC, 75 ºC, 80 ºC, 85 ºC, 90 ºC and 95 ºC). Aliquots were taken out at different time points (0 h, 0.5 h, 1 h, 2 h, 4 h, 8h, 12 h and 24 h) and immediately applied to enzyme activity measurement. The Glucose Oxidase reagent

set from Pointe Scientific Inc. (Canton, Michigan) was used to measure the enzyme activity. Four microliters of Cb486 was added to 16µl of the substrate (cellobiose) for 2 min, 4 min and 6 min. The reaction was stopped by boiling at 100 ºC for 2 min. The enzyme activity was measured at 37 ºC using a thermostated Synergy II multi-mode microplate reader from BioTek Instruments Inc. (Winooski). Two hundred microliters of assay solution were pipetted into a 96-well plate for each sample and pre-incubated at 37 ºC for 15 min. Six microliters of the reaction sample was added to the pre-incubated 200µl assay solution and then incubated for 5 min. The reading was taken at 510nm wavelength and the initial velocity of reaction in the first minute was calculated. The initial velocity of reaction for time 0 was set as 100; then the remaining activities (percentage) for time 0.5 h, 1 h, 2 h, 4 h, 8h, 12 h and 24 h were calculated by dividing the initial velocities of reaction for time 0.5 h, 1 h, 2 h, 4 h, 8h, 12 h and 24 h by the initial velocity of reaction at time 0, then multiplied by 100, respectively. This experiment was carried out by Michael Iakiviak of the Cann Lab.

HYDROLYSIS OF CELLO AND XYLO-OLIGOSACCHARIDES BY Cb486

The capacity of Cb486 to hydrolyze xylo- and cello-oligosaccharides was assessed by resolving and detecting the hydrolysis products utilizing thin layer chromatography (TLC). Initial biochemical studies had revealed that the optimum pH for activity for Cb486 was 5.5. Thus, for measuring the hydrolysis of xylo- and cello-oligosaccharides, reaction mixtures (10 µl) were prepared in citrate buffer (50mM sodium phosphate, 150 mM NaCl, pH 5.5) with X_1-X_6 (20mM) or G_2-G_6 (20mM) and reactions were initiated by the addition of Cb486 (2µM, final concentration). Following incubation at 80°C for 16h, hydrolysis products were centrifuged for

10mins and spotted onto a DC-Plastikfolien Silica Gel 60 F254 TLC plate from Merck (Whitehouse Station, NJ) to resolve the products as described above.

STEADY-STATE KINETIC MEASUREMENTS FOR Cb486

The steady state kinetic studies of Cb486 were performed on the six α- and β-*para*-nitrophenol-linked monosaccharides; (*p*NP-β-D-galactopyranoside, *p*NP-β-D-fucopyranoside, *p*NP-β-D-glucopyranoside, *p*NP-β-D-cellobioside, *p*NP-α-L-arabinopyranoside and *p*NP-β-D-xylopyranoside) and the natural substrate, cellobiose. The kinetic data was collected using Cary 300 UV-Vis spectrophotometer (Varian). *p*NP-β-D-fucopyranoside or *p*NP-α-L-arabinopyranoside or *p*NP-β-D-xylopyranoside (0 to 10mM) or *p*NP-β-D-glucopyranoside or *p*NP-β-D-cellobioside (0 to 20mM) or *p*NP-β-D-galactopyranoside (0 to 40mm) was incubated in citrate reaction buffer (100 µl) (50 mM sodium citrate, 150 mM NaCl [pH 5.5]). The reaction was initiated by adding 25µl of Cb486 (10nM final concentration) to substrates; *p*NP-β-D-galactopyranoside, *p*NP-β-D-fucopyranoside, and *p*NP-β-D-glucopyranoside or Cb486 (50nM final concentration) to substrates; *p*NP-β-D-cellobioside, *p*NP-α-L-arabinopyranoside and *p*NP-β-D-xylopyranoside, and mixed by pipetting up and down for several times at 85 ºC. The hydrolysis of *p*NP substrates was continuously monitored by recording the UV signal at 400 nm for 5 minutes.

The Glucose Oxidase reagent set from Pointe Scientific Inc was used for the natural substrate, cellobiose. Cellobiose (0 to 50mM) was incubated in citrate reaction buffer (100 µl) (50 mM sodium citrate, 150 mM NaCl [pH 5.5]). Four microliters of Cb486 (50nM final concentration) was added to 16µl of the substrate (cellobiose) for 2 min, 4 min and 6 min at 85

ºC. The reaction was stopped by boiling at 100 ºC for 2 min. The enzyme activity was measured at 37 ºC using a thermostated Synergy II multi-mode microplate reader from BioTek Instruments Inc. (Winooski). 200µl of assay solution was pipetted into a 96-well plate for each sample and pre-incubated at 37 ºC for 15 min. Six microliters of the reaction sample were added to the pre-incubated 200µl assay solution and then incubated for 5 min. The reading was taken at 510nm wavelength.

Initial velocities of the enzyme-catalyzed reactions were obtained by adjusting the protein concentrations such that the slopes of the resulting progress curves (change in absorbance per unit of time) were linear. Initial rate data were then plotted against the substrate concentration, and kinetic values were estimated by applying a nonlinear curve fit using GraphPad Prism v5.02 from GraphPad Software (San Diego, CA). The extinction coefficient for *para*-nitrophenol at pH 5.5 and at a wavelength of 400 nm was measured to be 0.673 mM^{-1} cm^{-1}.

HYDROLYSIS OF A MODEL XYLAN BY Cb486 AND Cb195

WAX (1% wt/vol, final concentration) was incubated alone or co-incubated with Cb486 (0.5µM final concentration) or Cb195 (0.5µM final concentration) or both in citrate buffer (50mM sodium citrate, 150mM NaCl, pH 5.5) at 75°C for 16 hours. The concentrations of reducing ends were estimated using the *para*-hydroxybenzoic acid hydrazide (PAHBAH) assay as described previously (Lever, 1972) with xylose as a standard. For qualitative identification of the hydrolysis products, the reactions were resolved by thin layer chromatography (TLC). Following incubation at 75°C for 16h, hydrolysis products were centrifuged for 10 min and spotted onto a DC-Plastikfolien Silica Gel 60 F254 TLC plate from Merck (Whitehouse Station,

NJ) to resolve the products using monomeric xylose (X_1) and xylo-oligosaccharides (X_2-X_6) (25 μg each) as standards. The mobile phase consisted of n-butanol: acetic acid:H2O, 10:5:1 (vol/vol/vol) and 20cm x 10cm TLC plates were used. The products were then visualized by spraying the plates with a 1:1 (v/v) mixture of methanolic orcinol (0.2% w/v) and sulfuric acid (20% v/v) followed by heating the plates at 65 °C for 10 min. The products of hydrolysis were also separated using high performance anion-exchange chromatography (HPAEC) with a System Gold high-performance liquid chromatograph (HPLC) instrument from Beckman Coulter (Fullerton, CA) fitted with a CarboPac PA1 guard column (4 by 50 mm) and a CarboPac PA1 analytical column (4 by 250 mm) from Dionex Corporation (Sunnyvale, CA). The eluted saccharides were then detected by HPAEC with pulse amperometric detection (PAD) with a pulsed model 5040 amperometric analytical cell and a Coulochem III electrochemical detector from ESA Biosciences (Chelmsford, MA) as described by Dodd et al; 2010.

HYDROLYSIS OF POLYSACCHARIDES BY Cb486 AND FOUR ENDOGLUCANASES

Avicel (10% wt/vol, final concentration), konjac glucomannan (5% wt/vol, final concentration) and phosphoric acid swollen cellulose (5% wt/vol, final concentration) was each incubated alone or with several endoglucanase from *C. bescii* (Cb1953WT, Cb1952WT, Cb1946WT and Cb629 [0.5μM final concentration]). The incubations were either with endoglucanases alone or together with Cb486 (0.5μM final concentration) in citrate buffer (50mM sodium citrate, 150mM NaCl, pH 5.5) at 75°C for 16 hours. Pretreated Miscanthus (50% wt/vol, final concentration) was incubated alone or co-incubated with each or all four endoglucanases (0.5μM final concentration) and Cb486 (0.5μM final concentration) in citrate buffer (50mM sodium citrate, 150mM NaCl, pH 5.5) at 75°C for 16 hours. The concentrations of

reducing ends were estimated using the *para*-hydroxybenzoic acid hydrazide (PAHBAH) assay as described previously (Lever, 1972) with glucose as a standard. For qualitative identification of the hydrolysis products, the reactions were resolved by thin layer chromatography (TLC). Following incubation at 75°C for 16h, hydrolysis products were centrifuged for 10 min and spotted onto a DC-Plastikfolien Silica Gel 60 F254 TLC plate from Merck (Whitehouse Station, NJ) to resolve the products using monomeric glucose (G_1) and cello-oligosaccharides (G_2-G_6) (25 μg each) as standards. The mobile phase consisted of n-butanol: acetic acid:H2O, 10:5:1 (vol/vol/vol) and 20cm x 10cm TLC plates were used. The products were then visualized by spraying the plates with a 1:1 (v/v) mixture of methanolic orcinol (0.2% w/v) and sulfuric acid (20% v/v) followed by heating the plates at 65 °C for 10 min. The products of hydrolysis were also separated using high performance anion-exchange chromatography (HPAEC) with a System Gold high-performance liquid chromatography (HPLC) instrument from Beckman Coulter (Fullerton, CA) fitted with a CarboPac PA1 guard column (4 by 50 mm) and a CarboPac PA1 analytical column (4 by 250 mm) from Dionex Corporation (Sunnyvale, CA). The eluted saccharides were then detected by HPAEC with pulse amperometric detection (PAD) with a pulsed model 5040 amperometric analytical cell and a Coulochem III electrochemical detector from ESA Biosciences (Chelmsford, MA) as described by Dodd et al; 2010. To identify and quantify the mono- and oligo-saccharides produced from enzymatically degraded polysaccharides, peak retention times and peak areas from the chromatographs of samples were compared to those of commercially available saccharides analyzed as standards.

RESULTS

DOMAIN ARCHITECTURE OF A MULTIFUNCTIONAL β-GLUCOSIDASE FROM *CALDICELLULOSIRUPTOR BESCII*

A putative β-glucosidase was identified in the genome of *C. bescii*. The domain architecture of the protein (ORF486) is shown in Fig 13A. The amino acid sequence analysis of this protein revealed the presence of a single GH1 catalytic domain. Known activities of the enzymes with a GH1 catalytic domain include: β-glucosidase (EC 3.2.1.21); β-galactosidase (EC 3.2.1.23); β-mannosidase (EC 3.2.1.25); β-glucuronidase (EC 3.2.1.31); β-D-fucosidase (EC 3.2.1.38); exo-β-1,4-glucanase (EC 3.2.1.74); 6-phospho-β-galactosidase (EC 3.2.1.85); 6-phospho-β-glucosidase (EC 3.2.1.86); strictosidine β-glucosidase (EC 3.2.1.105); lactase (EC 3.2.1.108); amygdalin β-glucosidase (EC 3.2.1.117); prunasin β-glucosidase (EC 3.2.1.118); raucaffricine β-glucosidase (EC 3.2.1.125); thioglucosidase (EC 3.2.1.147); β-primeverosidase (EC 3.2.1.149); isoflavonoid 7-O-β-apiosyl-β-glucosidase (EC 3.2.1.161) etc.

CLONING, EXPRESSION AND PURIFICATION OF A PUTATIVE β-GLUCOSIDASE FROM *CALDICELLULOSIRUPTOR BESCII*

The gene for Cb486 was amplified by PCR and cloned into an expression vector for recombinant protein expression in *E. coli*. Cb486 was expressed as an N-terminal hexahistidine fusion protein to facilitate purification by metal affinity chromatography. The predicted molecular mass for the hexahistidine fusion protein, His-Cb486, 54.9 kDa, was in agreement with the size of the purified protein estimated by comparison with molecular mass markers through SDS-PAGE analysis (Fig 13B).

Cb486 IS A MULTIFUNCTIONAL ENZYME

To determine whether the putative glucosidase possesses its predicted activity, the enzyme was examined for release of products from fifteen *p*NP substrates (Fig 14A). The substrates were: *p*NP-α-L-arabinopyranoside, *p*NP- α-L-arabinofuranoside, *p*NP-β-D-fucopyranoside, *p*NP-α-L-fucopyranoside, *p*NP-α-D-galactopyranoside, *p*NP-β-D-galactopyranoside, *p*NP-α-D-glucopyranoside, *p*NP-β-D-glucopyranoside, *p*NP-β-D-maltopyranoside, *p*NP-α-D-maltopyranoside, *p*NP-α-D-mannopyranoside, *p*NP-β-D-mannopyranoside, *p*NP-α-L-rhamnopyranoside, *p*NP-β-D-xylopyranoside, and *p*NP-β-D-cellobioside. The result of the screen on the *p*NP substrates showed activity in five (*p*NP-α-L-arabinopyranoside, *p*NP-β-D-fucopyranoside, *p*NP-β-D-galactopyranoside, *p*NP-β-D-glucopyranoside, *p*NP-β-D-xylopyranoside and *p*NP-β-D-cellobioside) of the fifteen *p*NP substrates. The highest activity was observed in *p*NP-β-D-galactopyranoside followed by *p*NP-β-D-fucopyranoside with the least activity seen in *p*NP-β-D-xylopyranoside.

Cb486 was co-incubated with cello- and xylo- oligosaccharides to confirm its glucosidase and xylosidase activities, respectfully. Resolving the hydrolysis products on TLC showed the release of glucose as the only product from the cello-oligosaccharides (G2 to G5) and small amounts of G2, G3, G4, and G5 in case of G6 (Fig 14B). This confirms that Cb486 has a cellodextrinase activity. Hydrolysis products from the xylo-oligosaccharides showed the release of mainly xylose and xylo-oligosaccharides of different lengths depending on the xylo-oligosaccharide substrate (Fig 14C). HPLC analysis of the hydrolysis products from the xylo-oligosaccharides also showed the same pattern of released products as resolved with the TLC (Fig 15A, 15B, 15C,

15D, 15E and 15F). This result confirms the presence of a xylosidase activity in Cb486. Co-incubating with glucose or xylose produced no long chain oligosaccaharides.

OPTIMAL pH, TEMPERATURE AND THERMOSTABILITY OF CB486

The pH and temperature profiles (Fig 16A and 16B respectively) of Cb486 showed that it works best at a pH of 5.5 at 85°C. It is however not thermostable at this temperature (Fig 16C). The thermostability assay carried out on Cb486 showed that Cb486 has 77%, 75% and 65%, activity after incubation at 80 ºC, 75 ºC and 70 ºC for 24 h, respectively (Fig 16C).

STEADY-STATE KINETIC PARAMETERS OF Cb486

To determine the catalytic properties of Cb486, the steady-state kinetic parameters of the enzyme in the presence of six α- and β-*para*-nitrophenol-linked monosaccharides; (*p*NP-α-L-arabinopyranoside, *p*NP-β-D-fucopyranoside, *p*NP-β-D-galactopyranoside, *p*NP-β-D-glucopyranoside, *p*NP-β-D-xylopyranoside and *p*NP-β-D-cellobioside) and natural substrate cellobiose were analyzed. Cb486 was incubated in a sodium citrate buffer in the presence of various concentrations of the various *p*NP substrates, and the change in magnitude of the *A*400 signal was monitored by UV spectroscopy. Initial rate data Cb486 were obtained for each of the substrate concentrations, and plots of the initial velocity of each *p*NP substrate hydrolysis (nmol/s) versus the substrate concentration (mM) were generated (Fig 17A, 17B, 17C, 17D, 17E, 17F and 17G). Cb486 has the highest affinity for *p*NP-α-L-arabinopyranoside with a *K*m of 0.7 ± 0.1mM. Its catalytic efficiency of 78.4 ± 11.5 $s^{-1}mM^{-1}$ was relatively low due to a low *k*cat of 54.9 ± 1.7s^{-1}. Cb486 showed its highest catalytic efficiency towards pNP-β-D-fucopyranoside

(465.9 ± 27.7s^{-1}) followed by *p*NP-β-D-glucopyranoside (333.4 ± 28.8s^{-1}). Even though the highest *k*cat value of 910.2 ± 27.2s^{-1} was observed for Cb486 on *p*NP-β-D-galactopyranoside, it recorded a catalytic efficiency of 101.1 ± 8.4$s^{-1}mM^{-1}$ due to the very high *K*m of 9.0 ± 0.7mM. Cb846 has the lowest affinity for the only natural substrate (cellobiose) tested with a *K*m of 9.9 ± 1.1mM and the lowest catalytic efficiency of 15.5 ± 1.8$s^{-1}mM^{-1}$. Table 3 shows a summary of the kinetic parameters.

HYDROLYSIS OF THREE POLYSACCHARIDES BY FOUR ENDOGLUCANASES AND Cb486

Cb1953WT, Cb1952WT, Cb1946WT and Cb629 are endoglucanases from the genome of *C. bescii* that are able to hydrolyze different cellulosic polysaccharides. The polysaccharides used for this study were avicel, phosphoric acid swollen cellulose (PASC) and konjac glucomannan (KGM). Reducing sugar assay on the hydrolysis products from each substrate showed activity from each individual endoxylanase and slightly higher activity when the substrate was co-incubated with endoglucanases and Cb486 (glucosidase) (Fig 18A, 18B, and 18D). Resolving the hydrolysis products by TLC (Fig 18C and 18E) and HPLC (Fig 19A: Avicel, 19B: PASC) revealed the products present in the hydrolysates. The various endoglucanases released mainly cellobiose and some other oligosaccharides. Mannobiose was also released from konjacglucomannan. In the presence of Cb486 however, the cellobiose released was converted to glucose. This was evident in both TLC and HPLC analyses.

All four endoglucanases released only cellobiose from PASC that was converted to glucose in the presence of Cb486 as seen from resolving the hydrolysis products by both TLC and HPLC.

No TLC analysis was performed on the hydrolysis products from avicel; however HPLC showed similar results as seen in the two other substrates with cellobiose released by the four endoglucanases being converted to glucose by Cb486.

HYDROLYSIS OF WAX BY Cb195 AND Cb486

WAX was incubated alone or co-incubated with Cb486 or Cb195 or both in order to determine the synergism between these two enzymes. Cb195 is an endoxylanase from the genome of *Caldicellulosiruptor bescii* that is able to hydrolyze WAX to produce xylo-oligosaccharides of various lengths (X2 to X6). The reducing sugar assay recorded almost no reducing ends when WAX was incubated with only Cb486 as expected. On the other hand the concentration of reducing ends obtained from incubation with Cb195 alone was high and slightly higher when both Cb195 and Cb486 were used (Fig 18F). Resolving the hydrolysis products by TLC showed that incubation with Cb195 released products that migrated in similar pattern to xylo-oligosaccharides of various lengths with barely any product with similar migration to xylose seen. Hydrolysis products from co-incubation of WAX with both enzymes showed an increase in the production of a product that migrated similarly to xylose with a slight decrease in the amount of products that migrated similarly to other xylo-oligosaccharides (Fig 15H). This result showed that Cb486 with a xylosidase activity is able to work synergistically with Cb195, an endoxylanase to release xylose from xylans (WAX).

HYDROLYSIS OF MISCANTHUS BY FOUR ENDOGLUCANASES AND Cb486

Cb486 and the four endoglucanases from above were also incubated with pre-treated (microwaved) Miscanthus. Fig 20 shows the results from a reducing sugar assay on the hydrolysis products of microwaved miscanthus. It showed an increase in glucose production in the presence of Cb486. The hydrolysis products were also resolved on the HPLC and the concentrations of the various sugars determined (Table 4). When the concentration of each enzyme was doubled (from 0.5μM to 1μM), there was about three-fold increase in amount of glucose released and about two and half-fold increase in the amount of cellobiose released. These results show synergism between each englucanase and Cb486 in working to release glucose from cellulosic polysaccharides.

DISCUSSION

Cb486 was able to hydrolyze the linkages present in six different aryl glycoside substrates with the highest activity in *p*NP-β-D-galactopyranoside with a *k*cat value of 910.2 ± 27.2s^{-1} and a high *K*m of 9.0 ± 0.7mM followed by *p*NP-β-D-fucopyranoside, *p*NP-β-D-glucopyranoside, *p*NP-β-D-cellobioside, *p*NP-β-D-xylopyranoside and *p*NP-α-L-arabinopyranoside. Results from the TLC analysis of the hydrolysis products from incubation of Cb486 with cello- and xylo-oligosaccharides showed the release of glucose and xylose from the long chain cello- and xylo-oligosaccharides respectively. This result confirmed that Cb486 has both β-glucosidase and β-xylosidase activities. For biotechnological applications, enzymes exhibiting broad substrate specificity are desirable.

In the enzymatic hydrolysis of cellulose, β-glucosidases hydrolyze cellobiose to free glucose molecules after it has been degraded to cellobiose by endoglucanases and exoglucanases. Cb486 was found to be capable of converting all the cellobiose produced by four different endoglucanases (Cb1953WT, Cb1952WT, Cb146WT and Cb629) from a number of cellulosic substrates (PASC, Avicel, KGM and pre-treated Miscanthus) into glucose units. These endoglucanases are from a gene cluster from *C. bescii* as well. Cb486 was also able to hydrolyze xylobiose released by Cb195 (an endoxylanase from *C. bescii*) from WAX into xylose units. This was however not as efficient as in the case of cellobiose hydrolysis as there was still some xylobiose seen on the TLC plate.

C. bescii is known to be able to utilize both cellulose and xylan simultaneously. It therefore possesses a variety of cellulolytic enzymes. In addition to this, being able to induce multi-functionalization of certain enzymes to hydrolyze different kinds of substrates will be of great advantage to this organism for survival in its natural environment. Cb486 is obviously one of these multi-functional enzymes and is capable of working synergistically with both endoglucanases as well as endoxylanases to release glucose and xylose from cellulose and xylan respectively.

CHAPTER V

DISCUSSION

Future expansion of biofuel production must be increasingly based on bioethanol from lignocellulosic materials, such as agricultural byproducts, forest residues, industrial waste streams or energy crops (Claassen *et al*., 1999; Solomon *et al*., 2007). Plant tissue varies widely in structure and composition and, as might be expected, in its response to pretreatment and enzymatic saccharification (Himmel *et al*., 2007). Microorganisms have to synthesize a number of different enzymes in order to hydrolyze cellulose or hemicellulose in order to invade or live successfully in the plant tissues (Khandeparker and Numan, 2008). Both *C. bescii* and *T. bryantii* are thermostable anaerobes which have been found to be endowed with a number of plant cell wall degrading enzymes in their respective genomes.

The gene cluster from *T. bryantii* investigated in this study was found to contain a number of accessory enzymes which we thought should work with the xylanase in the breakdown of xylan. Almost all xylanases that have been described to date are endo-acting; only two bacteria have been reported to produce exo-acting xylanases, in both cases these enzymes were mesophilic (Gasparic *et al*., 1995; Kubata *et al*., 1994, 1995). One of the critically important enzymatic activities required for the depolymerization of xylans is endo-1, 4-*β*-xylanase (xylanase) activity (Dodd and Cann, 2009). Tb888 based on its amino acid sequence was thought to be a putative xylanase with a GH10 catalytic domain. With this thought in mind, we set out to determine if it has a xylanase activity. Spotting it on two agar plates containing pectin or oat spelt xylan overnight, clearing zones observed suggested activity on both substrates. Tb888 was also able to release xylose equivalents when incubated with five different xylans (WAX, BWX, OSX, LWX and RAX) with highest activity seen in WAX and RAX. No activity

was observed when Tb888 was incubated with XGC and this was not a surprise since XGC has a backbone of β-1-4 glucose residues instead of the backbone of β-1-4 xylose residues in the other substrates. Xylanases catalyze the endo-hydrolysis of 1,4-β-D-xylosidic linkages in a seemingly random fashion, although more recent evidence would suggest the cleavage sites used by GH10 and 11 enzymes are influenced by side chain substituents (Dodd and Cann, 2009; Kolenova et al., 2006; Maslen et al., 2007).

Tb882 and Tb884 were both designated as putative *β*-xylosidases based on the analysis of their amino acid sequences. They were both screened for activity on fifteen artificial substrates and were both found to be active on two of them (*p*NP-α-L-arabinopyranoside and *p*NP-β-D-xylopyranoside) with both showing higher activity on the *p*NP-β-D-xylopyranoside. They were both found also to be able to hydrolyze xylo-oligosaccharides (X2-X6) producing mainly xylose units from these oligosaccharides. Xylan-1,4-*β*-xylosidase (*β*-xylosidase) enzymes release xylose monomers from the non-reducing end of xylo-oligosaccharides (Dodd and Cann, 2009). Incubating Tb882 or Tb884 together with xylose however produced no long chain oligosaccharides implying that both enzymes are not involved in transglycosylation. We thought the endoxylanase (Tb888) may work together with two different β-xylosidases aiding *T. bryantii* to effectively utilize xylans that exhibit different substitutions in the context of the plant cell wall. This hypothesis was supported by the synergy observed between the xylanase and the two accessory proteins. Tb882 or Tb884 or both were able to work synergistically with Tb888 to sufficiently release xylose units from xylans (BWX, LWX, OSX, WAX and RAX) as well as xylo-oligosaccharides. They were able to hydrolyze the xylobiose released by Tb888 to xylose units from the polysaccharides. *β*-D-xylosidases are important in the relief of end-product inhibition of xylanases caused by xylobiose and the performance of β-xylosidases is typically

inhibited by increasing concentrations of their end-product, xylose (Yeoman *et al*., 2010). Interestingly, a thermophilic *β*-xylosidase from the fungus *Scytalidium thermophilum* was, however, found to be immune to xylose-mediated inhibition (Zanoelo *et al*., 2004). In some substrates (OSX, LWX and BWX) there was an unknown product seen from co-incubation with Tb888 and Tb882 that was removed when the incubation was done in the presence Tb884. This shows that the two xylosidases are not redundant in their functions in the organism on different substrates. In all cases investigated, Tb884 seemed to work better with Tb888 in the release of xylose in comparison to Tb882. Tb887, the only α-glucuronidase in the gene cluster has been to shown to work synergistically with the two β-xylosidases (Tb882 and Tb884) to release xylose from aldouronic acids.

On the basis of the results from the present study, a model for utilization of xylan by *T. bryantii* likely involves secretion of Tb888 into the extracellular space to degrade this complex plant cell wall polysaccharide. This enzyme hydrolyzes the xylan into a variety of oligosaccharides that are transported into the cell as substrates for further degradation by the other enzymes (Tb882 and Tb884) predicted to be intracellularly located. The β-xylosidases Tb882 and Tb884 degrade xylobiose into xylose.

β-Glucosidases based on their substrate specitivity are divided into three groups. They are aryl-β-glucosidase that has strong affinity for aryl-β-glucoside, cellobiase that only hydrolyzes celloligosaccharides, and broad specific β-glucosidase that have multifunction (Kim *et al*., 2007). β-Xylosidases may also be monofunctional or multifunctional (Wagschal *et al*., 2009; Teng *et al*., 2011). A number of studies have looked at bifunctional β-glucosidase/xylosidases, such as *bgx1* from *Phytophthora infestan* (Brunner *et al*., 2002), and *bgxA* from *Erwinia chrysanthemi* (Vroemen *et al*, 1995). In these researches, the β-xylosidase

activities of these enzymes were not fully exploited as well as the β-glucosidase activities. The β-xylosidase activity of multifunctional glucosidases is however important in understanding the advantages these enzymes might have over monofunctional glucosidases in lignocellulose degradation.

Cb486 from *C. bescii* in this study was found to be able to hydrolyze the linkages present in six different aryl glycoside substrates with the highest activity in *p*NP-β-D-galactopyranoside with a k*cat* value of 910.2 ± 27.2s^{-1} and a high *K*m of 9.0 ± 0.7mM followed by *p*NP-β-D-fucopyranoside, *p*NP-β-D-glucopyranoside, *p*NP-β-D-cellobioside, *p*NP-β-D-xylopyranoside and *p*NP-α-L-arabinopyranoside. A recombinant β-glucosidase from *Dictyoglomus turgidum* characterized by Kim *et al* was also found to have hydrolytic activity of on a number of aryl-glycoside substrates; with the highest for *p*-nitrophenyl (*p*NP)-β-D-glucopyranoside (with a K_m of 1.3 mM and a k_{cat} of 13900 1/s), followed by *o*NP-β-D-glucopyranoside, *p*NP-β-D-xylopyranoside, *p*NP-β-D-fucopyranoside, and *p*NP-β-D-galactopyranoside (Kim *et al*, 2011).

Results from the TLC analysis of the hydrolysis products from incubation of Cb486 with cello- and xylo-oligosaccharides showed the release of glucose and xylose from the long chain cello- and xylo-oligosaccharides respectively. These results confirmed that Cb486 has both β-glucosidase and β-xylosidase activities. Two β-glucosidase/xylosidases (RuBG3A and RuBG3B) were cloned from the yak rumen uncultured microorganisms and were found to effectively hydrolyze cellooligosaccharides as well as working synesgistically with xylanase to release xylose from xylan hrolysis (Bao *et al*., 2012)

Being a thermostable enzyme with multiple specificity, Cb486 can be utilized for different valuable applications in development of new bio-fuel feed stock, processing of cellulose or lactose containing by-products in food and wine industries. For biotechnological applications, enzymes exhibiting broad substrate specificity are desirable.

In the enzymatic hydrolysis of cellulose, β-glucosidases hydrolyze cellobiose to free glucose molecules after it has been degraded to cellobiose by endoglucanases and exoglucanases. Cb486 was found to be capable of converting all the cellobiose produced by four different endoglucanases (Cb1953WT, Cb1952WT, Cb146WT and Cb629) from a number of cellulosic substrates (PASC, Avicel, KGM and microwaved Miscanthus) into glucose units. These endoglucanases are from a gene cluster from *C. bescii* as well. Cb486 was also able to hydrolyze xylobiose released by Cb195 (an endoxylanase from *C. bescii*) from WAX into xylose units. This was however not as efficient as in the case of cellobiose hydrolysis as there was still some xylobiose seen on the TLC plate.

C. bescii is known to be able to utilize both cellulose and xylan simultaneously. It therefore possesses a variety of cellulolytic enzymes. In addition to this, being able to induce multi-functionalization of certain enzymes to hydrolyze different kinds of substrates will be of great advantage to this organism for survival in its natural environment. Cb486 is obviously one of these multi-functional enzymes and is capable of working synergistically with both endoglucanases as well as endoxylanases to release free glucose and xylose from cellulose and xylan respectively.

The use of biofuels provides a means to reduce the use of fossil fuels as well as to reduce the global emission of greenhouse gases into the environment (Lynd *et al*., 1991). The utilization of hemicellulose and lignin, in addition to cellulose, may greatly improve the productivity and

yield of fuels from biomass (Linden *et al*., 1994). Acid hydrolysis of biomass is faster but is accompanied by the formation of toxic compounds that hinder subsequent microbial fermentations (Biely, 1985). Using enzymes obtained from these organisms therefore provides a means for the hydrolysis of plant biomass without the formation of toxic compounds to enable relatively easy microbial fermentation.

For future work on the hemicellulase gene cluster from *T. bryantii*, the acetyl xylan esterase and the two oxido-reductases should be characterized and used together with the other enzymes in the cluster to determine exactly how they synergistically hydrolyze xylans.

CHAPTER VI

CONCLUSIONS

This work presents data on the purification and characterization of a β-1,4-endoxylanase (Tb884), two β-xylosidases (Tb882 and Tb884) and an α-glucuronidase from *T. bryantii*; and a multifunctional cellodextrinase (Cb486) from *C. bescii*.

All enzymes were purified using TALON® Polyhistidine-Tag Purification Resin from Clontech (Mountain View, CA) as described by the manufacturer. The optimal temperatures of 60°C, 65°C, 60°C and 85°C of Tb888, Tb882, Tb884 and Cb486 respectively show that these enzymes are thermophilic enzymes.

The accessory enzymes from *T. byrantii* together work with the endoxylanase to hydrolyze hemicellulosic substrates releasing xylose as the major sugar. Together with the α-glucuronidase (Tb887), the two β-xylosidases (Tb882 and Tb884) were also able to release xylose from aldouronic acids.

Cb486 from *C. bescci* was found to be able to hydrolyze the linkages present in six different aryl glycoside substrates with the highest activity in *p*NP-β-D-galactopyranoside with a k*cat* value of 910.2 ± 27.2s^{-1} and a high *K*m of 9.0 ± 0.7mM followed by *p*NP-β-D-fucopyranoside, *p*NP-β-D-glucopyranoside, *p*NP-β-D-cellobioside, *p*NP-β-D-xylopyranoside and *p*NP-α-L-arabinopyranoside. The enzyme was also able to release glucose and xylose from cellulosic and hemicellulosic substrates respectively when incubated with four different endoglucanases and an endoxylanase from *C. bescii.* It is therefore a β-glucosidase/β-xylosidase.

CHAPTER VII

FIGURES AND TABLES

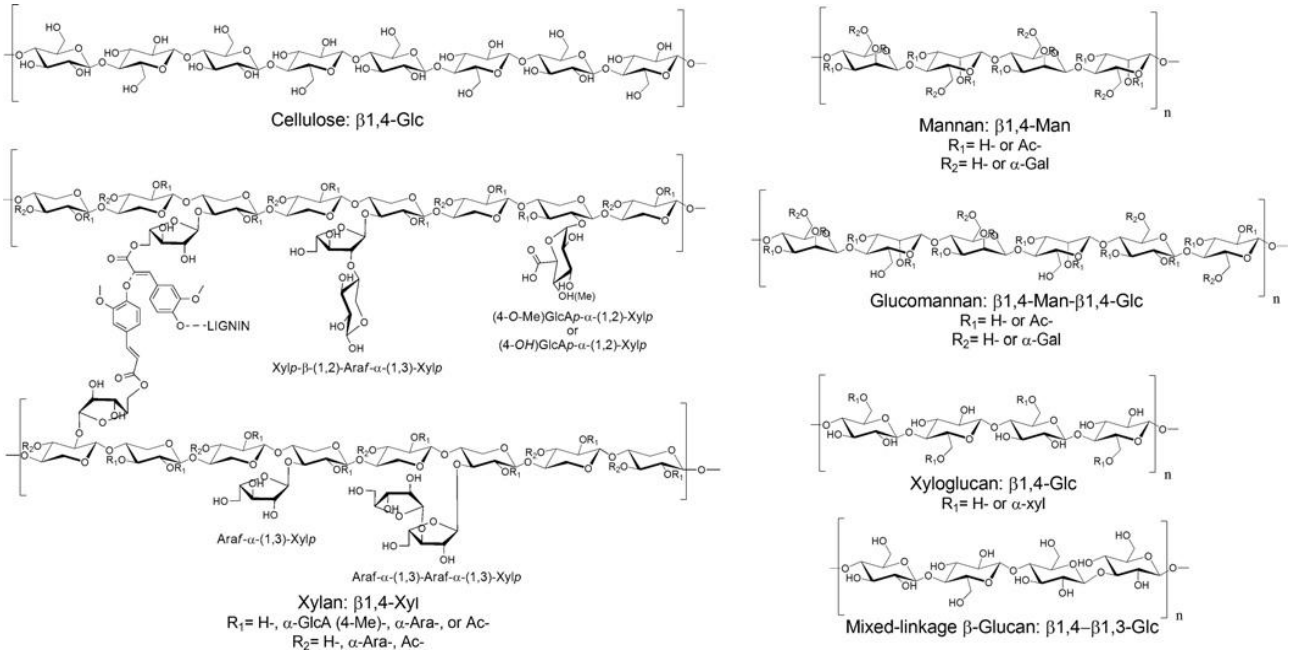

FIGURE 1 Polymeric structures of cellulose and hemicellulose chains
Cellulose consists of repeating β-(1,4)-linked D-glucose residues. Adjacent D-glucose residues are flipped, making cellobiose the fundamental repeating unit. The major hemicelluloses are shown. Xylan consists of repeating β-(1,4)-linked D-xylose residues with the potential for L-arabinose or acetyl substitutions at either the 2-O or 3-O positions or both; 2-O substitution with 4-hydroxy- or 4-methyl-glucuronic acid; and added complexity from substitutions (hexose, pentose and/or phenolics) on the L-arabinose side-chain residues [18,189–192]. Mannan consists of a β-(1,4)-linked D-mannose backbone, whereas the glucomannan backbone has both D-mannose and D-glucose residues with β-(1,4) linkages. Xyloglucan has a β-(1,4)-linked D-glucose backbone with D-xylose side chains, and the mixed-linkage β-glucan backbone has both β-(1,4)- and β-(1,3)-linked glucose residues.

(Adapted from reference 36, Jordan *et al*., 2012)

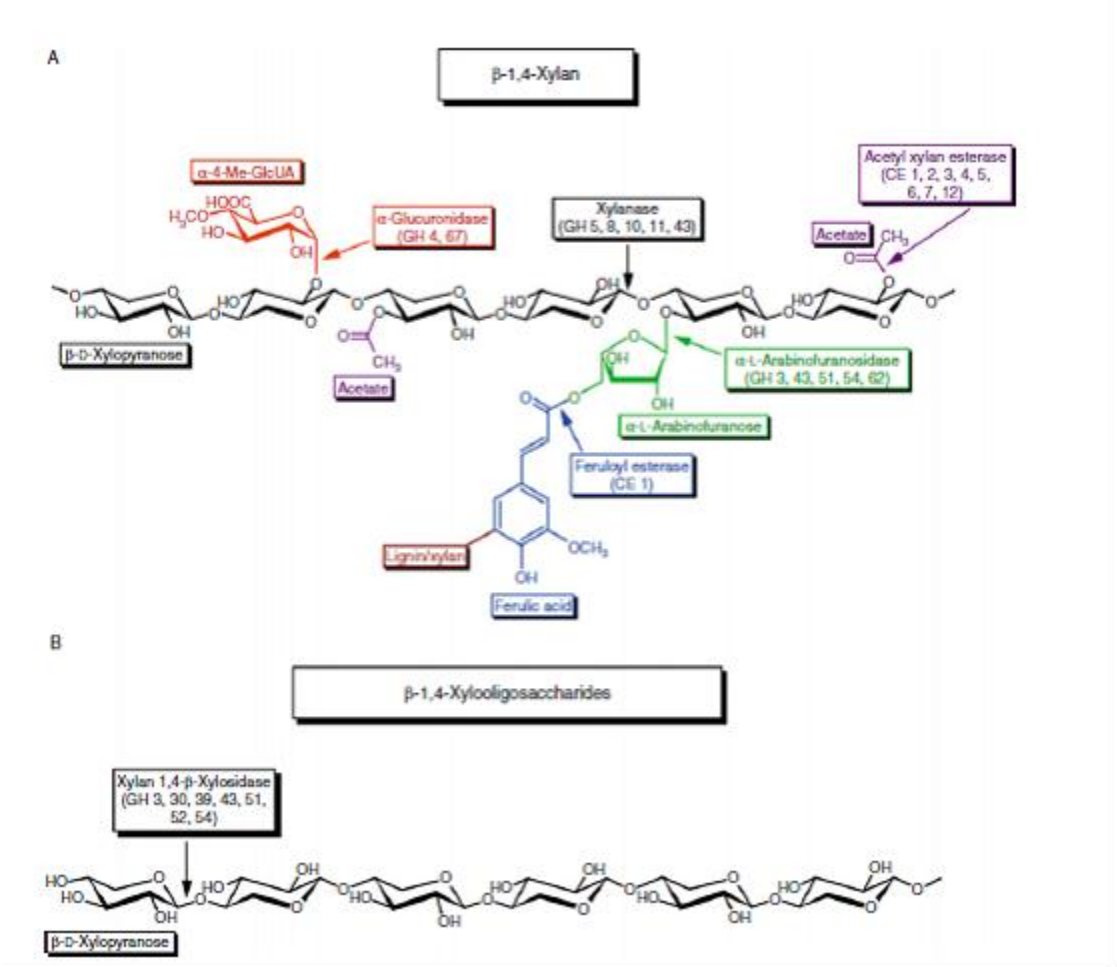

FIGURE 2 Enzymatic activities associated with xylan deconstruction. (A) Endoxylanases cleave the backbone of xylan chains to release shorter xylo-oligosaccharides which are further debranched by accessory enzymes. (B) b-Xylosidases release xylose monomers from the nonreducing ends of debranched xylo-oligosaccharides.

Adapted from Dodd and Cann (2009)

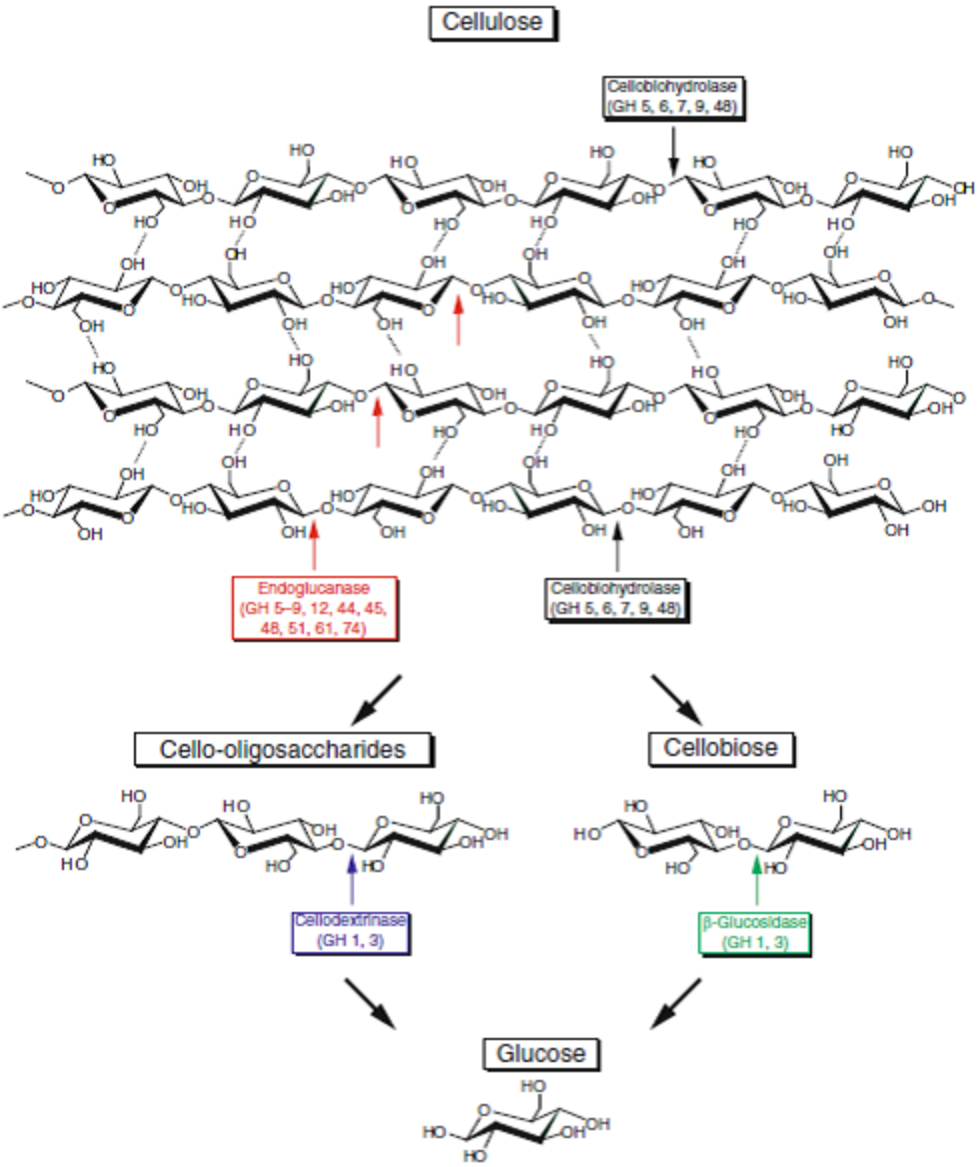

FIGURE 3 Enzymatic activities associated with cellulose deconstruction. Endoglucanase enzymes (indicated by red arrows) randomly cleave β-1,4 glucosidic linkages within the backbone of cellulose. Cellobiohydrolase enzymes (also known as exoglucanases) cleave cellobiose from either the reducing end or the nonreducing end of cellulose chains in a processive manner. Oligosaccharides released as a result of these activities are converted to glucose by the action of cellodextrinases, whereas the cellobiose released mainly by the action of cellobiohydrolases is converted to glucose by β-glucosidases.

Adapted from Dodd and Cann (2009)

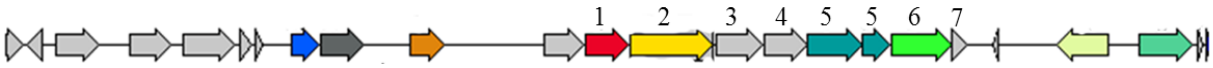

FIGURE 4: Genes in a hemicellulase gene cluster from *T. bryantii*.

Table 1a: Genes in a hemicellulase gene cluster and their predicted functions

Number	Gene	Predicted function
1	Tb888	endo-1,4-β-xylanase
2	Tb887	α-glucuronidase
3	Tb886	oxidoreductase
4	Tb885	oxidoreductase
5	Tb884/3	β-xylosidase
6	Tb882	β-xylosidase
7	Tb881	acetyl xylan esterase

Table 1b. Primers used for the expression of the genes in the hemicellulase gene cluster

Gene	Position	Primer sequence
tb881	Forward	5'-GACGACGACAAGATGGGACTTTTTGATATGCCATTA C-3'
	Reverse	5'-GAGGAGAAGCCCGGTTAAAGCTCCAGTAAAAATTGC -3'
tb882	Forward	5'-GACGACGACAAGATGATAAAAATAAAGATACCAAAAAATTC-3
	Reverse	5'-GAGGAGAAGCCCGGTCAATATCCGTTTATCTTGCTATC-3
tb884	Forward	5'-GACGACGACAAGATGATAAGTAAATCTTTTTATGCGC -3'
	Reverse	5'-GAGGAGAAGCCCGGTTAT TCATCCAC AGTATGCTGG -3'
tb885	Forward	5'-GACGACGAC AAGATGAGCAAAGAAAACGGCATGTAC -3'
	Reverse	5'-GAGGAGAAGCCCGGTCATTCTACCTTTATTGCATTTG -3'
tb886	Forward	5'-GACGACGACAAGATGATTAATATAGCCATTATTGGCGC -3'
	Reverse	5'-GAGGAGAAGCCCGGTTACTTAATATCTCTTCCAAATG -3'
tb887	Forward	5'-GACGACGACAAGATGTACGACTGCTGGCTTAGGTATAAG -3'
	Reverse	5'-GAGGAGAAGCCCGGTTATTCATAAATTTTCCTTCCATG -3'
tb888	Forward	5'-GACGACGACAAGATGCCTTCAAAGGGA AAAATG -3'
	Reverse	5'-GAGGAGAAGCCCGGTTAAAAATCAACTATGCTGTAAAAG -3'

Nucleotides added to facilitate ligation-independent cloning are underlined.

(All the genes above were cloned by Xiaoyun Su of the Cann Lab)

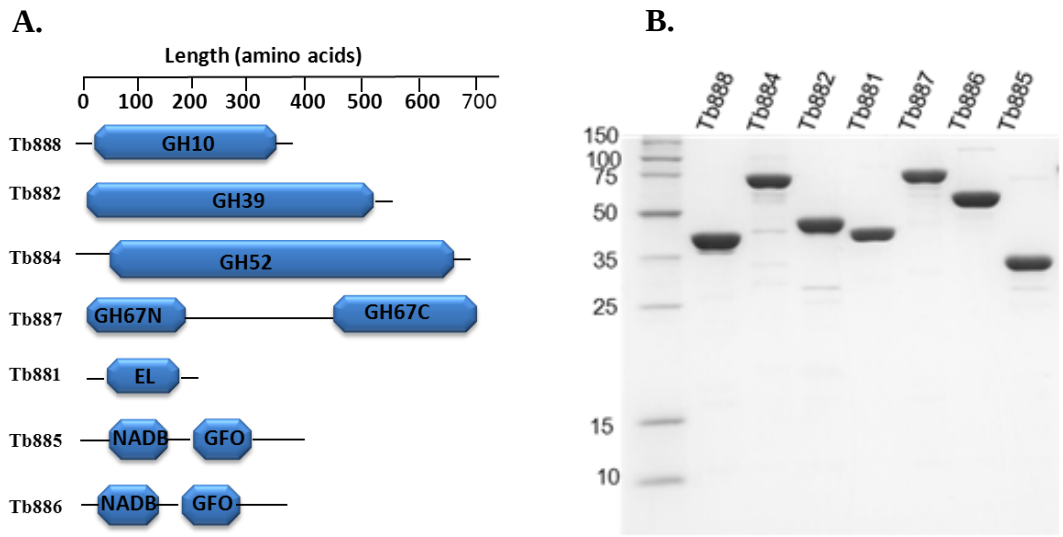

FIGURE 5 Hemicellulose-degrading enzymes of *T. bryantii*.

(A) Domain architectures of the putative endoxylanase (Tb888) and six putative accessory enzymes identified in genome sequence of *T. bryantii*. The functional domains were assigned by using the Pfam online server (http://www.sanger.ac.uk/Software/Pfam/). The numbers in the names refer to the predicted GH family of the protein.

(B) Purification of the predicted GH family proteins described in panel A. The elution fractions from cobalt affinity chromatography were pooled for each protein and analyzed by 12% SDS-PAGE.

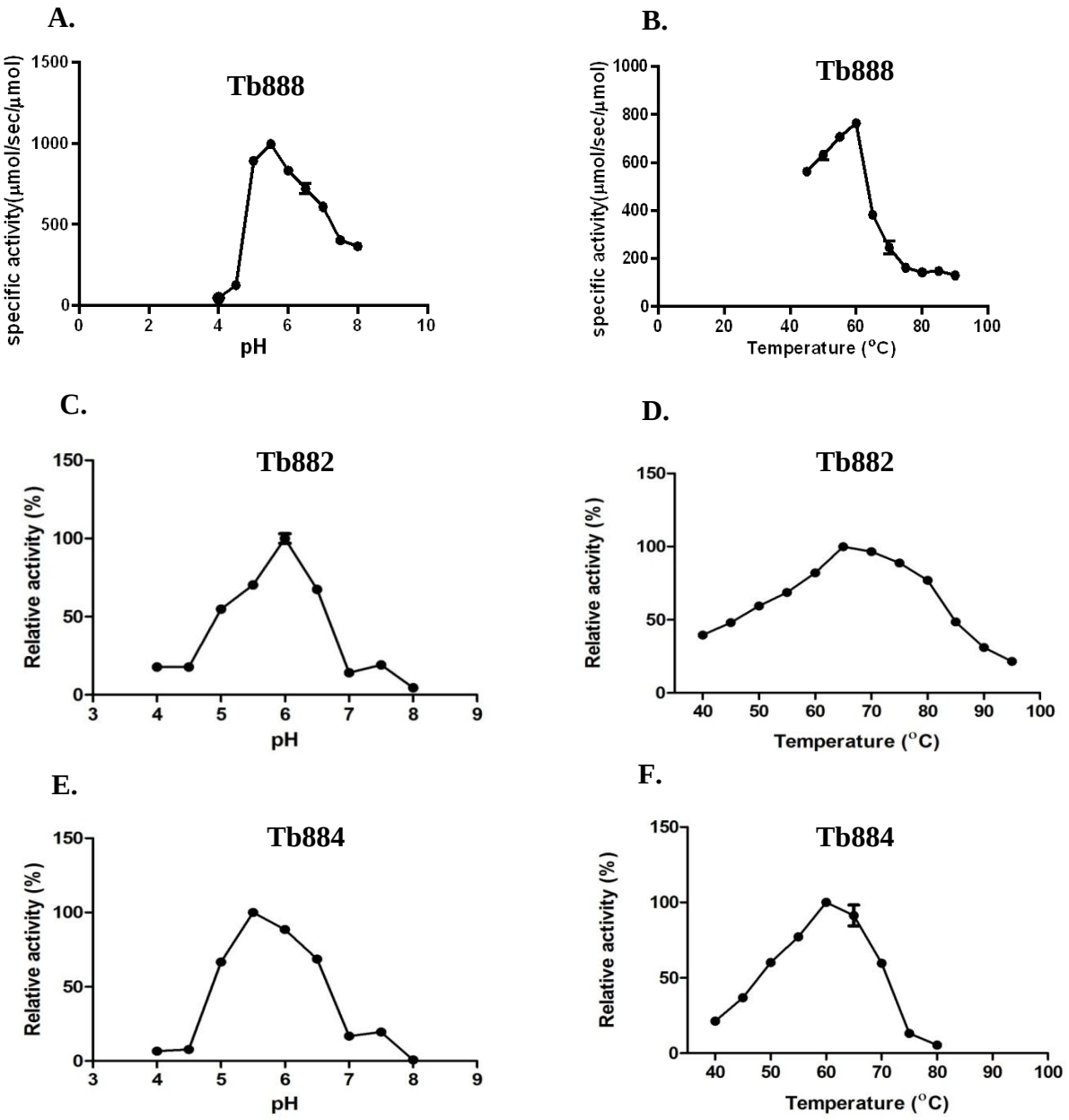

FIGURE 6 pH and temperature profiles of the Tb888, Tb882 and Tb884

Using WAX as a substrate, the optimum pH (A) and temperature (B) were determined for Tb888. *p*NP-β-D-xylopyranoside was used in case of both Tb882 and Tb884. The pH profiles for Tb882 and Tb884 are shown in (C) and (E) and temperature profiles in (D) and (F) respectively. Each protein was incubated with its substrate in either citrate buffer (50mM Na-Citrate with 150mM NaCl, pH 4.0-6.0) or phosphate buffer (50mM Na-Phosphate with 150mM NaCl, pH 6.0-8.0) in order to determine its optimum pH. Following the determination of the optimum pH values of the various proteins, they were each incubated with their substrates at different temperatures (40-95°C) in citrate buffer (50mM Na-Citrate with 150mM NaCl, pH 5.5 for Tb888 and Tb884, pH 6.0 for Tb882) for the determination of their optimum temperature values.

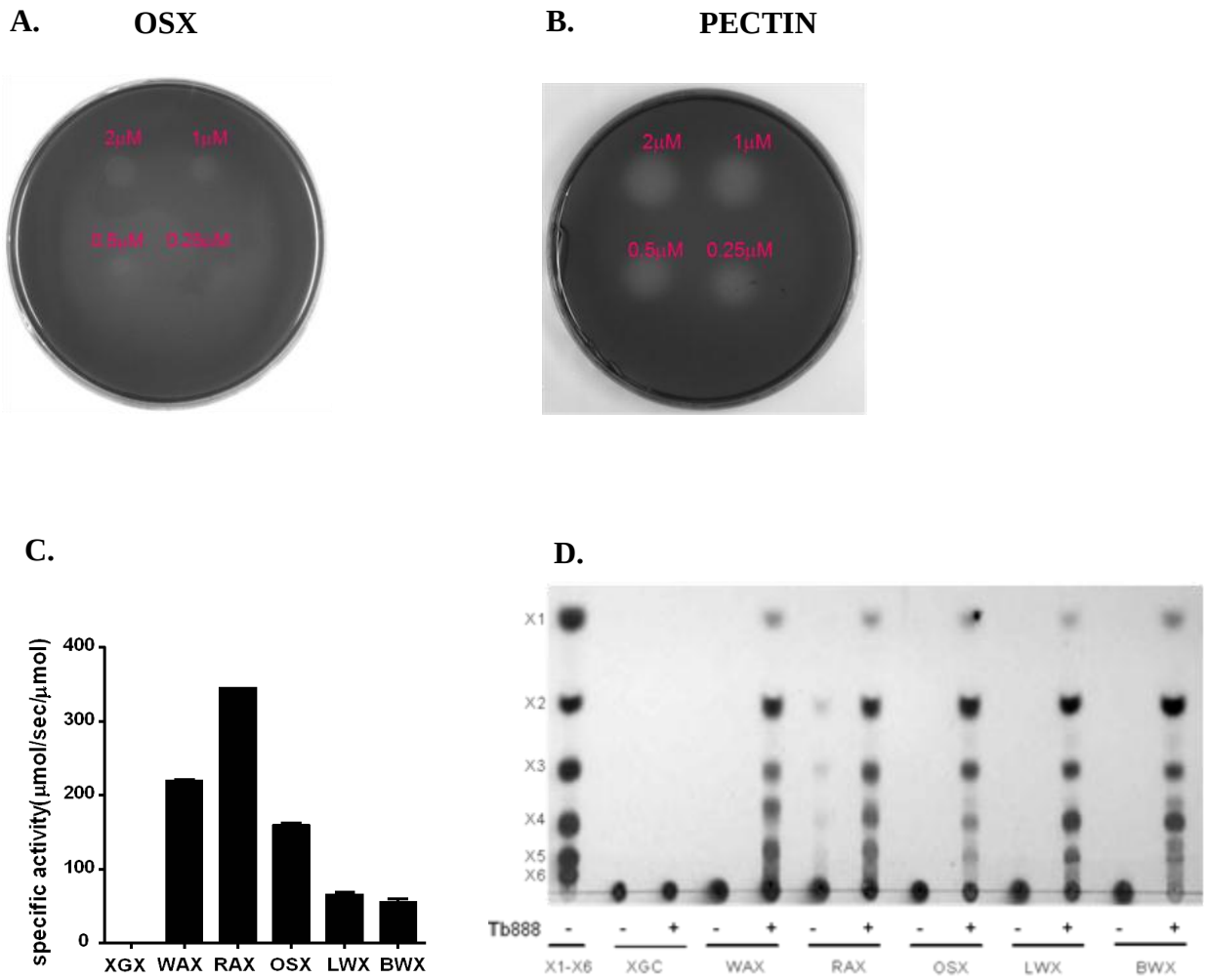

FIGURE 7 Hydrolysis of xylan substrates by the putative endoxylanase (Tb888) from *T. bryantii*.

Depolymerization of OSX (A) and pectin (B). Tb888 was assessed for its capacity to depolymerize OSX or pectin by incubating the protein on an agar plate infused with OSX or pectin followed by staining with Congo red. (C) Specific activity of Tb888. The final concentrations of the enzymes were 50 nM for reactions with all substrates. Each substrate was at 1% (wt/vol) in the reaction mixture. Bars are shown with standard errors for three independent experiments.(D) Hydrolysis products from (C) were concentrated and spotted on DC-Plastikfolien Silica Gel 60 F254 TLC plate from Merck (Whitehouse Station, NJ) with xylose and xylo-oligosaccharides as controls.

(The depolymerization of OSX and Pectin assays were done by Xiaoyun Su of the Cann Lab)

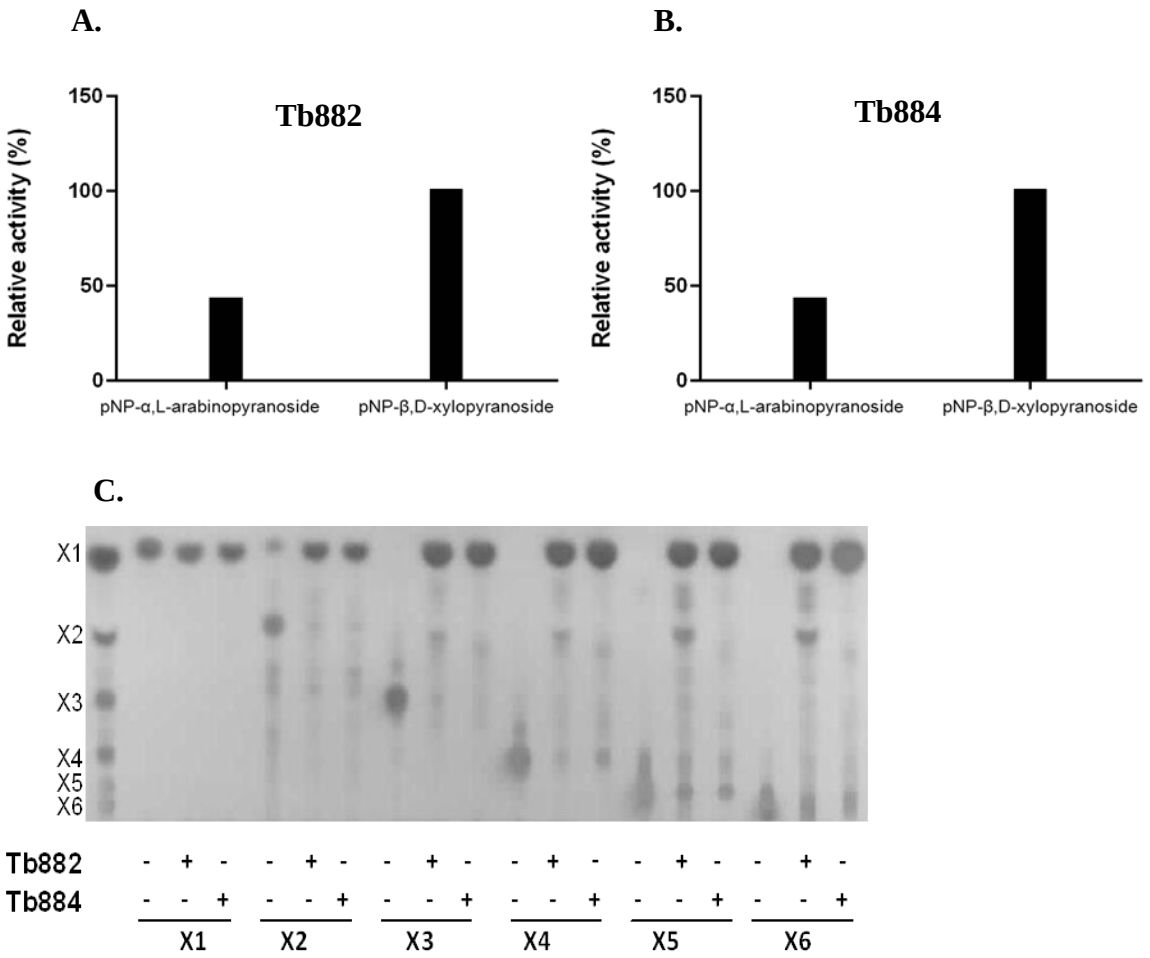

FIGURE 8 Hydrolytic activities of Tb882 and Tb884

To determine the substrate specificity for Tb882 (A) and Tb884 (B), the recombinant proteins were screened for activity on a library of α- and β-*para*-nitrophenol-linked monosaccharides. Incubation of enzymes with the substrates led to release of products that were quantified as a concentration of *p*NP equivalents from two of the fourteen *p*NP substrates (*p*NP-α-L-arabinopyranoside and *p*NP-β-D-xylopyranoside). (C) For measuring the hydrolysis of xylo-oligosaccharides, reaction mixtures (10 µl) were prepared in citrate buffer (50mM sodium phosphate, 150mM NaCl, pH 6.0 (Tb882) or pH 5.5 (Tb884)) with X1-X6 (20mM) and reactions were initiated by the addition of Tb882 and Tb884 (2µM, final concentration). Following incubation at 60 °C for 16h, hydrolysis products were centrifuged for 10mins and spotted onto a DC-Plastikfolien Silica Gel 60 F254 TLC plate from Merck (Whitehouse Station, NJ) to resolve the products described above.

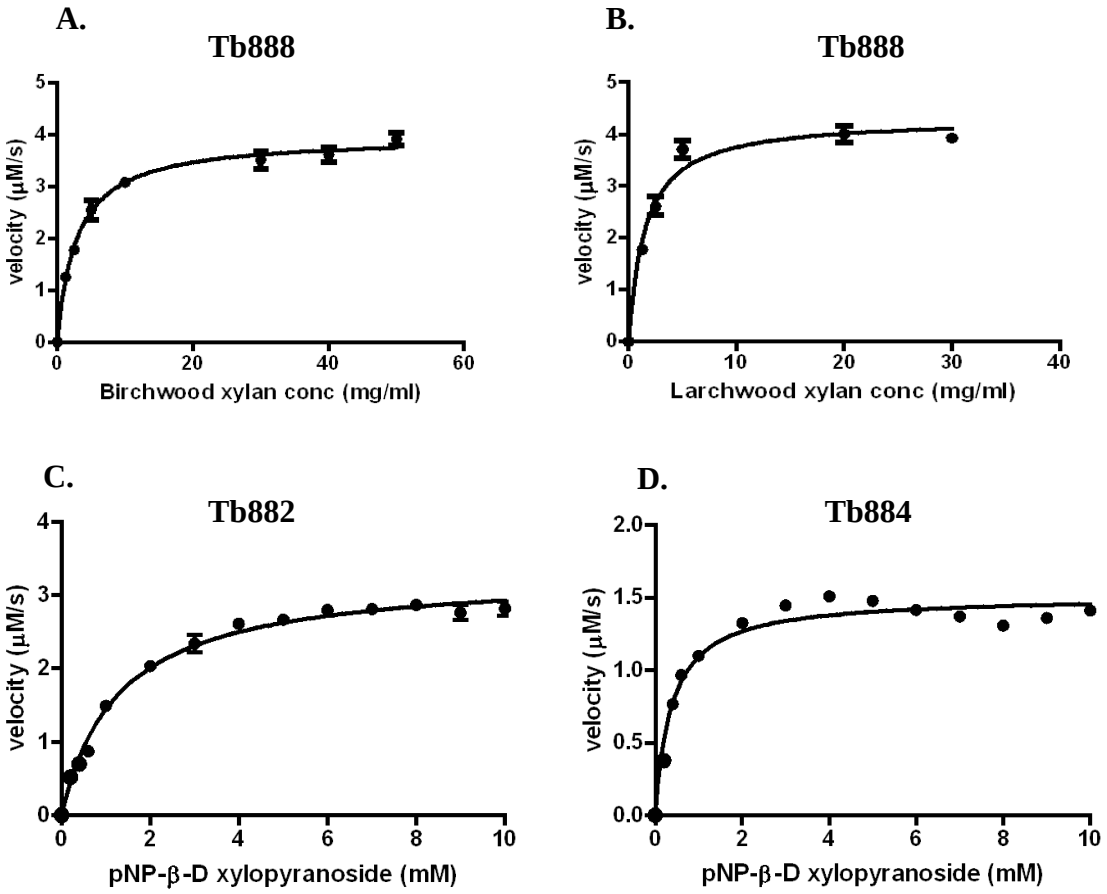

FIGURE 9 steady state kinetics of Tb888, Tb882 and Tb884

Tb888 was incubated with various concentrations (0-40mg/ml) of BWX and LWX and reducing ends estimated at different time points (3, 6 and 9min) using the PAHBAH assay. *p*NP-β-D-xylopyranoside (0-10 mM) was incubated in citrate buffer (50 mM sodium citrate, 150 mM NaCl, pH 6.0 (Tb882) or pH 5.5 (Tb884)) in a 1 cm path-length quartz cuvette and reactions were initiated by the addition of Tb882 (50nM) or Tb884 (10nM). Hydrolysis of each *p*NP substrate was continuously monitored by recording the UV signal at 400 nm. Initial rate data for all enzymes were then plotted against the various substrate concentrations and kinetic values were estimated by applying a nonlinear curve fit using GraphPad Prism v5.01 from GraphPad Software (San Diego, CA). The extinction coefficient for *para*-nitrophenol at pH 5.0 and a wavelength of 400 nm was measured as 319 M^{-1} cm^{-1}.

Table 2a: Determination of kinetic parameters of Tb888 with 2 substrates

Substrate	k_{cat} (s^{-1})	K_m (mg/mL)	k_{cat}/K_m ($mg/mL^{-1}s^{-1}$)
Larch wood xylan	172.52	1.51	114.25
Birch wood xylan	158.44	2.874	55.13

Table 2b: Determination of kinetic parameters of Tb882 and Tb884 with pNP-β,D-xylopyranoside

Enzyme	Substrate	k_{cat} (s^{-1})	K_m (mM)	k_{cat}/K_m ($mM^{-1}s^{-1}$)
Tb882	pNP-β,D-xylopyranoside	66.06± 1.04s^{-1}	1.29 ± 0.08	51.21
Tb884	pNP-β,D-xylopyranoside	150.9 ± 2.24 s^{-1}	0.38±0.03	394.97

Tables 2a shows the summary of the kinetic parameters of Tb888 as shown in fig 9A and B and Table 2b shows that of Tb882 and Tb884 as shown in fig 9C and D.

Tb888 was incubated with various concentrations (0-40mg/ml) of BWX and LWX and reducing ends estimated at different time points (3, 6 and 9min) using the PAHBAH assay. pNP-β-D-xylopyranoside (0-10 mM) was incubated in citrate buffer (50 mM sodium citrate, 150 mM NaCl, pH 6.0 (Tb882) or pH 5.5 (Tb884)) in a 1 cm path-length quartz cuvette and reactions were initiated by the addition of Tb882 (50nM) or Tb884 (10nM). Hydrolysis of each pNP substrate was continuously monitored by recording the UV signal at 400 nm. Initial rate data for all enzymes were then plotted against the various substrate concentrations and kinetic values were estimated by applying a nonlinear curve fit using GraphPad Prism v5.01 from GraphPad Software (San Diego, CA). The extinction coefficient for para-nitrophenol at pH 5.0 and a wavelength of 400 nm was measured as 319 M-1 cm-1.

A.

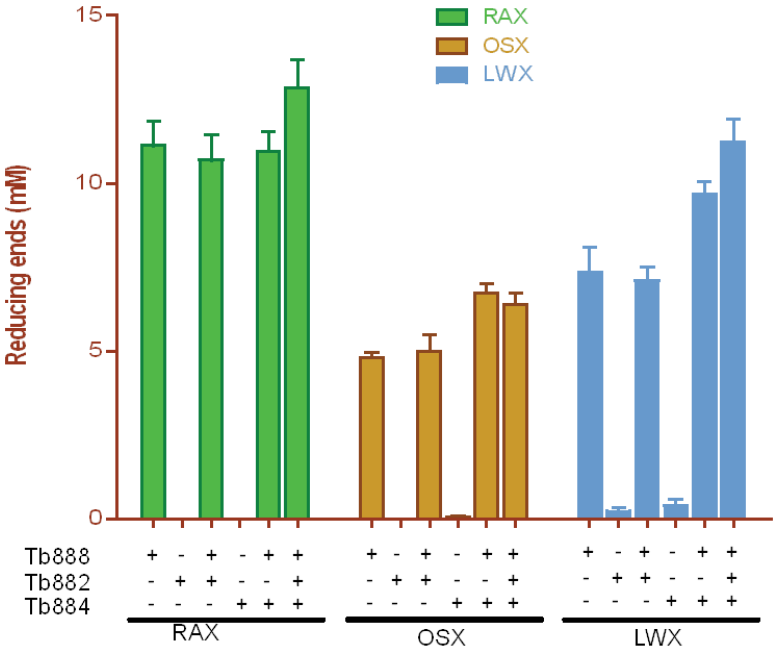

B.

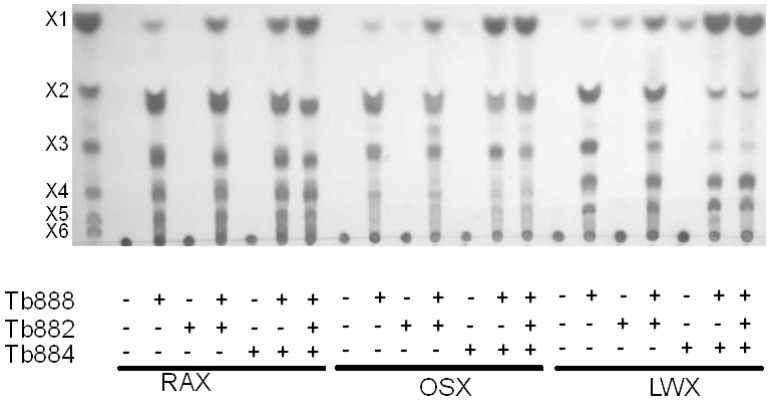

FIGURE 10 (cont. on the next page)

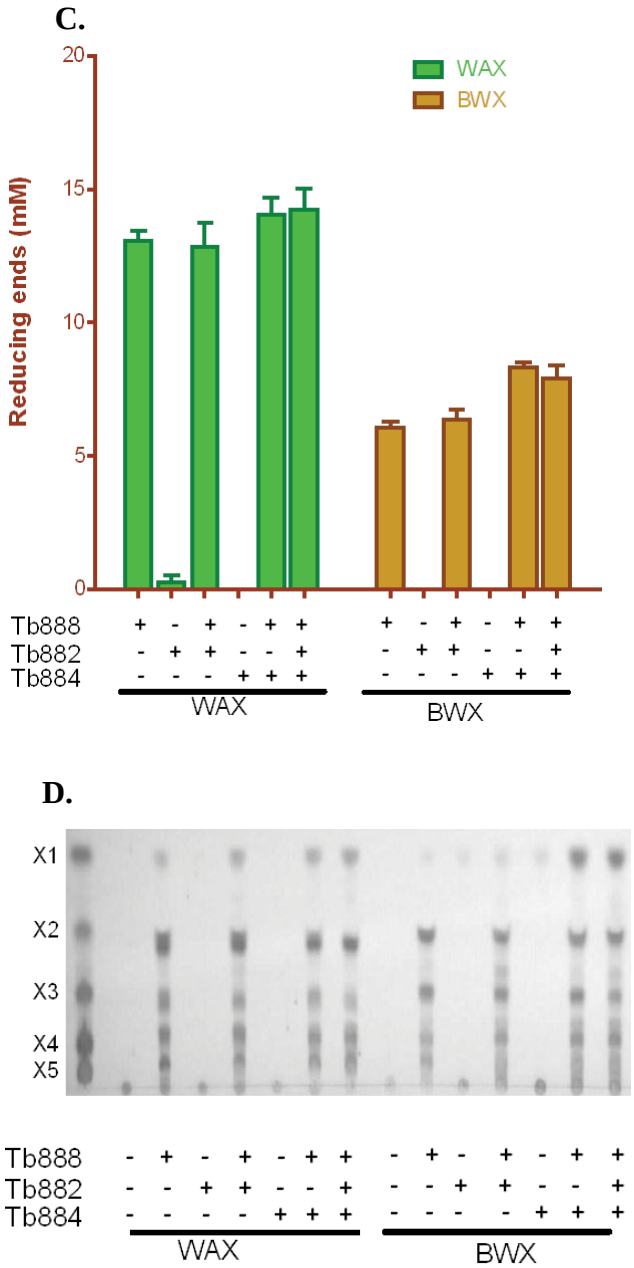

FIGURE 10. Functional analysis of Tb888, Tb882 and Tb884

Each substrate (1% wt/vol, final concentration) was incubated alone or co-incubated with Tb888 (5nM final concentration) or Tb882 (50nM final concentration) or Tb884 (5nM final concentration) or all three enzymes in various combinations in citrate buffer (50 mM sodium citrate, 150 mM NaCl, pH 5.5) at 60 °C for 16 hours. The concentration of reducing ends (A and C) were estimated using the *para*-hydroxybenzoic acid hydrazide (PAHBAH) assay as described previously (Lever, 1972) with xylose as a standard. For qualitative identification of the hydrolysis products, the reactions were resolved by thin layer chromatography (TLC) (B and D).

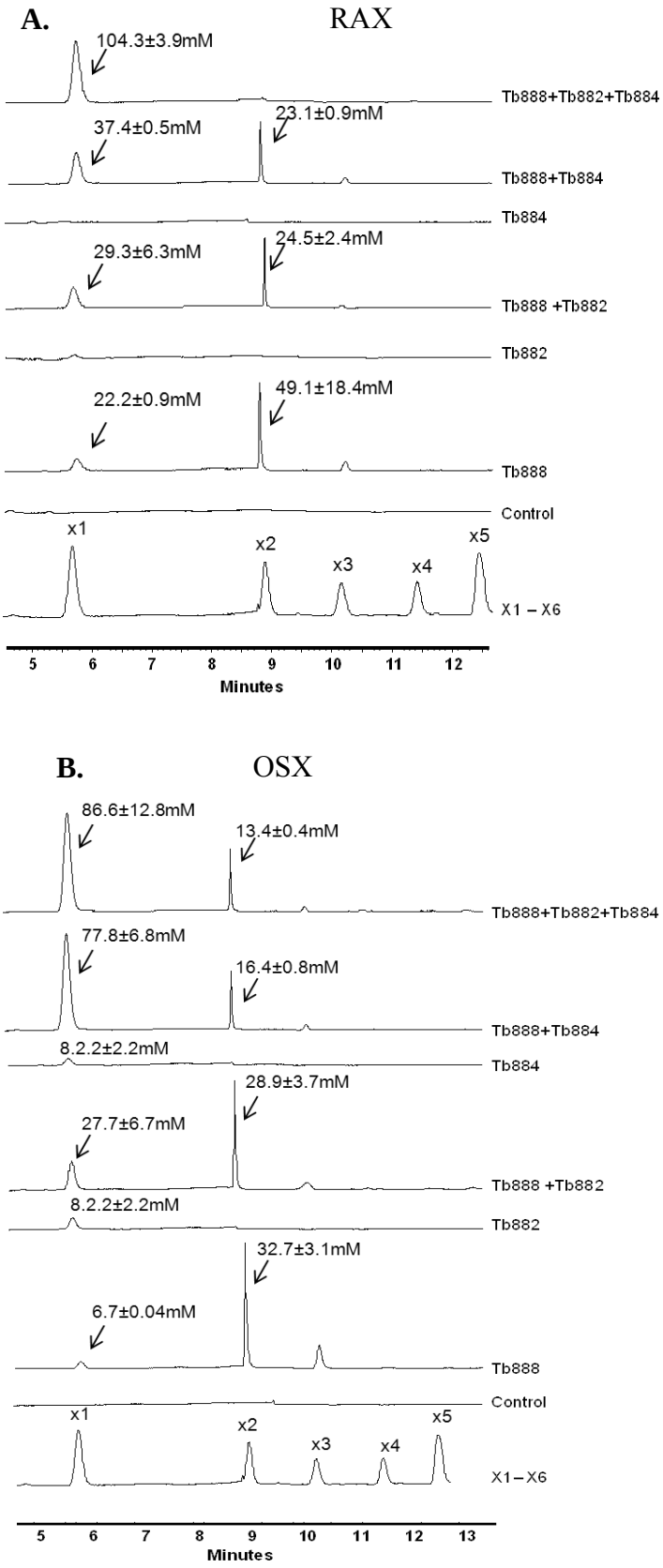

FIGURE 11 (cont. on the next page)

C. LWX

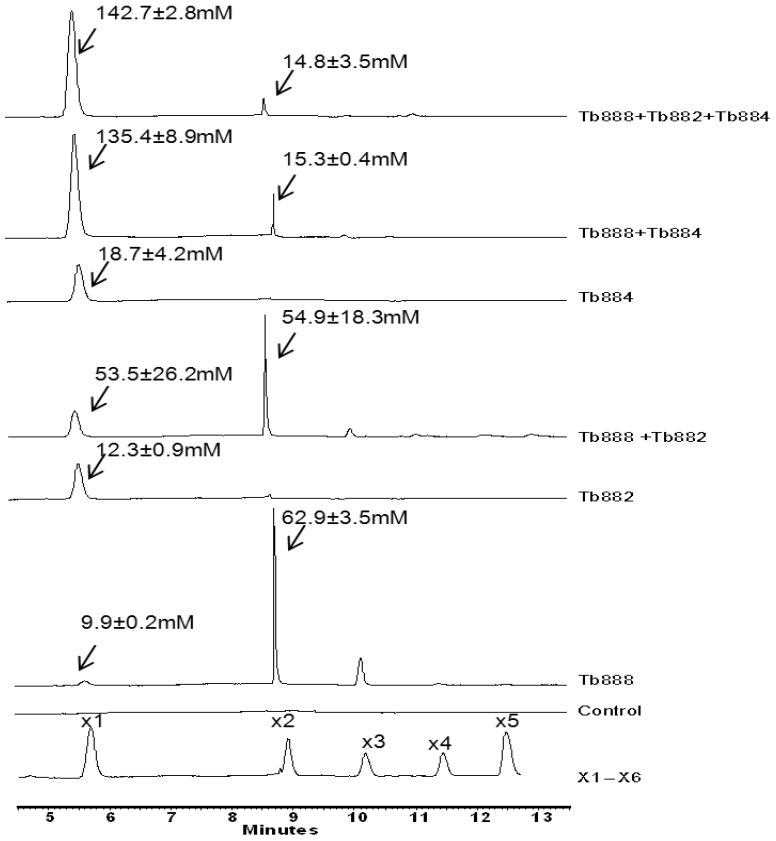

D. WAX

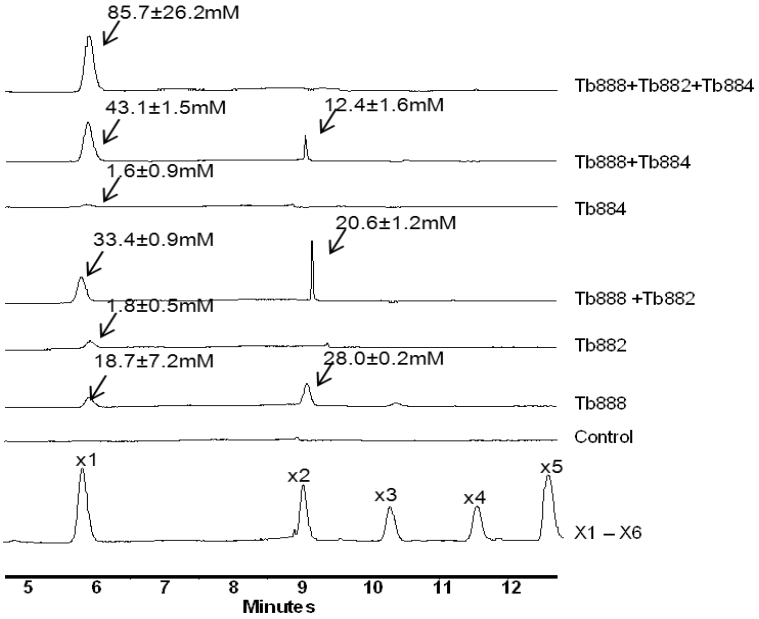

FIGURE 11 (cont. on the next page)

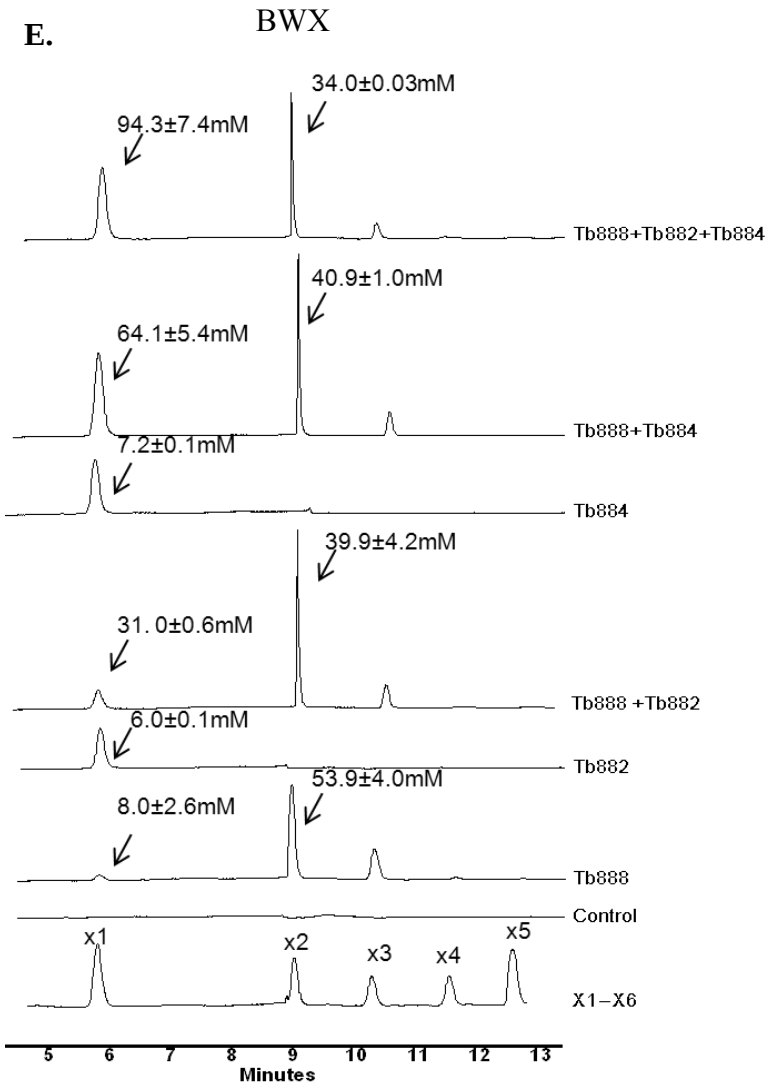

FIGURE 11 Functional analysis of Tb888, Tb882 and Tb884

Each substrate (1% wt/vol, final concentration) was incubated alone or co-incubated with Tb888 (5nM final concentration) or Tb882 (50nM final concentration) or Tb884 (5nM final concentration) or all three enzymes in various combinations in citrate buffer (50 mM sodium citrate, 150 mM NaCl, pH 5.5) at 60 °C for 16 hours. Resolving the hydrolysis products from Fig. 7 on HPLC. RAX (A), OSX (B), LWX (C), WAX (D) and BWX (E)

A.

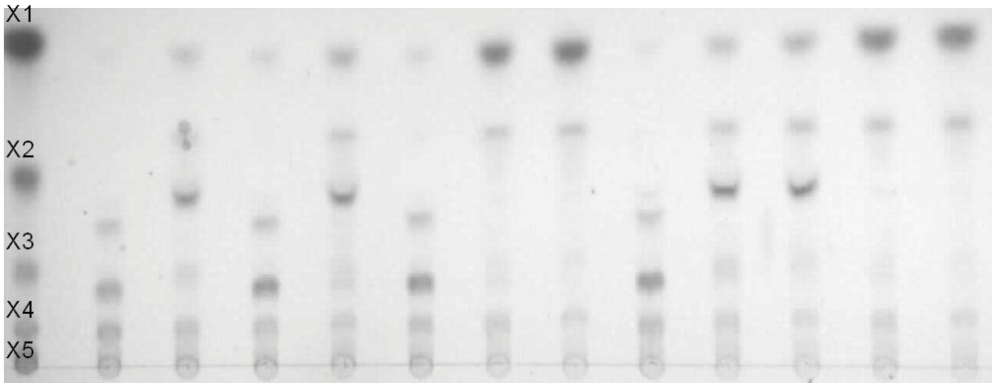

Tb887	-	+	-	+	-	+	+	-	+	+	+	+
Tb882	-	-	+	+	-	-	+	-	-	+	-	+
Tb884	-	-	-	-	+	+	+	-	-	-	+	+
Tb888	-	-	-	-	-	-	-	+	+	+	+	+

FIGURE 12. Catalytic activity of Tb887

The catalytic activity of the Tb887 was determined by its capacity to release xylo-oligosaccharides from aldouronic acids and also to function synergistically with a β-xylosidases (Tb882 and Tb884) and endoxylanase (Tb888) to release xylose from aldouronic acids. The hydrolytic products were analyzed by TLC using xylose (X1) and xylo-oligosaccharides (X2-X6) as standards

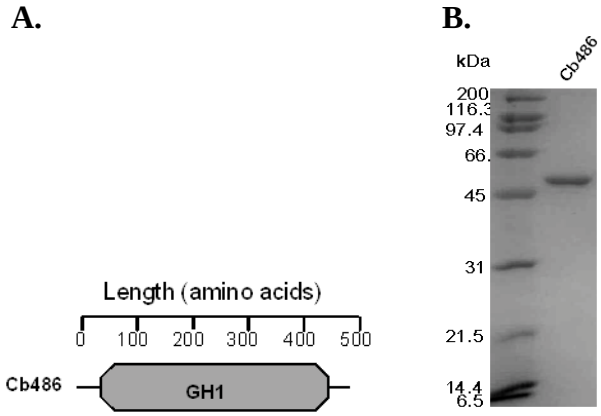

FIGURE 13 (A) Domain architecture of the putative β-glucosidase (Cb486) from the genome sequence C bescii. The functional domains were assigned by using the Pfam online server (http://www.sanger.ac.uk/Software/Pfam/). The number in the name refer to the predicted GH family of the protein.

(B) Purification of the predicted GH family protein described in panel A. The elution fractions from cobalt affinity chromatography were pooled for the protein and analyzed by 12% SDS-PAGE.

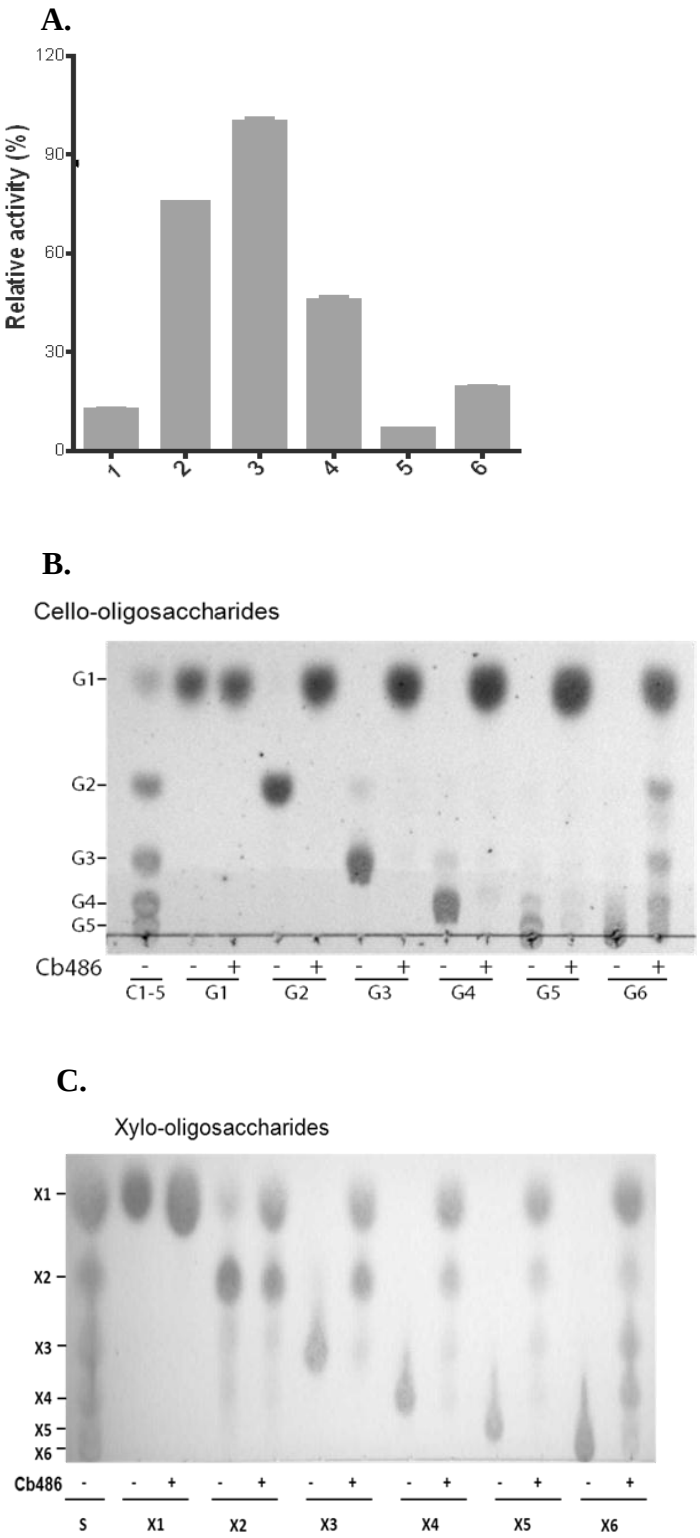

FIGURE 14 Hydrolytic activities of Cb486

(A) To determine the substrate specificity for Cb486, the recombinant protein was screened for activity on a library of α- and β-*para*-nitrophenol-linked monosaccharides. Incubation of enzymes with the substrates led to release of products that were quantified as a concentration of

*p*NP equivalents from six of the fourteen *p*NP substrates [(*p*NP-α-L-arabinopyranoside (1), *p*NP-β-D-fucopyranoside (2), *p*NP-β-D-galactopyranoside (3), *p*NP-β-D-glucopyranoside (4), *p*NP-β-D-xylopyranoside (5) and *p*NP-β-D-cellobioside (6)].

For measuring the hydrolysis of cello (B) and xylo-oligosaccharides (C), reaction mixtures (10 μl) were prepared in citrate buffer (50mM sodium phosphate, 150 mM NaCl, pH 5.5) with 20mM G1-G6 or 20mM X2-X6 and reactions were initiated by the addition of Cb486 (2μM, final concentration). This was followed by resolving of the products using TLC.

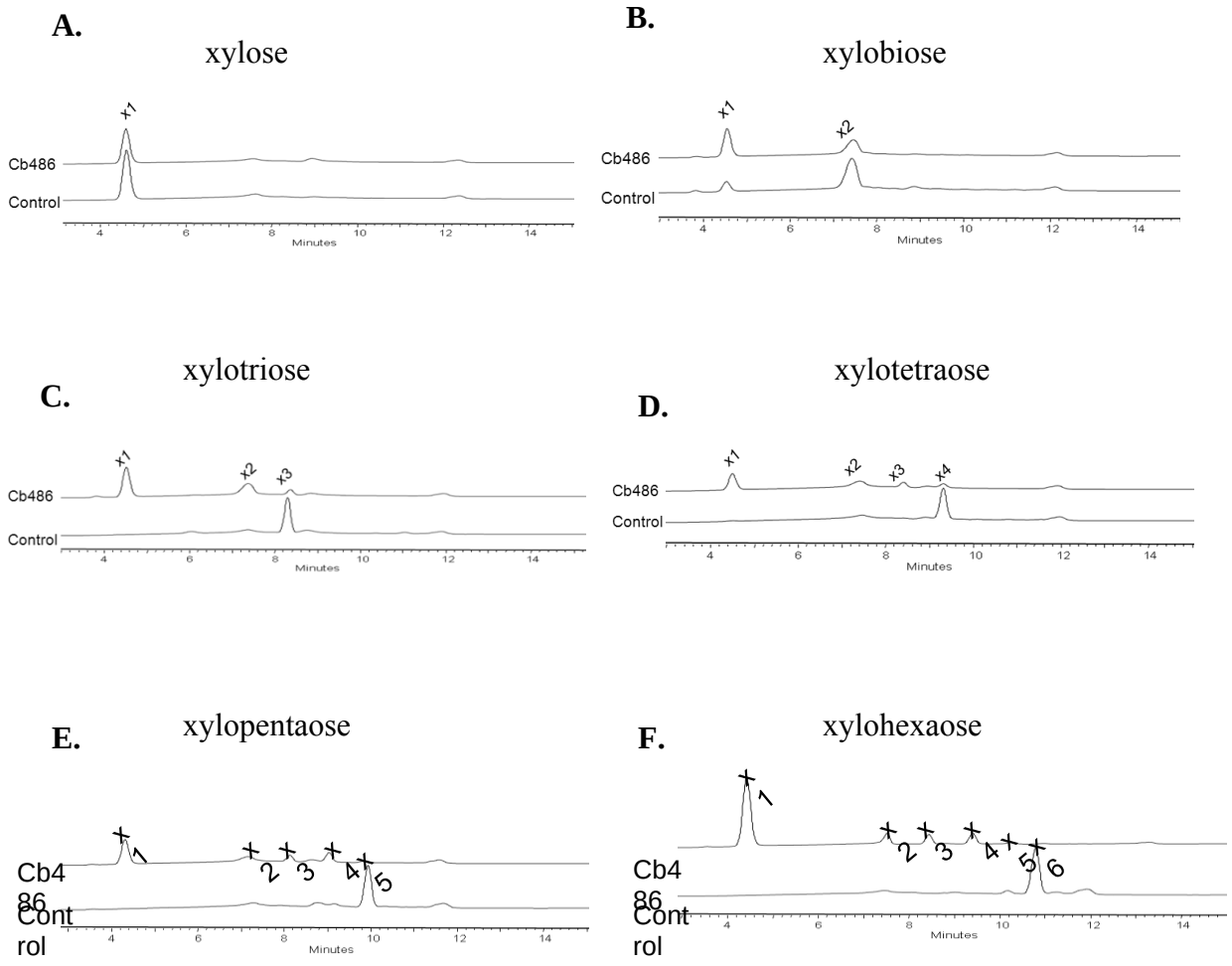

FIGURE 15 Hydrolytic activities of Cb486

For the detection of the hydrolysis products from the xylo-oligosaccharides, reaction mixtures (10 µl) were prepared in citrate buffer (50mM sodium phosphate, 150 mM NaCl, pH 5.5) with 20mM G1-G6 or 20mM X2-X6 and reactions were initiated by the addition of Cb486 (2µM, final concentration). Hydrolysis products from the xylo-oligosaccharides were then resolved using HPLC. (A) xylose (B) xylobiose (C) xylotriose (D) xylotetraose (E) xylopentaose (F) xylohexaose

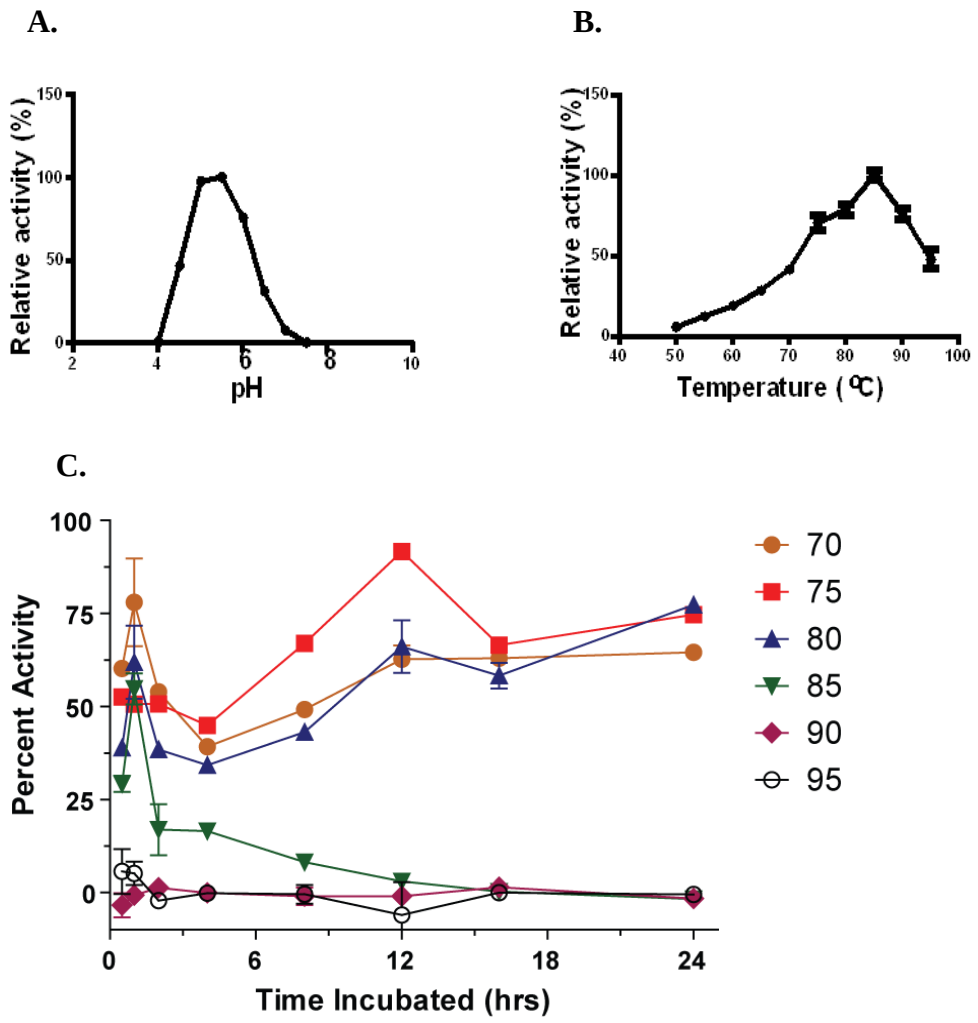

FIGURE 16 pH and temperature and thermostability profiles of Cb486

(A) pH profile of Cb486. 10nM Cb486 was incubated with *p*NP-β-D-galactopyranoside (1.0mM final concentration) prepared in citrate buffer (50mM Na-citrate with 150mM NaCl, pH 4.0-6.0) or phosphate buffer (50mM Na-phosphate with 150mM NaCl, pH 6.0-8.0). (B) Temperature of Cb486. 10nM Cb486 was incubated with *p*NP-β-D-galactopyranoside (1.0mM final concentration) prepared in citrate buffer (50mM Na-citrate with 150mM NaCl, pH 5.5). The release of *p*NP was continuously monitored by recording the UV signal at 400 nm for 5 minutes. (C) thermostability of Cb486. Five µM Cb486 was kept at different temperatures (50 ºC, 55 ºC, 60 ºC, 65 ºC, 70 ºC, 75 ºC, 80 ºC, 85 ºC, 90 ºC and 95 ºC). The samples were taken out at certain time points (0 h, 0.5 h, 1 h, 2 h, 4 h, 8h, 12 h and 24 h) and immediately applied to enzyme activity measurement.

(The thermostability assay was done by Michael Iakiviak of the Cann Lab)

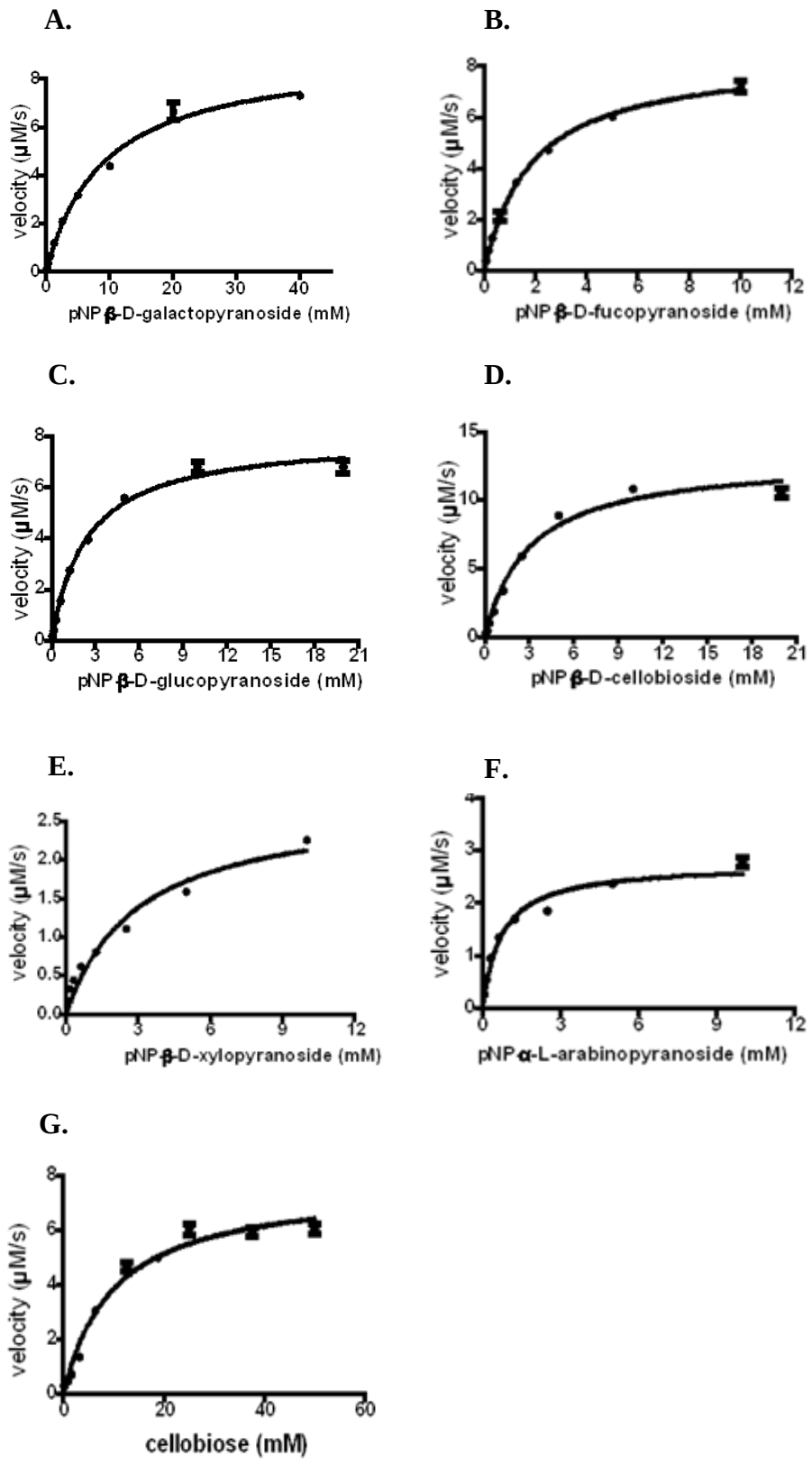

FIGURE 17 (cont. on the next page)

FIGURE 17 the kinetic data of Cb486 on the six α- and β-*para*-nitrophenol-linked monosaccharides and the natural substrate, cellobiose

*p*NP-β-D-fucopyranoside or *p*NP-α-L-arabinopyranoside or *p*NP-β-D-xylopyranoside (0 to 10mM) or *p*NP-β-D-glucopyranoside or *p*NP-β-D-cellobioside (0 to 20mM) or *p*NP-β-D-galactopyranoside (0 to 40mm) was incubated in citrate reaction buffer (100 µl) (50 mM sodium citrate, 150 mM NaCl [pH 5.5]). The reaction was initiated by adding 25µl of Cb486 (10nM final concentration) to substrates; *p*NP-β-D-galactopyranoside, *p*NP-β-D-fucopyranoside, and *p*NP-β-D-glucopyranoside or Cb486 (50nM final concentration) to substrates; *p*NP-β-D-cellobioside, *p*NP-α-L-arabinopyranoside and *p*NP-β-D-xylopyranoside, and mixed by pipetting up and down for several times at 85 ºC. The hydrolysis of *p*NP substrates was continuously monitored by recording the UV signal at 400 nm for 5 minutes.

The Glucose Oxidase reagent set from Pointe Scientific Inc was used in the case of the natural substrate, cellobiose as described above.

Table 3: Determination of kinetic parameters of Cb486 with various substrates

Substrate	k_{cat} (s^{-1})	K_m (mM)	k_{cat}/K_m ($mM^{-1}s^{-1}$)
pNP-β-D-galactopyranoside	910.2±27.2	9.0±0.7	101.1±8.4
pNP-β-D-fucopyranoside	838.7±17.8	1.8±0.1	465.9±27.7
pNP-β-D-glucopyranoside	800.2±18.1	2.4±0.2	333.4±28.8
pNP-β-D-cellobioside	261.6±8.5	3.0±0.3	87.2±9.2
pNP-β-D-xylopyranoside	55.0±3.7	3.0±0.5	18.3±3.3
pNP-α-L-arabinopyranoside	54.9±1.7	0.7±0.1	78.4±11.5
cellobiose	153.4±5.4	9.9±1.1	15.5±1.8

Table 3 shows a summary of the kinetic paramaters of Cb486 with various substrates.

*p*NP-β-D-fucopyranoside or *p*NP-α-L-arabinopyranoside or *p*NP-β-D-xylopyranoside (0 to 10mM) or *p*NP-β-D-glucopyranoside or *p*NP-β-D-cellobioside (0 to 20mM) or *p*NP-β-D-galactopyranoside (0 to 40mm) was incubated in citrate reaction buffer (100 µl) (50 mM sodium citrate, 150 mM NaCl [pH 5.5]). The reaction was initiated by adding 25µl of Cb486 (10nM final concentration) to substrates; *p*NP-β-D-galactopyranoside, *p*NP-β-D-fucopyranoside, and *p*NP-β-D-glucopyranoside or Cb486 (50nM final concentration) to substrates; *p*NP-β-D-cellobioside, *p*NP-α-L-arabinopyranoside and *p*NP-β-D-xylopyranoside, and mixed by pipetting up and down for several times at 85 ºC. The hydrolysis of *p*NP substrates was continuously monitored by recording the UV signal at 400 nm for 5 minutes.

The Glucose Oxidase reagent set from Pointe Scientific Inc was used in the case of the natural substrate, cellobiose as described above.

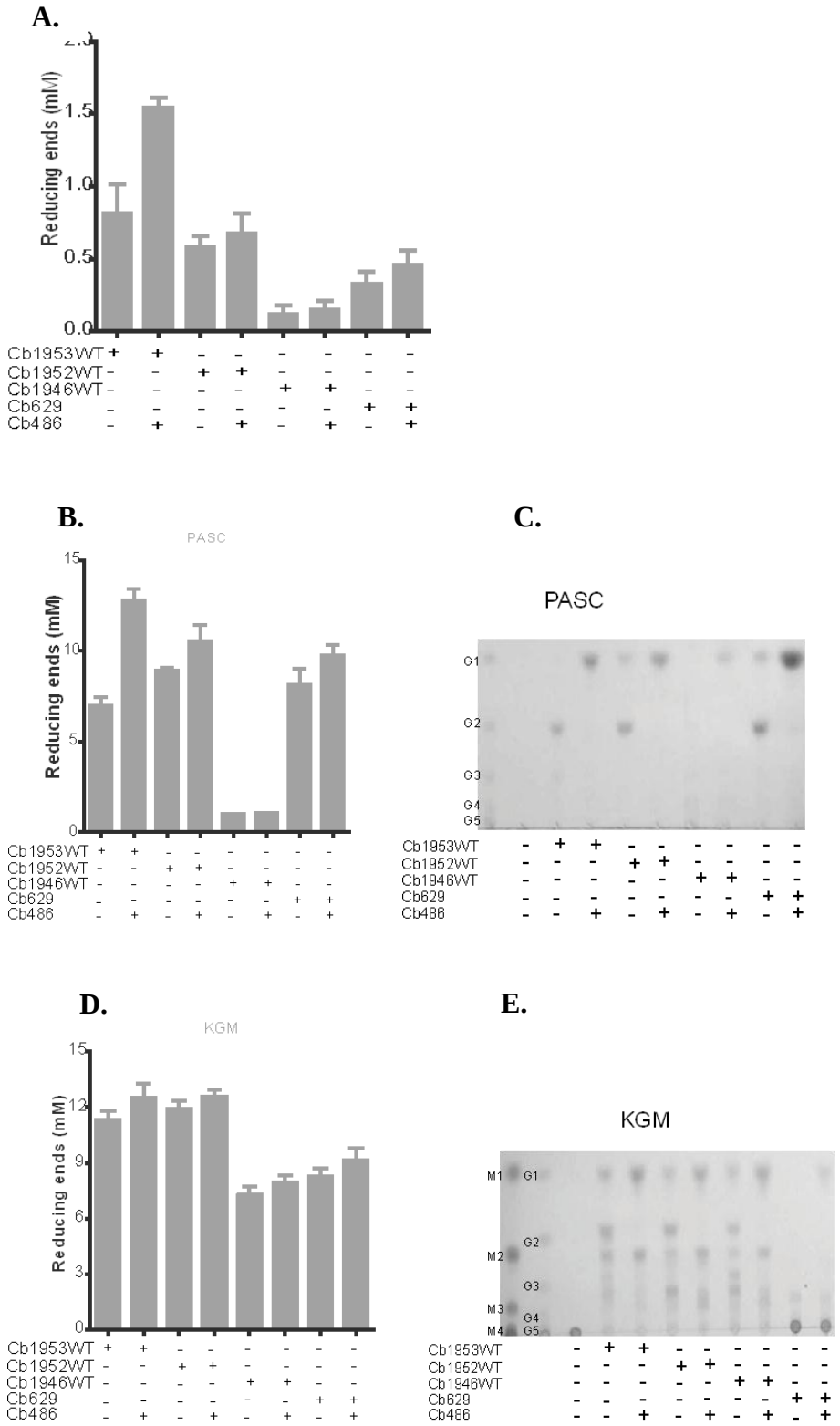

FIGURE 18 (cont. on the next page)

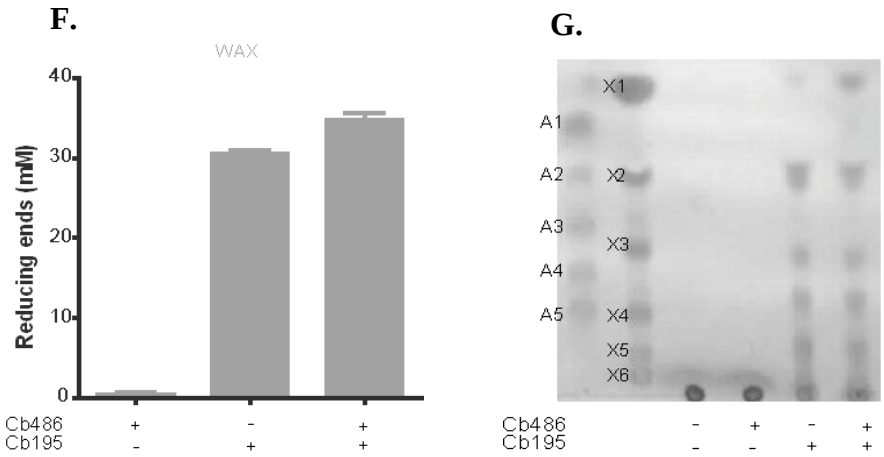

FIGURE 18 Hydrolysis of various polysaccharides by Cb486

Avicel (10% wt/vol, final concentration), konjac glucomannan (5% wt/vol, final concentration) and phosphoric acid swollen cellulose (5% wt/vol, final concentration) was each incubated alone or co-incubated with each endoglucanase (Cb1953WT, Cb1952WT, Cb1946WT and Cb629 [0.5µM final concentration]) alone or with Cb486 (0.5µM final concentration) in citrate buffer (50mM sodium citrate, 150mM NaCl, pH 5.5) at 75°C for 16 hours. The concentration of reducing ends, of Avicel (A), PASC (B) konjac glucomannan (D) and WAX (F) were estimated using the *para*-hydroxybenzoic acid hydrazide (PAHBAH) assay as described previously (Lever, 1972) with glucose as a standard. For qualitative identification of the hydrolysis products, the reactions were resolved by thin layer chromatography (TLC), PASC (D) konjac glucomannan (F) and WAX (H).

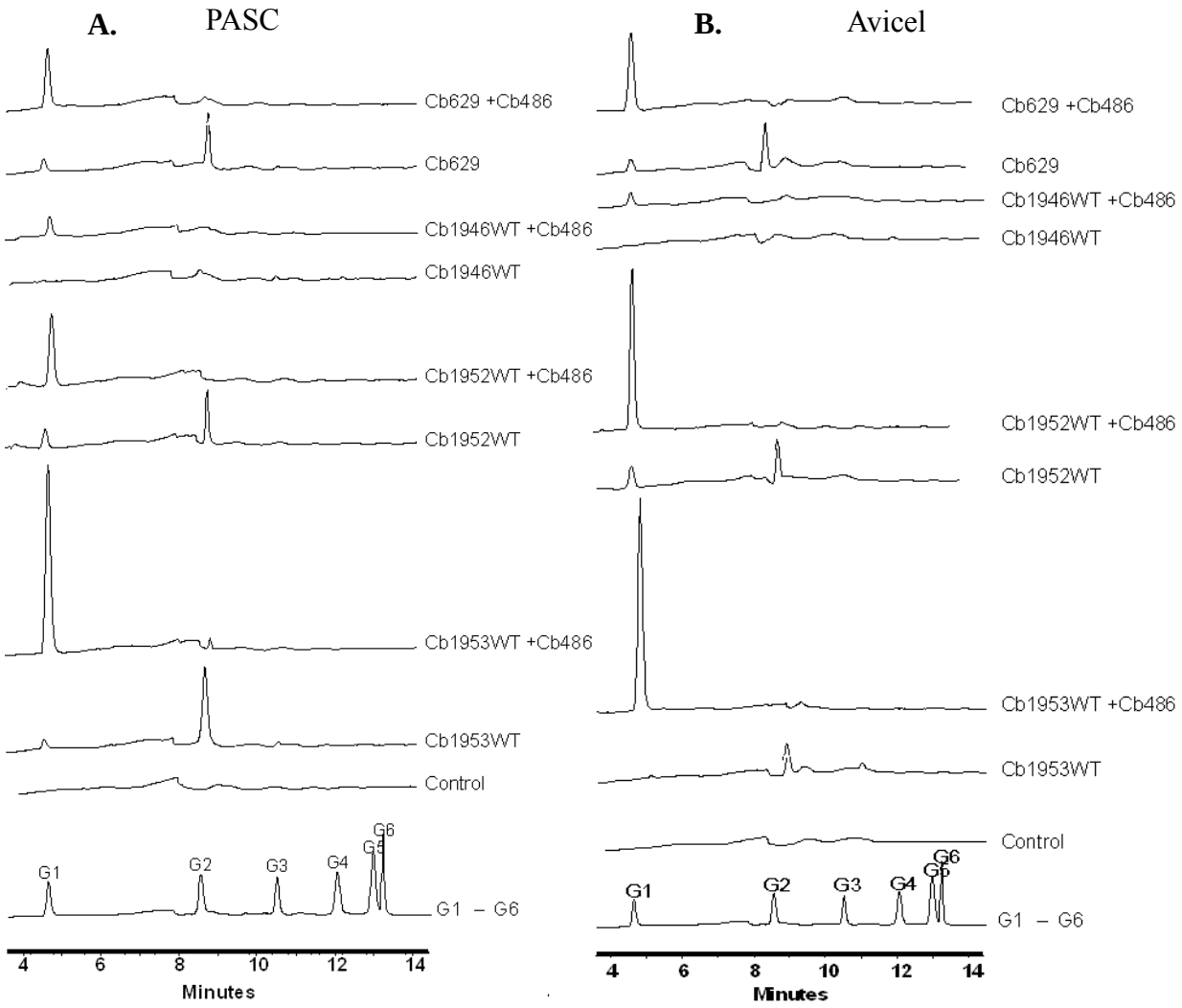

FIGURE 19 Hydrolysis of various polysaccharides by Cb486

Avicel (10% wt/vol, final concentration), and phosphoric acid swollen cellulose (5% wt/vol, final concentration) was each incubated alone or co-incubated with each endoglucanase (Cb1953WT, Cb1952WT, Cb1946WT and Cb629 [0.5µM final concentration]) alone or with Cb486 (0.5µM final concentration) in citrate buffer (50mM sodium citrate, 150mM NaCl, pH 5.5) at 75°C for 16 hours.Resolving the hydrolysis products from on the HPLC. PASC (A) and Avicel (B)

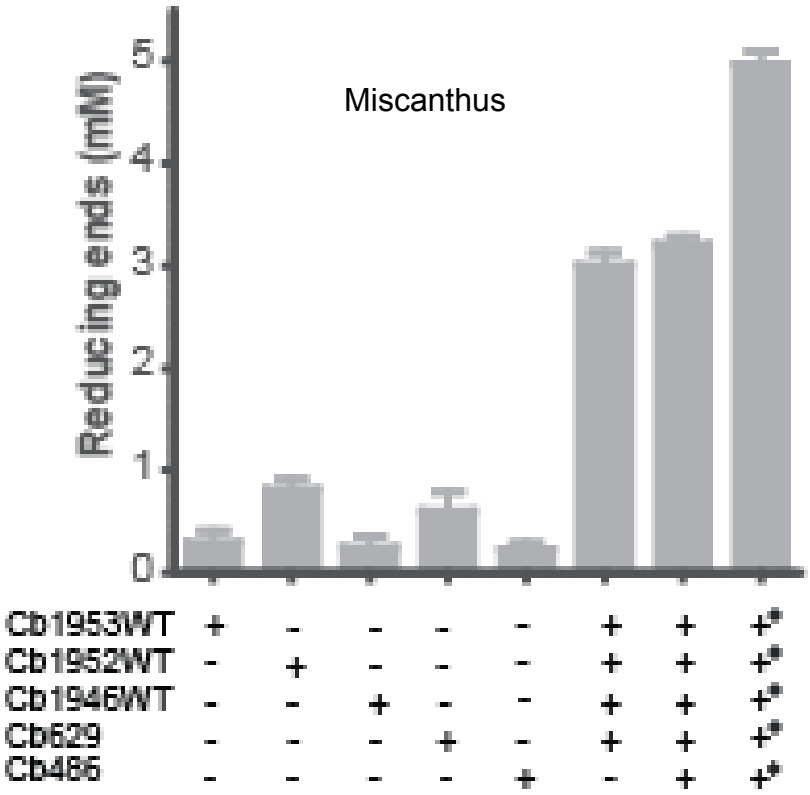

FIGURE 20 Hydrolysis of Pretreated (microwaved) Miscanthus

Pretreated Miscanthus (50% wt/vol, final concentration) was incubated alone or co-incubated with each or all four endoglucanases (0.5µM final concentration) and Cb486 (0.5µM final concentration) in citrate buffer (50mM sodium citrate, 150mM NaCl, pH 5.5) at 75°C for 16 hours. The concentration of reducing ends, in the hydrolysis product were estimated using the *para*-hydroxybenzoic acid hydrazide (PAHBAH) assay as described previously (Lever, 1972) with glucose as a standard

+*: Each enzyme was at 1µM concentration compared to 0.5µM in all other setups.

Table 4: Sugar concentrations in microwaved Miscanthus hydrolysis products

Protein	Glucose (μM)	Cellobiose (μM)	Cellotriose (μM)	Cellotetraose (μM)	% hydrolyzed
Cb1953WT	32.97± 0.41	85.28± 3.06	8.44± 0.09	0	0.069
Cb1952WT	0	164.47±2.08	27.76±0.34	0	0.124
Cb1946WT	0	8.30± 0.52	13.39± 1.01	22.59± 2.01	0.044
Cb629	1.44±0.04	91.57±6.19	15.98± 1.06	0.39±0.04	0.070
Cb486	0.35±0.03	0.22±0.02	0	0	0
4 enzymes	313.09± 32.02	1096.73± 25.30	25.52± 4.03	0	0.776
5 enzymes	866.97± 85.15	830.84± 66.13	20.32± 1.04	0	0.777
5 enzymes (1μM)	2465.92±322.23	1319.73± 119.09	0	0	1.533

Table 4 shows the concentrations of the various sugars from the hydrolysis products from Fig.17. This was obtained from HPLC analysis of the hydrolysis products.

REFERENCES

Bao, L., Huang, Q., Chang, L., Sun, Q., Zhou, J., Lu, H. (2012) Cloning and characterization of two β-glucosidase/xylosidase enzymes from yak rumen metagenome. Appl. Biochem. Biotechnol. 166:72-86.

Bertani, G. (1951) Studies on lysogenesis. I. The mode of phage liberation by lysogenic Escherichia coli. J. Bacteriol. 62:293–300.

Bertani, G. (2004) Lysogeny at mid-twentieth century: P1, P2, and other experimental systems. J. Bacteriol. 186:595–600.

Biely, P. (1985) Microbial xylanolytic systems, Trends Biotechnol. 3:286-290.

Biely, P. (2003) Xylanolytic enzymes. In ‘‘Handbook of Food Enzymology’’ (J. R. Whitaker, A. G. J. Voragen and D. W. S. Wong, Eds.), Marcel Dekker, New York.

Biely, P., de Vries, R. P., Vrsanska, M., Visser, J. (2000) Inverting character of α-glucuronidase A from *Aspergillus tubingensis*. Biochim. Biophys. Acta 1474:360–364.

Biely, P., Kratky, Z., Vrsanska, M. (1981) Substrate-binding site of endo-1,4-beta-xylanase of the yeast *Cryptococcus albidus*. Eur. J. Biochem. 119:559–564.

Biely, P., MacKenzie, C. R., Puls, J., Schneider, H. (1986) Co-operativity of esterases and xylanases in the enzymatic degradation of acetyl xylan. Nat. Biotechnol. 4:731–733.

Biely, P., Vrsanska, M., Tenkanen, M., Kluepfel, D. (1997b) Endo-beta-1,4-xylanase families: differences in catalytic properties. J. Biotechnol. 57:151–166.

Bouveng, H. O. (1961) Phenylisocyanate derivatives of carbohydrates. 11. Location of O-acetyl groups in birch xylan. Acta Chem. Scand. 15:96-100.

Bray, M. R., Clarke A. J. (1992) Action pattern of xylo-oligosaccharide hydrolysis by Schizophyllum commune xylanase A. Eur. J. Biochem. 204:191–196.

Brett, C. T., Waldren, K. (1996) Physiology of plant cell walls. In ‘‘Topics in plant functional biology’’ (M. Black and B. Charlewood, Eds.), Chapman and Hall, London.

Caffall, K.H., Mohnen, D., (2009) The structure, function, and biosynthesis of plant cell wall pectic polysaccharides. Carbohydr. Res. 344:1879-900.

Cann, I. K., Ishino, S., Yuasa, M., Daiyasu, H., Toh, H., Ishino, Y. (2001) Biochemical analysis of replication factor C from the hyperthermophilic archaeon *Pyrococcus furiosus*. J. Bacteriol. 183:2614–2623.

Cantarel, B. L., Coutinho, P. M., Rancurel, C., Bernard, T., Lombard, V., Henrissat, B. (2009) The carbohydrate-active enzymes database (CAZy), an expert resource for glycogenomics. Nucleic Acid. Res. 37:D233-238.

Catic, I., Rujnic-Sokele, M., (2008) Agriculture products - food for living being or for machinery. Polimeri 4:243-243.

Chen, F., Dixon, R. A. (2007) Lignin modification improves fermentable sugar yields for biofuel production. Nat. Biotechnol. 25:759–761

Claassen, P.A.M., van Lier, J.B., Contreras, A.M.L., van Niel, E.W.J., Sijtsma, L., Stams A.J.M., de Vries, S.S., Weusthuis, R.A.. (1999) Utilisation of biomass for the supply of energy carriers. Appl. Microbiol. Biotechnol. 6:741-755.

Debeire, P., Strecker, B., Vignon, M. (1990) Purification and properties of an endo-l,4- xylanase excreted by a hydrolytic thermophilic anaerobe, *Clostridium thermolacticum*. Eur. J. Biochem. 187: 573-580.

Dekker, R. F. H. (1983) Bioconversion of hemicellulose: Aspects of hemicellulase production by *Trichoderma reesei* QM 9414 and enzymatic saccharification of hemicellulose, Biotechnol. Bio Eng. 25:1127-1146

Derewenda, U., Swenson, L., Green, R., Wei, Y., Morosoli, R., Shareck, F., Kluepfel, D., Derewenda, Z. S. (1994) Crystal structure, at 2.6-Å resolution, of the *Streptomyces lividans* xylanase A, a member of the F family of β-1,4-D-glycanases. J. Biol. Chem. 269:20811–20814.

Dien, B. S., Sarath, G., Pedersen, J. F., Sattler, S. E., Chen, H., Funnell-Harris, D. L., Nichols, N. N. Cotta, M. A. (2009) Improved sugar conversion and ethanol yield for forage sorghum (Sorghum bicolor L. Moench) lines with reduced lignin contents. Bioenerg. Res. 2:153–164

Dodd, D., Cann, I. K. O. (2009) Enzymatic deconstruction of xylan for biofuel production. Glob. Change Biol. Bioener. 1:2–17.

Dodd, D., Kiyonari, S., Mackie, R. I., Cann I. K. O. (2010) Functional diversity of four glycoside hydrolase family 3 enzymes from the rumen bacterium *Prevotella bryantii* B14. J. Bacteriol. 192:2335–2345.

Ebringerova, A., Heinze, T. (2000) Xylan and xylan derivatives – biopolymers with valuable properties, 1.Naturally occurring xylans structures, isolation procedures and properties. Macromol. Rap.Comm. 21:542–556.

Ebringerova, A., Hromadkova, Z., Heinze, T. (2005) Hemicellulose. Adv. Polym. Sci. 186:1–67

Faix, O. (1991) Classification of lignins from different botanical origins by FI-IR spectroscopy Holzforshung 45:21-27.

Faure, D. (2002) The family-3 glycoside hydrolases: from housekeeping functions to host-microbe interactions. Appl. Environ. Microbiol. 68:1485–1490.

Freier, D., Mothershed, C. P., Wiegel, J. (1988) Characterization of *Clostridium thermocellum* JW20. Appl. Environ. Microbiol. 54:204-211.

Galbe, M., Zacchi G. (2002) A review of the production of ethanol from softwood. Appl. Microbiol. Biotechnol. 6:618-628

Garcia-Aparicio, M. P., Ballesteros, M., Manzanares, P., Ballesteros, I., Gonzalez, A., Negro, M. J. (2007) Xylanase contribution to the efficiency of cellulose enzymatic hydrolysis of barley straw. Appl. Biochem. Biotechnol. 137–140:353–365.

Gasparic, A., Martin, J., Daniel, A. S., Flint, H. J. (1995) A xylan hydrolase gene cluster in *Prevotella ruminicola* B(1)4, sequence relationships, synergistic interactions, and oxygen sensitivity of a novel enzyme with exoxylanase and beta-(1, 4)-xylosidase activities. Appl. Environ. Microbiol. 61:2958–2964.

Griswold, K. E., Mackie, R. I. (1997) Degradation of protein and utilization of the hydrolytic products by a predominant ruminal bacterium, *Prevotella ruminicola* B1(4). J. Dairy Sci. 80:167–175.

Harholt, J., Suttangkakul, A., Vibe, S.H., (2010) Biosynthesis of pectin. Plant Physiol. 153:384-95.

Harvey, A. J., Hrmova, M., De Gori, R., Varghese, J. N., Fincher, G. B. (2000) Comparative modeling of the three-dimensional structures of family 3 glycoside hydrolases. Proteins 41:257–269.

Henrissat, B., Davies, G. (1997) Structural and sequence-based classification of glycoside hydrolases. Curr. Opin. Struct. Biol. 7:637–644.

Himmel, M. E., Ding, S.-Y., Johnson, D. K., Adney, W. S., Nimlos, M. R., Brady, J. W. Foust, T. D. (2007) Biomass recalcitrance: engineering plants and enzymes for biofuels production. Science 315:804–807

Johnson, K. G., Harrison, B. A., Schneider, H., Mackenzie, C. R., Fontana, F. D. (1988) Xylan-hydrolyzing enzymes from *Streptomyces spp.* Enzyme Microb. Technol. 10:403409.

Jordan, D.B., Bowman, M.J., Braker, J.D., Dien, B.S., Hector, R.E., Lee, C.C., Mertens, J.A., Wagschal, K., (2012) Plant cell walls to ethanol. J. Biochem. 442:241-52.

Joseleau, J. P., Comtat, J., Ruel, K. (1992) Chemical structure of xylans and their interaction in the plant cell walls. In: Xylans and Xylanases. pp. 1-15. Visser, J., Beldman, G., Kusters-van Someren, M. A., and Voragen, A. G. J., Eds., Elsevier, Amsterdam.

Khandeparker, R., Numan, M. T. (2008) Bifunctional xylanases and their potential use in biotechnology. Ind Microbiol Biotechnol 35:635–644.

Kim, Y.S., Yeom, S.J., Oh, D.K. (2011) Characterization of a GH3 family β-glucosidase from *Dictyoglomus turgidum* and its application to the hydrolysis of isoflavone glycosides in spent coffee grounds. J. Agric. Food Chem. 59:11812–11818

Knocke, C., Vogt J., (2009) Biofuels - challenges & chances: How biofuel development can benefit from advanced process technology. Eng. Life Sci 2:96-99.

Kolenova, K., Vrsanska, M., Biely, P. (2006) Mode of action of endo-β-1, 4-xylanases of families 10 and 11 on acidic xylo-oligosaccharides. J. Biotechnol. 121:338–345.

Kormelink, F. J. M., Searle-van Leeuwen, M. J. F., Wood, T. M., Voragen, A. G. J. (199 la) (1,4)-β-D-arabinoxylan arabinofuranohydrolase: a novel enzyme in the bioconversion of arabinoxylan. Appl. Microbiol. Biotechnol. 35:231-232.

Kormelink, F. J. M., Searle-van Leeuwen, M. J. F., Wood, T. M., Voragen, A. G. J. (1991b) Purification and characterization of a (1,4)-β-D-arabinoxylan arabinofuranohydrolase from *Aspergillus awamori*. Appl. Microbiol Biotechnol. 35:753-758.

Kubata, B. K., Suzuki, T., Horitsu, H., Kawai, K., Takamizawa, K. (1994) Purification and characterization of *Aeromonas caviae* ME-1 xylanase V, which produces exclusively xylobiose from xylan. Appl. Environ. Microbiol. 60:531–535.

Kubata, B. K., Takamizawa, K., Kawai, K., Suzuki, T., Horitsu, H. (1995) Xylanase IV, an exoxylanase of *Aeromonas caviae* ME-1 which produces xylotetraose as the only low-molecular-weight oligosaccharide from xylan. Appl. Environ. Microbiol. 61:1666–1668.

Laemmli, U. K. (1970) Cleavage of structural proteins during the assembly of the head of bacteriophage T4. Nature 227:680–685.

Lamed, R., Bayer, E. A. (1988) The cellulosome concept: Exocellular enzyme reactor centers for efficient binding and cellulolysis. In: Aubert J.P, Beguin P, Millet J (eds) Biochemistry and genetics of cellulose degradation. Academic Press, London, pp 101–116

Laureano-Perez, L., Teymouri, F., Alizadeh, H., Dale, B. E. (2005) Understanding factors that limit enzymatic hydrolysis of biomass: characterization of pretreated corn stover. Appl. Biochem. Biotechnol. 121–124:1081–1099.

Lee, J. (1997) Biological conversion of lignocellulosic biomass to ethanol. Biotechnol., 56:1–24.

Lever, M. (1972) A new reaction for colorimetric determination of carbohydrates. Anal. Biochem. 47:273–279.

Lin, L. L., Thomson, J. A. (1991) An analysis of the extracellular xylanases and cellulases of *Butyrivibrio fibrisolvens* H17c. FEMS Microbiol. Lett. 84:197–204.

Linden, J. C., Decker, S. R., Samara, M. (1994) Role of Acetyl Esterase in Biomass Conversion. ACS Symposium Series, Vol. 566

Lynd, L. R., Cushman, J. H., Nichols, R. J., Wyman, C. E. (1991) Fuel ethanol from cellulosic biomass. Science 251:1318–1323.

Mackenzie, C. R., Bilous, D., Schneider, H., Johnson, K. G. (1987) Induction of cellulolytic and xylanolytic enzymes systems in *Streptomyces spp*. Appl. Environ. Microbiol. 53:2835-2839.

Madden, R. H. (1983) Isolation and characterization of *Clostridium stercorarium sp*. nov., cellulolytic thermophile. Int. J. Syst. Bacteriol. 33:837-840.

Manikandan, K., Bhardwaj, A., Ghosh, A., Reddy, V. S., Ramakumar, S. (2005) Crystallization and preliminary X-ray study of a family 10 alkali-thermostable xylanase from alkalophilic *Bacillus sp*. strain NG-27. Acta. Crystallogr. Sect. F. Struct. Biol. Cryst. Commun. 61:747–749.

Marcus, S. E., Verhertbruggen, Y., Herve, C., Ordaz-Ortiz, J. J., Farkas, V., Pedersen, H. L., Willats, W. G., Knox, J. P. (2008) Pectic homogalacturonan masks abundant sets of xyloglucan epitopes in plant cell walls. BMC Plant Biol. 22:8-60.

Maslen, S. L., Goubet, F., Adam, A., Dupree, P., Stephens, E. (2007) Structure elucidation of arabinoxylan isomers by normal phase HPLC-MALDI-TOF/TOF-MS/MS. Carbohyd. Res. 342:724–735.

Matsuo, N., Kaneko, S., Kuno, A., Kobayashi, H., Kusakabe, I. (2000) Purification, characterization and gene cloning of two a-L-arabinofuranosidases from *Streptomyces chartreusis* GS901. J. Biochem. 346:9–15.

McMillan, J.D., (1997) Bioethanol production: status and prospects. Renew. Ener. 2-3:295-302.

Mierzwa, M., Tokarzewska-Zadora, J., Deptula, T., Rogalski, J., Szczodrak, J. (2005) Purification and characterization of an extracellular α-D-glucuronidase from *Phlebia radiata*. Prep. Biochem. Biotechnol. 35:243–256.

Mohnen, D. (2008) Pectin structure and biosynthesis. Curr. Opin. Plant Biol. 11:266-277

Mohnen, D., Bar-Peled, M., Somerville, C. (2008) Cell wall polysaccharide synthesis. In Biomass Recalcitrance: Deconstructing the Plant Cell Wall for Bioenergy (Himmel, M. E., ed.). pp. 94–187, Blackwell Publishing, Oxford

Poutanen, K., Puls, J. (1988) Characteristics of *Trichoderma reesei* β-xylosidase and its use in the hydrolysis of solubilized xylans, Appl. Microbiol. Biotechnol. 28:425 - 432.

Poutanen, K.; Sundberg, M.; Korte, H.; Puls, J. (1990) Deacetylation of xylans by acetyl esterases of *Trichoderma reesei*. Appl. Microbiol. Biotechnol. 33:506-510.

Puls, J., Schmidt, O., Granzow, C. (1987) α-Glucuronidase in microbial xylanolytic systems. Enzyme Microbio. Technol. 9:83–88.

Rainey, F. A., Donnison, A.M., Janssen, P.H., Saul, D., Rodrigo, A., Bergquist, P.L., Daniel, R.M., Stackebrandt, E., Morgan, H.W. (1994) Description of

Caldicellulosiruptor saccharolyticus gen. nov., sp. nov: an obligately anaerobic, extremely thermophilic, cellulolytic bacterium. FEMS Microbiol. Lett. 120:263-266.

Saha, B.C. (1993) Hemicellulose bioconversion. J. Ind. Microbiol. Biotechnol. 30:279–291.

Scheller, H. V., Ulvskov, P. (2010) Hemicelluloses. Annu. Rev. Plant Biol. 61:263–289

Shao, W., Wiegel, J. (1995) Purification and characterization of two thermostable acetyl xylan esterases from *Thermoanaerobacterium sp*. strain JW/SL-YS485. Appl. Environ. Microbiol. 61:729–733.

Solomon, B.D., Barnes, J.R., Halvorsen, K.E., (2007) Grain and cellulosic ethanol: History, economics, and energy policy. Biom. Bioener. 6:416-425

Sommerville, C., Youngs, H., Taylor, C., Davis, S. C., Long, S. P. (2010) Feedstocks for lignocellulosic biofuels. Sci. 329:790-792

Sun, Y., Cheng, J. (2002) Hydrolysis of lignocellulosic materials for ethanol production: a review. Biore. Technol. 83:1–11.

Sunna, A., Antranikian, G. (1997) Xylanolytic enzymes from Fungi and Bacteria. Crit. Rev. Biotechnol. 17:39-67

Suresh, C., Kitaoka, M., Hayashi, K. (2003) A thermostable non-xylanolytic α-glucuronidase of *Thermotoga maritima* MSB8. Biosci. Biotechnol. Biochem. 67:2359–2364.

Svetlichny, V. A., Svetlichnaya, T. P., Chernykh, N., Zavarzin, G. A. (1990) *Anaerocellum thermophilum* gen. nov. sp. nov, an extreme thermophilic celluloselytic eubacterium isolated from hot springs in the Valley of Geysers. Microbiol. Mosc. 59:871-879.

Tan, K.T., Lee, K.T., Mohamed, A.R., (2008) Role of energy policy in renewable energy accomplishment: The case of second-generation bioethanol. Energ. Pol. 9:3360-3365.

Teng, C., Jia, H., Yan, Q., Zhou, P. and Jiang, Z. (2011) High-level expression of extracellular secretion of a β-xylosidase gene from *Paecilomyces thermophila* in *Escherichia coli*. Bioresour. Technol. 102:1822–1830.

Timell, T. (1964) Wood hemicelluloses: Part I. Adv. Carbohydr. Chem. Biochem. 19:247–299

van Peij, N.N., Brinkmann, J., Vrsanska, M., Visser, J., de Graaff, L.H. (1997) β-Xylosidase activity, encoded by xZnD, is essential for complete hydrolysis of xylan by *Aspergillus niger* but not for induction of the xylanolytic enzyme spectrum, Eur. J. Biochem. 245:164-173.

Vanholme, R., Demedts, B., Morreel, K., Ralph, J., Boerjan, W., (2010) Lignin biosynthesis and structure. Plant Physiol. 153:895–905

Vogel, K. P., Jung, H.-J. G. (2001) Genetic modification of herbaceous plants for feed and fuel. Crit. Rev. Plant Sci. 20:15–49

Vrsanska, M., Gorbacheva I. V., Kratky, Z., Biely, P. (1982) Reaction pathways of substrate degradation by an acidic endo-1,4-β-xylanase of *Aspergillus niger*. Biochimi. et Biophysi. Act. 704:114–122.

Wagschal, K., Heng, C., Lee, C. C., Wong, D. W. S. (2009) Purification and Characterization of a Glycoside Hydrolase Family 43 β-xylosidase from *Geobacillus thermoleovorans* IT-08. Appl. Microbiol. Biotechnol. 81:855–863.

Wheals, A.E., Basso, L.C., Alves, D.M.G., Amorim, H.V. (1999) Fuel ethanol after 25 years. Trends Biotechnol. 12:482-487

Williams, A. G., Withers, S. E. (1982) The effect of the carbohydrate growth substrate on the glycosidase activity of hemicellulose-degrading rumen bacterial isolates. J. Appl. Bacteriol.52:389-401.

Wolfenden, R., Lu, X., Young, G. (1998) Spontaneous hydrolysis of glycosides. J. Am. Chem. Soc. 120:6814–6815.

Wong, K. K., Tan, L. U., Saddler, J. N. (1998) Multiplicity of β-1,4-xylanase in microorganisms: functions and applications. Microbiology Reviews 52:305–317.

Woodward, J. (1984) Xylanases: functions, properties and applications. Top. Enzyme Ferment. Biotechnof. 8:9-30.

Yang, S.-J., Kataeva, I., Hamilton-Brehm, S. D., Engle, N. L., Tschaplinski, T. J., Doeppke, C., Davis, M., Westpheling, J. Adams, M. W. (2009) Efficient degradation of lignocellulosic plant biomass, without pretreatment, by the thermophilic anaerobe *Anaerocellum thermophilum* DSM 6725. Appl. Environ. Microbiol. 75:4762–4769.

Yeoman, C. J., Han Y., Dodd, D., Schroeder, C. M., Mackie, R. I., Cann, I. K. O. (2010) Thermostable enzymes as biocatalysts in the biofuel Industry. Ad. Appl. Microbiol. 70:1-55

Zanoelo, F. F., Polizeli, M.D., Mde, L., Terenzi, H. F., Jorge, J. A. (2004) Purification and biochemical properties of a thermostable xylose-tolerant β-D-xylosidase from *Scytalidium thermophilum*. J. Ind. Microbiol. Biotechnol. 31:170–176.

Zimmermann, W., Winter, B., Broda, P. (1988) Xylanolytic enzyme activities produced by mesophilic and thermophilic actinomycetes grown on graminaceous xylan and lignocellulose. FEMS Microbiol. Lett. 55:181-186.